N71-08397

PB 199 708

[illegible]

[illegible]

[illegible]

[illegible]

[illegible]

1 *Accession Number*

W 71-08397

2 *Subject Field & Group*

~~[illegible]~~ Ø5D, 5G

SELECTED WATER RESOURCES ABSTRACTS
INPUT TRANSACTION FORM

5 *Organization*

Syracuse University, Syracuse, New York

6 *Title*

PIPELINE FLOW OF SOLIDS-LIQUID SUSPENSIONS

10 *Author(s)*

Turian, Raffi
Yuan, Tran-Fu
Mauri, Giacomo

16 *Project Designation*

FWPCA Grant # 17070 DUQ

21 *Note*

Available from the National
Technical Information Service
as PB 199 708, $3.00 in
paper copy, $0.95 in microfiche

22 *Citation* ~~FWPCA Final Report on Grant # 17070 DUQ,~~ July1970, 122 p~~ages~~, 13 fig, 9 tab, 40 ref

23 *Descriptors (Starred First)*

*Slurry, *Hydrodynamics, Fluid friction, Pipes, Flow rates, Reynold's number, Headloss, Hydraulics, Suspended load, Particle size, Manometers, Flow meters, Mixing, Pressure, Analytical techniques, Laboratory tests, Statistical analysis, Sludge

25 *Identifiers (Starred First)*

Drag co-efficient, Glass

microns

27 *Abstract* Suspensions containing closely sized beads of varying diameters, made from two types of glass, were allowed to flow through 2,1 and 1/2 inch pipelines. Available slurry flow data in 1/2 inch pipe using glass, steel, and lead particles were combined with these data, resulting in a particle size range of from 31μ up to 4380μ. There were 12 particle sizes, and particle densities of 2.3, 3.0, 4.4, 7.5 and 11.3 gm/cc, with the entire data set consisting of 1511 points. From these data points, a slurry flow correlation was developed which predicts the slurry friction factor within an absolute average deviation of 9.5% for the entire data collection, with 74 data points having a deviation exceeding 30% and 9 data points with a deviation greater than 50%. Utilization of the correlation involved recasting of the drag coefficient —Reynold's Number relationship into an empirical expression valid for numbers well within the Stokes flow region, and up to nearly the so-called drag crisis. While most of the data presented ~~was~~ were taken in the laboratory, published data from two sources (selected after stringent scrutiny) were used to supplement certain ranges of the Reynold's number. ~~(Lowry-Texas)~~

(WRSIC abstract)

Abstractor Mark V. Lowry | *Institution* Texas Univ, Austin

WR:102 (REV. JULY 1969)
WRSIC

SEND, WITH COPY OF DOCUMENT, TO: WATER RESOURCES SCIENTIFIC INFORMATION CENTER
U.S. DEPARTMENT OF THE INTERIOR
WASHINGTON, D. C. 20240

GPO: 1970 - 407 - 89

RESEARCH REPORT

PIPELINE FLOW OF SOLIDS-LIQUID SUSPENSIONS

by

Raffi M. Turian, Principal Investigator
Tran-Fu Yuan
and
Giacomo Mauri

Department of Chemical Engineering and Metallurgy
Syracuse University
Syracuse, New York 13210

Submitted to:
Federal Water Pollution Control Administration
As a Final Report
Under Grant No. 17070 DUQ
July 1970

ABSTRACT

An experimental study of suspended solid flow in 2, 1 and 1/2-inch pipelines was carried out. The suspensions were composed of closely sized beads of various diameters made from two types of glass. These data were combined with available slurry flow data in 1/2-inch pipe using suspended glass, steel and lead particles. Altogether the particle size range represented by the combined set of data is from a mean particle diameter of 31μ up to 4380μ, consisting of 12 different particle sizes in this range. The types of solids represented in these data cover particle densities, in round figures, of about 2.3, 3.0, 4.4, 7.5, and 11.3 gm/cc. The entire set of data consisted of 1,511 points.

The set of 1,511 data points were used to develop a slurry flow correlation. The correlation predicts the slurry friction factor with an absolute average deviation of 9.5% for the entire collection of data. Of the total number of data points, 74 have a deviation exceeding 30%, and only 9 points have a deviation exceeding 50%. The correlation can be used in slurry pipeline design, which entail entirely straightforward calculations. To preclude the need for trial and error computations in using the correlation, the drag coefficient-Reynolds number relationship for free settling spheres, which is utilized in the main slurry flow correlation, is recast into an empirical expression valid over an unprecedented range of nearly 14 cycles in Reynolds number; from well within the Stokes flow region up to nearly the region of the so-called drag crisis. The free settling sphere data used to develop this empirical equation were, for the most part, taken in this laboratory. However, published data from two sources (ones which withstood the stringent critical scrutiny imposed on all the falling sphere data) were used to supplement certain ranges of the Reynolds number.

TABLE OF CONTENTS

Page

ABSTRACT

TABLE OF CONTENTS i

LIST OF TABLES iii

LIST OF FIGURES iv

CHAPTER I - INTRODUCTION 1

CHAPTER II - FLOW OF SUSPENSIONS IN PIPELINES 4

CHAPTER III - EQUIPMENT AND MATERIALS 11

- 3.1. General Description of Overall System 11
- 3.2. Detailed Description of Special Features of the Equipment 16
  - 3.2-1. Pressure Taps 17
  - 3.2-2. Solid Traps 17
  - 3.2-3. Manometers 19
  - 3.2-4. Transparent Removable Section 19
  - 3.2-5. Slurry Reservoir and Weigh Tank 19
  - 3.2-6. Magnetic Flowmeter 19
  - 3.2-7. Pump, Motor, and Control 21
- 3.3. Materials 22

CHAPTER IV - PROCEDURE AND EXPERIMENTS 24

- 4.1. Physical Properties 24
  - 4.1-1. Densities of Glass Beads 24
  - 4.1-2. Sizes of Glass Beads 24
- 4.2. Operation of the Flow System and Experimental Procedure 28
  - 4.2-1. Calibration of the Magnetic Flowmeter 28
  - 4.2-2. Charging and Recovery of Solids 28
  - 4.2-3. Determination of Concentration 30
    - a. Discharge Concentration 31
    - b. Spatial Concentration 31
- 4.3. Flow Experiments 32
  - 4.3-1. Pressure Drop 32
  - 4.3-2. Critical Velocities 32

TABLE OF CONTENTS (Cont'd.)

Page

CHAPTER V - EXPERIMENTAL RESULTS AND CORRELATIONS 36

5.1. Introduction 36

5.2. Critical Velocities 36

5.3. Free Falling Velocity of Spheres 39

5.4. Pipe Flow of Homogeneous Liquids 45

5.5. Slurry Flow Correlation 47

5.6. Summary 57

CHAPTER VI - CONCLUSION 66

NOMENCLATURE 69

LITERATURE CITED 72

APPENDIX A - GLASS SPHERE SLURRY FLOW IN 2, 1, and 1/2-INCH PIPELINES 74

APPENDIX B-1 - SIZE MEASUREMENTS OF GLASS BEADS 114

APPENDIX B-2 - GLASS SPHERE SLURRY FLOW IN 2-INCH PIPELINE 117

LIST OF TABLES

TABLE NO.	TITLE	Page
3.1	Properties of Glass Beads in Flow Experiments Using 2-inch Pipeline Only	22
3.2	Properties of Glass Beads in Flow Experiments Using 2, 1, and 1/2-inch Pipelines	23
5.1	Measured and Calculated Critical Slurry Velocities	37
5.2	Constants for Equations (14) and (15)	43
5.3	Constants for Equation (16)	45
5.4	Variables Relating to Pipeline Flow of Suspended Solids	48
5.5	Constants for Equation (37)	53
5.6	Solid Particles Used in Suspension Flow Experiments in 1/2-inch Pipeline by Murphy, Young, and Burian (40)	54
5.7	Values of Constants Obtained by Least Squares Scheme Using the Linearized Equation (38)	55

LIST OF FIGURES

FIGURE NO.	TITLE	PAGE
1	Schematic Representation of Equipment	12
2	Transparent and Removable Section	15
3	Pressure Tap and Solid Trap	18
4	Manometer Bank	20
5	Size Distribution for 4380μ Spheres	27
6	Pressure Drop-Velocity for Water in the 2-inch Pipe	33
7	Pressure Drop-Velocity for Water in the 1-inch Pipe	34
8	Pressure Drop-Velocity for Water in the 1/2-Inch Pipe	35
9	Plot of Reciprocal $[(i_m-i_w)/i_w C]$ against Slurry Velocity	39
10	Drag Coefficient-Reynolds Number Relation for Settling of a Solid Sphere in Unbounded Newtonian Fluids	41
11	Plot of $(f-f_w)$ against ξ° for 2, 1, and 1/2-inch Pipes	58
12	Plot of $(f-f_w)$ against ξ for 2, 1, and 1/2-inch Pipes	60
13	Plot of $(f-f_w)$ against ξ for 2, 1, and 1/2-inch Pipes (Data from this work shown only)	62

CHAPTER I

INTRODUCTION

The research problem under consideration in this report concerns the understanding of the pipe flow behavior of solids suspended in liquids, and, in particular, from the engineering viewpoint, the determination of the pressure drop-flow rate relationship relating to this type of flow. These solid-liquid suspensions are heterogeneous systems with a very strong tendency for settling. Indeed for most of the solid-liquid systems of interest the settling tendency is so pronounced that it is virtually impossible to obtain uniform distributions of the solids through the agitation caused by the flow within the pipeline, or, for that matter, by means of supplementary mixing within vessels. The number of variables which govern this type of flow is quite large, and the hydrodynamic problem relating to suspension flow, in general, is so complicated that all solution attempts to the present time have left it virtually intact.

Suspended solids flow in pipelines is of interest because it is applicable in problems relating to the handling and transportation of solid raw materials and products, solid wastes, sludges and so on. Largely because the variety of suspension systems is almost unlimited published reports in this area pertain to studies which are, necessarily, circumscribed in some manner. Clearly, it would be expedient to study only, or at least primarily, the suspension systems of particular importance to the individual researcher, and this is precisely the type of work which prevails in the literature on slurry flow. Therefore, the literature abounds with very useful results relating to particular slurries in specific flow situations, but these usually cannot be readily incorporated in a store of data which can ultimately be used to establish general design correlations. The main limitations in these types of published works are that: 1. they are so specific as to cover a very limited range of the variables involved, 2. the slurry systems are not well defined with respect to, say, solids shape and size distribution, and 3. incomplete data, which are often impossible to retrieve, are presented in the published versions.

A primarily experimental approach to the problem is inevitable, because of the hopelessness of, perhaps, ever achieving a mathematical solution to the general hydrodynamic problem. In this particular research problem an experimental study is burdened by three principal considerations: 1. the enormous number of variables governing the flow, 2. the vast ranges over which most of the variables can vary, and 3. the inherent limitations on accuracy and reproducibility of the data which can be obtained with these complicated heterogeneous settling slurries. This last consideration is quite crucial, and it clearly resides in the fact that one is really dealing with an unstable system. In many systems of practical interest the settling tendency is so pronounced, indeed often so predominant, that vast variations in the data, from experiments conducted under apparently identical conditions, are observed. Accordingly, it is quite important to make replicate measurements to insure satisfactory reproducibility under each set of operating conditions. This procedure is a mark of good experimental practice in most other problems, but in the problem under consideration here it is a necessity.

In practical applications of hydraulic transport of solids the objectives depend upon the particular function that this mode of solids conveyance serves. Generally, in short-distance handling operations the main objective is to insure easy and trouble-free transport of the material, often within the same plant site. Accordingly, under these circumstances, little or no consideration is given to modifying the design to account for differences in flow behavior between suspension and suspending liquid, except, perhaps, for insuring that a sufficiently high flow velocity can be maintained to inhibit settling. In addition, very dilute suspensions are invariably handled. In long-distance hydraulic transport, however, the objective is usually to convey the maximum amount of solids possible within, sometimes, rigid technical and economic constraints. Proper design, the right operating conditions, and the optimum slurry formulation are all intimately involved in solutions to the problem, and the interrelationships among these are largely unknown.

An experimental study of the flow of slurries made up of well-defined solids in a 2-inch, 1-inch, and 1/2-inch pipe was carried out. Two densities of glass spheres were used and the particle size ranged between 90μ and 4380μ. Available data from the literature were added to the data taken in this work, and the entire collection of data was used to develop a correlation. The drag coefficient-Reynolds number relationship for free-falling spheres in an unbounded Newtonian medium was recast into a polynomial expression suitable for direct calculation of the settling velocity, which is a needed parameter in the slurry flow correlation. The polynomial expression is based on very accurate free-falling velocity data, taken, for the most part, in this laboratory, and satisfactorily predicts the drag coefficient-Reynolds number relationship over 14 cycles in Reynolds number; covering the Stokes flow region at one end and going up to the so-called drag crisis (i.e. $Re = 2.5 \times 10^5$). Also, in order to facilitate use of the slurry flow correlation, the friction factor-Reynolds number relationship for Newtonian flow in a smooth pipe was cast into a simple polynomial expression.

CHAPTER II

FLOW OF SUSPENSIONS IN PIPELINES

The large body of published work relating to suspension transport includes basic studies typified by those of Goldsmith and Mason (1,2), Happel and Byrne (3), and Happel and Brenner (4). These types of basic studies are concerned with particle-fluid and particle-particle interactions in single-, double-, or multiple-sphere or rod suspensions. A basic and mathematically rigorous treatment can be successfully applied to these types of highly idealized "dilute" suspensions, provided some rather severe restrictions on the flow conditions are imposed. Such studies are of intrinsic value, of course, and may be useful in some practical situations, but within the context of hydraulic transport of solids they represent limiting situations, if we choose to view them in this light, too far removed from the actual situation to be of material consequence.

A somewhat basic approach, i.e. one which attempts to relate the flow to measurable internal parameters related to the momentum transfer processes prevailing, is based upon the researches of Bagnold (5,6,7), and his concept of the dispersive stress. The approach is phenomenological, depending, as it does, upon the experimental determination of the so-called dispersive stress. Bagnold demonstrated that by shearing a concentrated suspension of neutrally-buoyant spheres in an annular region that a dispersive stress, which could be correlated in terms of the variables of the system, existed between the particles. The approach was utilized, to some extent, by Daniel (8) in his study of the flow of suspensions in a rectangular channel. The experimental determination of the dispersive stress parameter is precluded in suspensions with a strong tendency to settle, because it is exceedingly difficult to maintain a uniform distribution of solids. Moreover, this approach is of marginal value in hydraulic transport of solids because of the difficulties of applying it to circular conduits.

Effective viscosity correlations for suspensions of spheres and other iso-dimensional particles, such as those proposed in the studies of Rutgers (9), Kynch (10), and Ting and Luebbers (11) and many others which have appeared, represent, in the main, empirical extensions of Einstein's theoretical expression (12) for the viscosity of very dilute suspensions of non-interacting spheres in Newtonian fluids. The application of the effective viscosity concept in the treatment of the pipeline flow of settling suspensions entails merely a recasting of the actual pressure drop-flow rate data into a different form; an unnecessarily cumbersome and round-about procedure with no demonstrable merit. The main allure of the effective viscosity concept resides in the implied promise that it will reduce the treatment of the suspension flow problem to that of a simple Newtonian or at least homogeneous, fluid, i.e. given the effective viscosity for a suspension the correlations developed for simple homogeneous Newtonian fluids (or, for that matter, non-Newtonian fluids) can be used. The procedure, therefore, depends crucially upon the possibility of making meaningful (in the restricted sense just stated) independent viscometric measurements; a rather difficult trick with the strongly settling, manifestly heterogeneous suspensions of practical interest. Nonetheless, effective viscosity correlations are quite useful for the purposes they have been used, which have rarely, if ever, included the correlation of the flow behavior of settling suspensions in pipelines.

Generally, when the maximum particle size in the suspension is quite small, and the flow velocity is sufficiently high, the distribution of solids across the pipe is, more or less, uniform, and the continuum approach is applied. For the flow of water suspensions of thoria and kaolin in pipes, Thomas (13) used the Bingham plastic model in establishing his correlations, but the largest mean particle size was about 13μ. The use of a continuum non-Newtonian approach is predicated upon the ability to provide a rheological characterization of the suspension through suitable viscometric means. Some rather important problems relating to the correlation of pressure drop-flow rate data in non-Newtonian fluids remain unresolved, and, in particular, those arising from ambiguities surrounding the definition of a suitable generalized Reynolds number are most persistent. Nonetheless, useful correlation procedures, based largely on data for aqueous, essentially homogeneous, high polymer solutions have been proposed (14,15). It is of interest to add here that the observation that, in some suspended flows at sufficiently high velocities, the solid material is concentrated within the central core with an outer annular region of clear liquid near the pipe wall, had led many investigators to presume that Bingham plastic flow prevailed. This type of behavior is generally common in paper pulp suspensions, and the connection with Bingham plastic flow rests upon the fact that in laminar pipe flow of this ideal, essentially fictitious, material there is always a central elastic plug surrounded by an annular region of liquid. The possible relationship between the two flows is quite deceptive, of course, because the suspension is not a continuum. The continuum non-Newtonian approach has been moderately successful with suspensions of fines which are frequently viewed as plastic materials with a yield stress (16,17).

Research on hydraulic transport has had a long history, and interest in it has endured and grown. Over a half a century ago Blatch (see ref. 18) proposed the relation

$$h_m = h_w + AC \qquad (1)$$

where h_m and h_w are the head losses, in ft. of water per ft. of pipe, for the mixture and for the suspending liquid at the same flow rate, respectively, and C is the mean solids concentration. In Equation (1) A was assumed constant, but Blatch, who took data using 1-inch brass and galvanized pipe and suspensions of -20 +40 mesh and -60 +100 mesh sand, found that the value of A depended on solid size. Later Howard (19), using 0.4 mm sand in 4-inch pipe, showed that A depended on pipe diameter as well.

Based on the idea of summing the work needed to maintain the solids in suspension together with the energy dissipation for the flowing water Wilson (20) derived the relation

$$h_m = h_w + A' \frac{v_\infty}{V} C \tag{2}$$

where v_∞ is the free-falling velocity of the particle and V is the mean suspension velocity. Wilson's treatment does not account for interactions among the various energy contributions in the flow. Newitt _et_ _al_ (21) conducted experiments with solids of sizes from -240 mesh to 3/16-inch and a specific gravity between 1.18 and 4.6 in a 1-inch pipe. Using Wilson's approach they proposed the relation

$$\frac{i_m - i_w}{i_w C} = 1100(s-1) \frac{v_\infty}{V} \frac{gD}{V^2} \tag{3}$$

where i_m and i_w are the head losses for the mixture and water at the same mean velocity, respectively, and C is the discharge concentration of solids. Equation (3) is applicable in the so-called _suspended_ _flow_ regime. For the _sliding_ _bed_ regime the relation

$$\frac{i_m - i_w}{i_w C} = 66(s-1) \frac{gD}{V^2} \tag{4}$$

was proposed, and for the regime with a _stationary_ _deposit_ they derived the equation

$$\frac{i_m - i_w}{i_w C} = 0.8(s-1) \tag{5}$$

In the area of solids suspension flow the work of Durand and his co-workers in Grenoble (22,23,24,25) is singular. In a series of papers, published in the early fifties, this group of researchers revealed the results of a study so extensive that it exceeded, or at least equaled, the combined effort of all other researchers up to that time. Durand and his group studied sand and gravel suspensions with particle sizes ranging between 0.2 mm to 25 mm, pipe diameters of from 1-1/2 inches up to 23 inches, and solids concentrations up to 60% by weight. Based upon this work they proposed the following criteria for delineating the main flow regimes observed in suspended solids flow:

1. For $d < 30\mu$: Homogeneous Flow, i.e. a uniform distribution of solids in flow exhibiting plastic behavior.
2. For $30\mu < d < 50\mu$: Intermediate Flow, i.e. depending upon the suspension velocity either homogeneous or heterogeneous flow can occur.
3. For $d > 50\mu$: Heterogeneous Flow
   - (a) For $50 < d < 0.2$ mm: Suspended Flow
   - (b) For 0.2 mm $< d < 2$ mm: Transition Flow
   - (c) For $d > 2$ m: Saltation Flow

Despite the fact that the foregoing criteria have been confirmed by others (of course, for the same solids) the particle size alone is, clearly, entirely too inadequate a measure of the nature of the flow regime which prevails.

A principal result of the work by Durand's group is the correlation

$$\frac{i_m - i_w}{i_w C} = K \left\{ \frac{V^2}{gD} \sqrt{C_D} \right\}^{-1.5} \tag{6}$$

where C_D is the drag coefficient for the free falling particle, assumed spherical, given by

$$C_D = \frac{4}{3} \frac{gd(s-1)}{v_\infty^2} \tag{7}$$

Based on a very large number of tests on sand slurries, the constant K in Equation (6) was found to be 176. To account for the effect of particle density, moreover, a modification of Equation (6) given by

$$\frac{i_m - i_w}{i_w C} = \bar{K} \left\{ \frac{V^2}{gD(s-1)} \sqrt{C_D} \right\}^{-1.5} \tag{8}$$

For the sand slurries Durand's group used (s-1) = 1.65, and, obviously, by comparing Equations (6) and (8) $\bar{K} = 83$.

A further result of Durand's work is an empirical equation for predicting the critical velocity of the slurry, i.e. the velocity below which a stationary deposit of solids forms in the pipe. The critical velocity correlation is given by

$$V_c = F_L \sqrt{2gD(s-1)} \tag{9}$$

where F_L is a dimensionless function of slurry concentration and particle diameter reported as a family of curves. The result in Equation (9) is of considerable practical value, since the critical velocity, if sufficiently high in a given case, may be the limiting parameter.

Ellis and Round (26) took data using Nickel (s = 8.90) slurries with particle size of 106μ in a 1-inch pipe. In order to get a satisfactory description of their data using Equation (8), they found that it was necessary to change the value of $\bar{K}$ and also the exponent, -1.5. That a correlation based on so extensive a piece of research work, as that of Durand and his co-workers, should fail to describe these data is testimony to the magnitude of the research problem and the vastness of the variables which govern it.

Other published work of interest includes Worster and Denny's (27) who used 0.1-inch to 1-inch gravel and coal slurries in 3, 4, and 6-inch pipe. Smith (28) took data in slurries with mixed particle size in 2 and 3-inch pipe. In using Durand's relation (6), Smith recommends using the expression

$$d_e = \sum_i w_i / \sum_i (w_i/d_i) \tag{10}$$

for calculation of an equivalent particle diameter d_e. In Equation (10) w_i is the weight fraction of particles of diameter d_i. Miller and Cloete (29,30) and Oedjoe et al (31,32,33,34) report pumping sand slurries at extremely high concentrations; intermediate between those of freely settled and vibration packed beds of these solids. Among the rare works in which liquids other than water has been used is that of Gay (35) who suspended particles of alumina, nickel, copper, and glass in sodium, xylene and glycerin. The use of liquids other than water in pilot size pipelines, a scale which ultimately must be used in this type of research, is somewhat impractical.

CHAPTER III

EQUIPMENT AND MATERIALS

3.1. General Description of Overall System

The slurry flow equipment used in our experiment is shown schematically in Figure 1. A brief description of the overall system will be presented, followed by a more detailed discussion of special features of this equipment. The system consisted of a cylindrical stainless steel reservoir having a conical bottom with a 3-inch flanged outlet at the center. The diameter and the height of the reservoir were 3 feet. The flanged bottom outlet of the reservoir was connected to a 3-inch gate valve followed by a 3-inch flanged tee leading to the pump inlet. The tee was oriented so that the fluid made a 90° turn in going into the pump inlet. The opening of the tee opposite the pump inlet was sealed with a blind flange, which later was drilled and tapped to accept a 3/4-inch pipe used for draining the system. The pump was of the centrifugal slurry type with a 3-inch inlet and a 2-inch outlet. The pump drive used was a 5 HP solid state controlled induction motor. The pump and the motor assembly were set on vibration mounts. A two foot length of 2-inch flexible rubber hose (A) connected the pump discharge to the flow test pipe. The flow test pipe was a flow loop consisting of two parallel legs of 2-inch pipe, approximately 37 ft. in length each, mounted on the same horizontal plane, 3 feet above floor level. The two parallel legs of the loop were connected together using a short section of straight pipe, a tee at one corner and a 90° elbow at the other corner. The tee was used to install the 1-inch and 1/2-inch test pipes which were mounted in the same horizontal plane above the 2-inch test loop. The longest continuous pieces of 2-inch pipe used in the construction of the loop were 10 feet. Thus, three ten foot lengths and one seven foot length of pipe were needed for each leg. Ten feet sections were also used for the 1-inch and

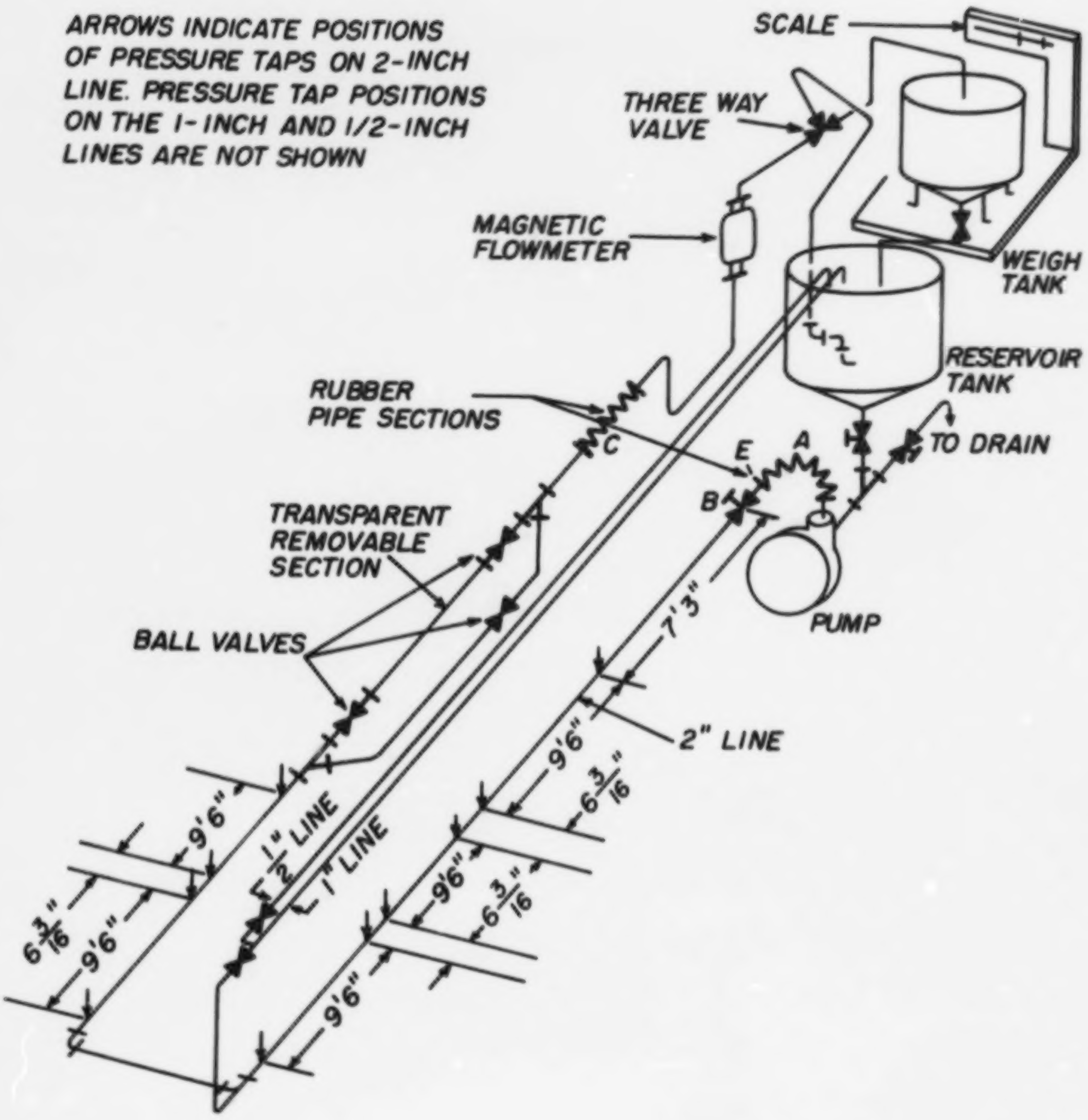

SCALE
THREE WAY VALVE
MAGNETIC FLOWMETER
WEIGH TANK
RESERVOIR TANK
RUBBER PIPE SECTIONS
C
E
A
B
TO DRAIN
TRANSPARENT REMOVABLE SECTION
BALL VALVES
PUMP
7'3"
2" LINE
9'6"
6 3/16"
9'6"
1/2" LINE
1" LINE
9'6"
6 3/16"
9'6"
9'6"
6 3/16"
9'6"
C

ARROWS INDICATE POSITIONS OF PRESSURE TAPS ON 2-INCH LINE. PRESSURE TAP POSITIONS ON THE 1-INCH AND 1/2-INCH LINES ARE NOT SHOWN

FIGURE I. SCHEMATIC REPRESENTATION OF EQUIPMENT

1/2-inch test pipes, which were 37 feet long each.

All pipe connections in the loop were made using Victaulic couplings, the grooving dimensions for which were set to give minimum pipe end-to-end separation. All pipe used in the loop was standard wall PVC pipe of 2-inches, 1-inch, and 1/2-inch nominal diameter, except for a 5 ft. transparent section in the 2-inch loop which was 2 inches I.D., plexiglas pipe. Plastic pipe was chosen for its smoothness which eliminates roughness as a consideration in analyzing the data, for its corrosion resistance and for its desirable machining and working properties. The entire flow loop was supported independently from the pump-motor assembly on a frame constructed from slotted angle, and a section of flexible rubber hose was also used to connect the end of the return branch of the flow loop to the piping leading to the reservoir and/or a weigh tank. This type of arrangement was planned in order to minimize the transmission of vibrations from the pump to the pipe test sections. The flexible hose connected to the downstream end of the flow loop led to the measuring head of a 2-inch magnetic flow meter, which was mounted so that the flow in it was in a vertical direction, with a 3 foot length of vertical pipe preceding it to prevent excessive impingement of solids on the inner wall of the flowmeter. The discharge from the flowmeter led to a 2-inch three-way valve, which could be used to direct the flow back into the slurry reservoir or into a weigh tank. The weigh tank was a cylindrical stainless steel tank having a conical bottom with a 3-inch flanged outlet at the center. The diameter and the height of the weigh tank were 2' 3". The flanged outlet from the bottom was connected to a 3-inch butterfly valve. In addition, the weigh tank had two 2-inch overflow outlets near the top. The weigh tank was placed on a 1000 lb. scale, and the entire assembly was mounted on a 5 foot high platform which was high enough such that the 3-inch outlet pipe from the weigh tank was approximately 2 inches above the slurry reservoir tank. A stirrer was mounted in each of the tanks. The 1-inch and 1/2-inch test sections emptied directly into the reservoir. The flowrate and solids concentrations in these test sections could be determined using a long, square, calibrated plexiglas column, with 7" x 7" cross-section and a height of 63 inches.

A few more details regarding the flow loop itself are of interest. We will identify, for the sake of this presentation, the rubber hose connection point to the flow loop as the entrance point (E in Figure 1). With this entrance point as a reference we will describe various features of the flow loop. Approximately 20 inches from the entrance point, a 2-inch gate valve was installed and used both for throttling and shutting off the flow when necessary. A bimetallic thermometer, with the stem almost reaching the opposite wall of the pipe, was mounted into the pipe 5 feet downstream of the entrance point. Upstream from the thermometer, a distance of 4 feet from the entrance point, a pressure transducer was installed. The signal from this transducer could be used to automatically control the pressure at that point by adjusting the motor speed. Our slurry flow system was set up so that the automatic controller of the pump-motor could be actuated by either this transducer, thereby giving control of the pump discharge pressure, or by a tachometer mounted on the motor shaft, which signal, when used, would result in control of the impeller speed. Pressure taps on the outgoing leg of the loop were located at the points indicated in Figure 1. The locations of the pressure taps on the 1-inch and 1/2-inch test pipes are not shown in Figure 1, but they were essentially similar to those on the main 2-inch loop. The first pressure tap on the 2-inch line was about 8 feet from the entrance point. Pairs of pressure taps connected to the same manometer were always on the same continuous section of pipe, which helped in decreasing the possible distortion of the

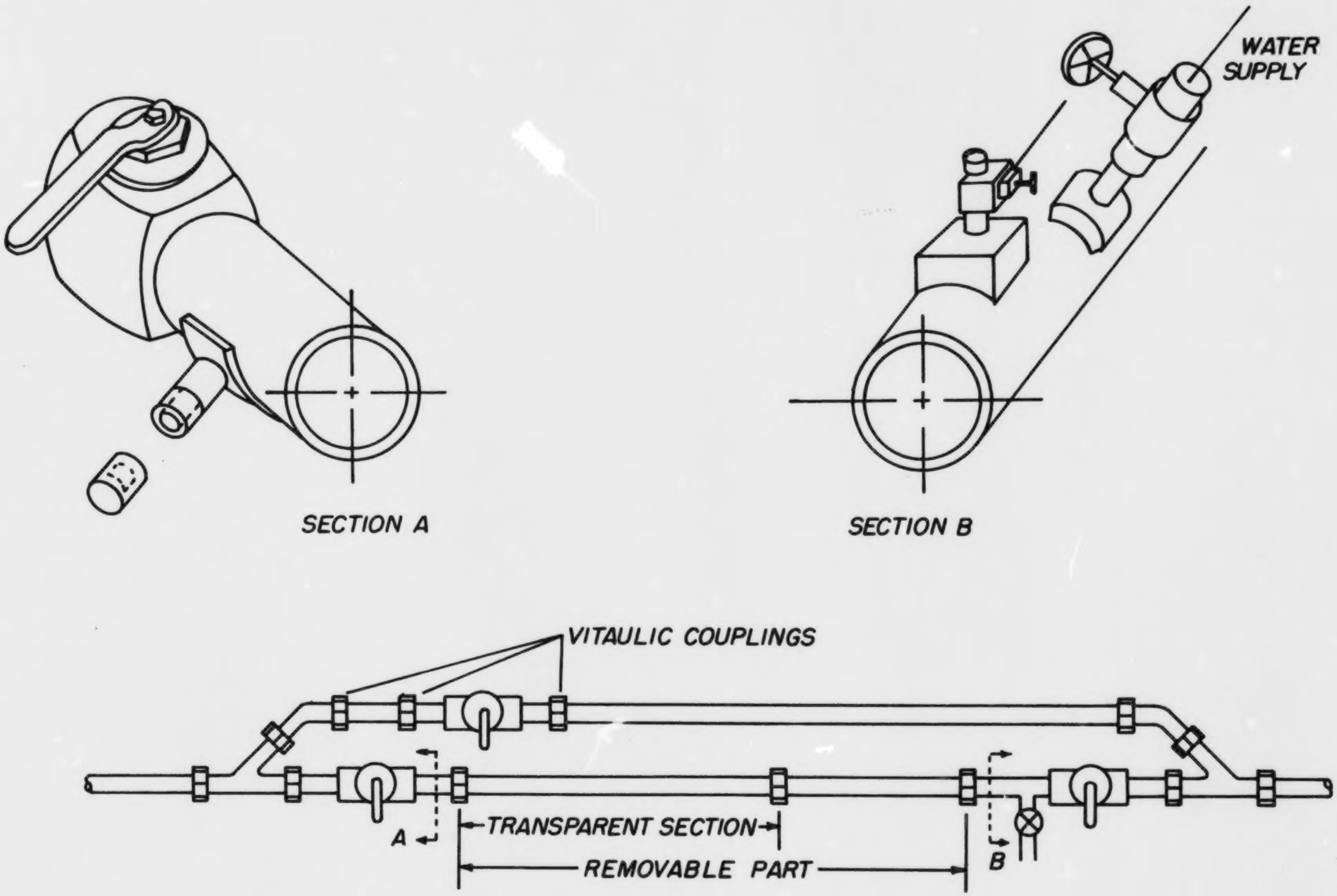
WATER SUPPLY
VITAULIC COUPLINGS
A
TRANSPARENT SECTION
REMOVABLE PART
B

SECTION A

SECTION B

FIGURE 2. TRANSPARENT AND REMOVABLE SECTION

pressure drop readings by disturbances from an intervening pipe joint. The pressure taps, which were made by drilling a 1/16-inch hole through the pipe wall and cementing a tapped PVC mount on the outside to accept a 1/4-inch fitting, were drilled near the ends of the 10-foot lengths of pipe used in constructing the main loop, and also the other test pipes. The location of the holes near the ends of the pipe section was necessary to permit inspection of the hole for possible burrs and other imperfections. Continuing with details of the flow loop, the tee leading to the smaller diameter test pipes was approximately 38 ft. from the entrance point, and it was followed by a straight 25-inch length of pipe and the 90° return elbow leading to the return leg of the 2-inch loop.

Pressure taps on the return leg of the loop were located as in Figure 1. The first was only 3 inches after the bend. Needless to say the same procedure as with the outgoing leg of the loop was used with reference to pairing pressure taps on the same continuous length of pipe to the same manometer. Twenty feet from the elbow a lateral was installed for inserting a bypass. The lateral joining the two pipes again was 32 ft. from the return elbow. Between the two laterals, two 2-inch ball valves were installed on the pipe, a distance of 9 ft. apart (Figure 2). A five foot section of the pipe here was plexiglas. Another 2-inch ball valve was installed on the bypass. The two ball valves on the pipe, when shut off simultaneously, could be used to isolate a section of the flow. When this was done, the bypass valve was opened at the same time to maintain the circulation, and avoid possible problems of solids settling in other parts of the system. The return leg of the loop was connected to a rubber hose leading to the piping connecting the magnetic flowmeter.

3.2. Detailed Description of Special Features of the Equipment

Special features of the design of the system, and the specific details, such as size, capacity, power, etc., of the equipment will be described here.

3.2-1. Pressure Taps

The pressure taps were constructed by drilling a 1/16-inch hole through the pipe wall. To make connections a mount was made by machining a block of PVC, and tapping a 1/4-inch thread through it. With the 1/4-inch hole in the block concentric with the 1/16-inch hole in the pipe, the block was cemented to the pipe wall. Each pressure tap was connected to a solids trap, from which the lines to the manometer were connected (Figure 3).

3.2-2. Solid Traps

The solid traps were made of 2-inch O.D. plexiglas cylinders of 6 inches height and 1/4-inch wall thickness. The ends of the cylinders were sealed with circular plexiglas plugs. One end of the cylinder was tapped for a 1/2-inch fitting and the other for a 1/4-inch fitting. In addition, a 1/4-inch tap was made through the center of the cylindrical wall. This last center hole was connected to the pressure taps on the pipe. The 1/4-inch hole through the end of the trap was used for connecting to the manometer lines. The 1/2-inch holes were plugged, and generally used for cleaning the traps. The solid traps could be mounted vertically with either the 1/2" or the 1/4" at the top, so that the setup could be used with slurries of solids heavier and also lighter than the liquid. Instead of connecting the 1/4" opening on the solids trap directly to the manometer lines, a 1/4" tee was used to install a valve. The axis of the valve was the same as that of the trap cylinder, and it was used for purging the manometer lines of air bubbles. The manometer lines were 1/4-inch rigid polyethylene tubing, which was semi-transparent

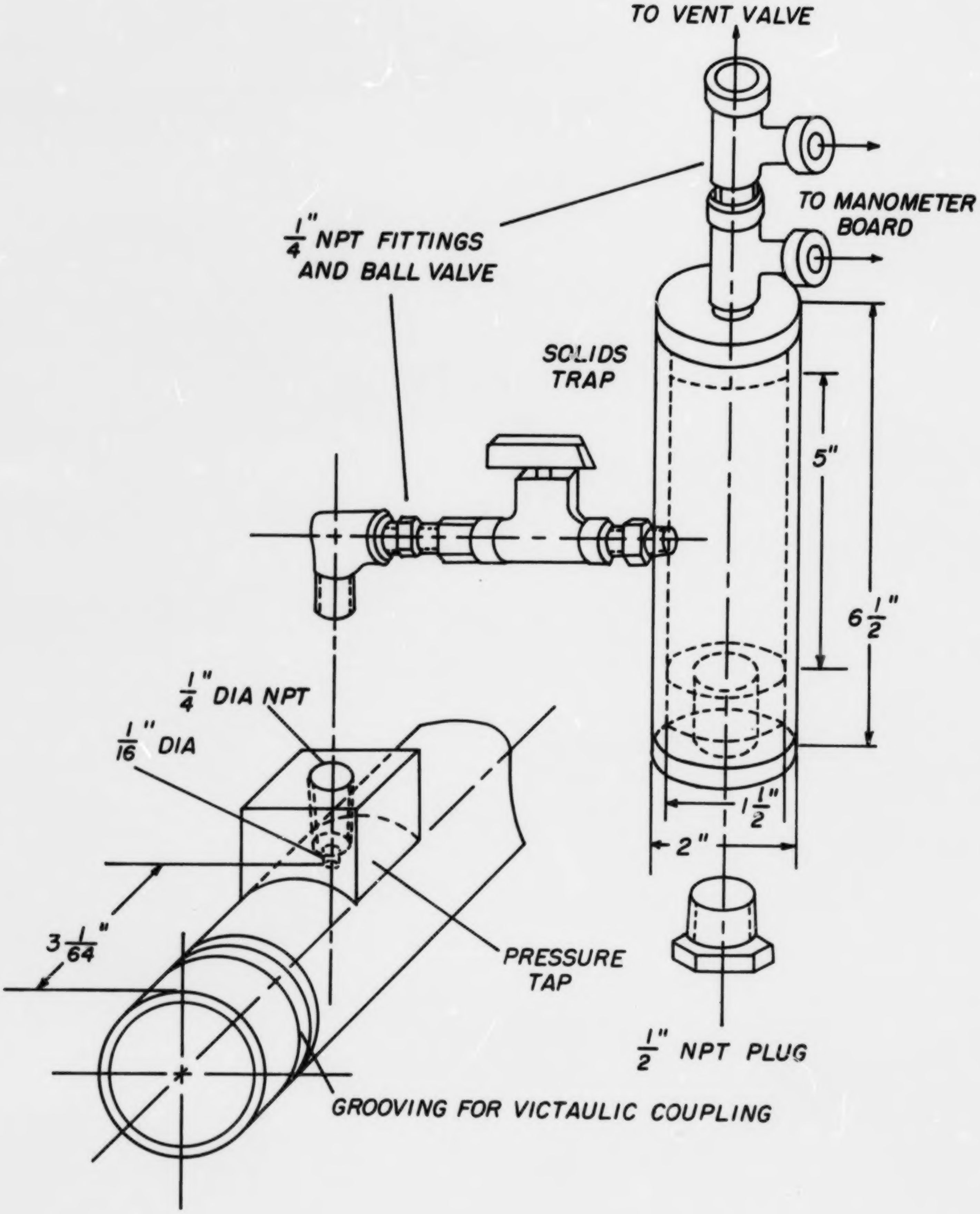
TO VENT VALVE
TO MANOMETER BOARD
1/4" NPT FITTINGS AND BALL VALVE
SOLIDS TRAP
5"
6 1/2"
1/4" DIA NPT
1/16" DIA
1 1/2"
2"
3 1/64"
PRESSURE TAP
1/2" NPT PLUG
GROOVING FOR VICTAULIC COUPLING

FIGURE 3. PRESSURE TAP AND SOLID TRAP

and permitted the detection of trapped air bubbles.

3.2-3. Manometers

A bank of 8 manometers (Figure 4) was used to measure pressure differences. All were Meriam Model No. A-324, well type manometers with a range of 30 inches. Three manometer fluids were used: Meriam Blue Fluid No. D-8325, specific gravity 1.75, Meriam Red Fluid No. 2883, specific gravity 2.95, and mercury. The density-temperature dependence of these fluids was determined by using a pycnometer. A piping manifold was used to connect the pressure taps to the desired manometer, and also to isolate manometers from the system.

3.2-4. Transparent Removable Section

The removable section of pipe on the return leg of the loop was described above. It was used for determining the "spatial concentration" of solids, which in such heteregenous slurry systems is not necessarily the same as the "transport concentration". Part of the removable section was constructed of plexiglas pipe to permit observation of the flow.

3.2-5. Slurry Reservoir and Weigh Tank

The slurry reservoir had a capacity of 160 U.S. gallons, and was equipped with 1/3 HP Lightnin mixer. A cooling coil made by winding 30 ft. of 1/2 copper tubing was installed in the reservoir tank. The weigh tank had a capacity of 80 U.S. gallons, and was equipped with 1/8 HP Lightnin mixer. This tank was mounted on a Howe-Richardson Mechano Weigh 54XL beam scale with 1000 lb. capacity.

3.2-6. Magnetic Flowmeter

A 2-inch Foxboro magnetic flowmeter was installed in our system. The three parts of this flowmetering system are:

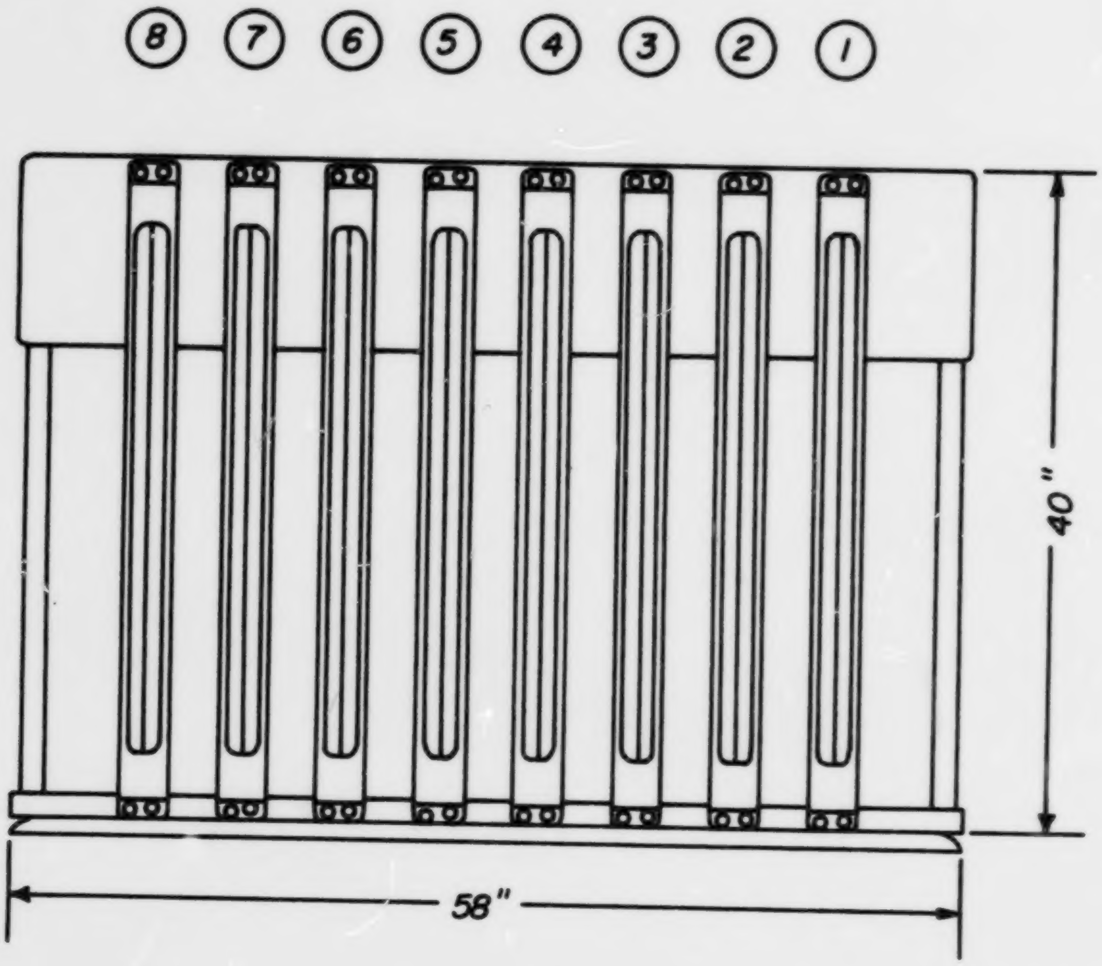
8
7
6
5
4
3
2
1
40"
58"

FIGURE 4. MANOMETER BANK

(I) Measuring Head; Foxboro Magnetic Flow Transmitter, type k802 SATS-BA, style B, size 2 inch, Material 304ss, Electrode 316ss, liner Teflon, 115 Volts, 60 cycles, 7.0 amps, 80 watts, parallel connection. Output: .05819 millivolt per GPM.

(II) Magnetic Flow to Current Converter Foxboro Model 696 with internal span switching

(III) Recorder: Foxboro Recorder Model 6410 HF, input 10-50 ma.

3.2-7. Pump, Motor, and Control

A centrifugal slurry pump made by Morris Machine works was used. The pump was a model 2JC8 with 3" I.D. suction, 2" I.D. discharge and 8-inch impeller diameter. Operated at 1780 RPM it is rated to develop 70 ft. of head. One of the special features of this pump was that the pump casing could be opened easily for cleaning in case of blockage with solids. No problems of this sort were encountered, however. The pump was coupled to a 5 HP variable speed induction motor, made by Delco Products. The motor specifications were 5 HP, DBB, Horizontal Foot Mounted, 3 Phase, 60 Cycle, 208 Volt Design D Motor in a 254 V Frame. The motor came with a solid state control panel which was used to provide the power to the motor and also the electronic controls for varying the motor speed. As mentioned earlier we could, in the setup used in the present work, control either the discharge pressure or the motor speed itself. It should be mentioned that we could add a 10 HP motor to our existing control panel, and also operate either the 5 HP and 10 HP in simplex or both in a duplex mode. The control panel specifications were 5 HP, OBB, 208V, Simplex V/Speed System with Tachometer for manual speed control. The pressure transducer was a Sostman Pressure Transducer, Model 3010-100 PG-5WH with a range of 0 to 1000 psig. Morris Machine Works did the coupling and mounting of the motor and pump on a steel base. In order to lubricate the packing of the pump thrust bearing we used a 2-oz. spring loaded grease cup filled with waterproof lubricant. A little water was allowed to flow through the bearing to prevent the grease from flowing into the circuit. This system was preferred to lubrication with water, because it avoided the flow of an unknown amount of water into the test loop.

3.3 Materials

The slurries used in our experiments consisted of glass beads suspended in water. Spheres made from two different glasses, having different densities, were used. In a preliminary set of experiments, reported earlier in Mauri's thesis (36), the 2-inch pipeline was used only, and the spheres had the following properties:

TABLE 3.1 - Properties of Glass Beads in Flow Experiments Using 2-inch Pipeline Only (36)

Average Diameter (microns)	Density gm/cc
48.8	2.451
214	2.455
314	2.454
475	2.481

Besides the experiments with the spheres listed in Table 3.1 in the 2-inch pipeline, flow experiments in the 2, 1, and 1/2-inch pipelines and the following glass spheres were performed:

TABLE 3.2 - Properties of Glass Beads in Flow Experiments Using 2, 1, and 1/2-inch Pipelines

Average Diameter (microns)	Density gm/cc
90	4.434
505	4.430
1015	4.400
475	2.486
1340	2.977
4380	2.964

CHAPTER IV

PROCEDURE AND EXPERIMENTS

4.1 Physical Properties

Aside from the determination of the densities of the manometer fluids and tap water at various temperatures about the ambient, size and density measurements for the glass beads were made.

4.1-1. Densities of Glass Beads

The densities of the glass beads were determined by displacement with distilled water using a calibrated, 50 ml, pycnometer. The procedure we followed entailed partially filling the pycnometer with distilled water and adding a pre-weighed quantity of the beads. The pycnometer was then filled completely with distilled water for a second weighing. Allowing the beads to settle through the distilled water in the partially pre-filled pycnometer seemed to prevent the entrapment of air bubbles. The glass beads used in the density determination were sampled as follows:

Approximately 200 ml of beads were removed from the entire batch, and this quantity of beads was divided into two parts. One part was returned to the container, while the other was retained. This procedure was repeated until the quantity of beads retained was suitable for the density of determination, i.e. approximately 25 ml. For each nominal sphere size used in our experiments only one determination of the density was made. The results of the density measurements are given in Tables 3.1 and 3.2.

4.1-2. Sizes of Glass Beads

To determine the size distribution of the spheres, the same sampling procedure described in the preceding section was used, though with a much smaller quantity of beads retained at the end.

The sphere sizes were determined using a microscope equipped with a micrometer vernier. The sample of spheres was laid on a slide and the cross hairs were focused on one edge of a given sphere and the micrometer reading recorded, and then with cross hairs focused on the opposite end of the same sphere the reading was taken again. For each sphere measured, two size determinations were made; one with the cross-hairs traversing the sphere in one direction, and the second with cross-hairs traversing the sphere in the reverse direction. This procedure helped to offset the effect of play in the micrometer screw. The micrometer vernier was checked using two spheres of accurately known diameter. The difference between the measured and known values of diameter was less than 0.5%. The traversing microscope method was used with those spheres of nominal size larger than 50µ. For the beads of nominal size 50µ, a more powerful microscope (eyepiece 7.5 X and objective 43 X) was used. On this microscope, made by American Optical Company, the eyepiece had a reticulum of which the subdivisions were checked against a micrometric segment (2 mm divided into 0.01 mm subdivisions). Two samples of about 200 beads each were obtained with the procedure already described and were used in the diameter determinations of each nominal size of spheres. However, on each sample only 10 spheres were measured, and this was done by measuring diameters of two groups of 5 neighboring spheres each in the sample. The two groups of spheres measured were in different positions in the field of view. Altogether the diameters of 20 different spheres of each size were measured. The procedure described above was used in obtaining the average sphere diameters listed in Table 3.1. A more complete listing of the individual diameter determinations is given in Appendix B-1.

In order to provide a more detailed picture concerning the diameter variations of the glass beads, the 4380μ beads listed in Table 3.2 were used in a somewhat more extensive determination, using the powerful microscope described previously. These beads have a size range, based on screening experiments, of 4000μ to 4760μ, which according to a simple averaging procedure would yield a value of 4380μ as given in Table 3.2. In this determination a sample consisting of 539 beads were measured. The results are shown plotted in Figure 5 as sphere diameter d_i against cumulative number percent of beads having diameters equal to or exceeding d_i. If we define n_i as the number of beads of diameter d_i, the number average diameter is given by

$$\bar{d}_n = \sum_i n_i d_i / \Sigma\, n_i \qquad (11)$$

Based on the data with the 539-bead sample the following results regarding variations in particle size are obtained:

(i) The maximum and minimum bead sizes in the sample are 4801μ and 3810μ, respectively.

(ii) The range $4039\mu \leq d_i \leq 4615\mu$ corresponds to cumulative number percent beads with diameter $\geq d_i$ of from 5% to 95%, i.e. 5% of the beads have $d_i \leq 4039\mu$, and 5% have $d_i \geq 4615\mu$.

(iii) The number average bead diameter, $\bar{d}_n$, is 4315μ.

(iv) The variation of bead sizes about the average diameter approximately obeys a normal distribution.

The fact that some of the particles are not spherical must be borne in mind in evaluating the results just presented. The marked departure from spherical shape of some of the particles accounts, to a large extent, for the discrepancy between the size range

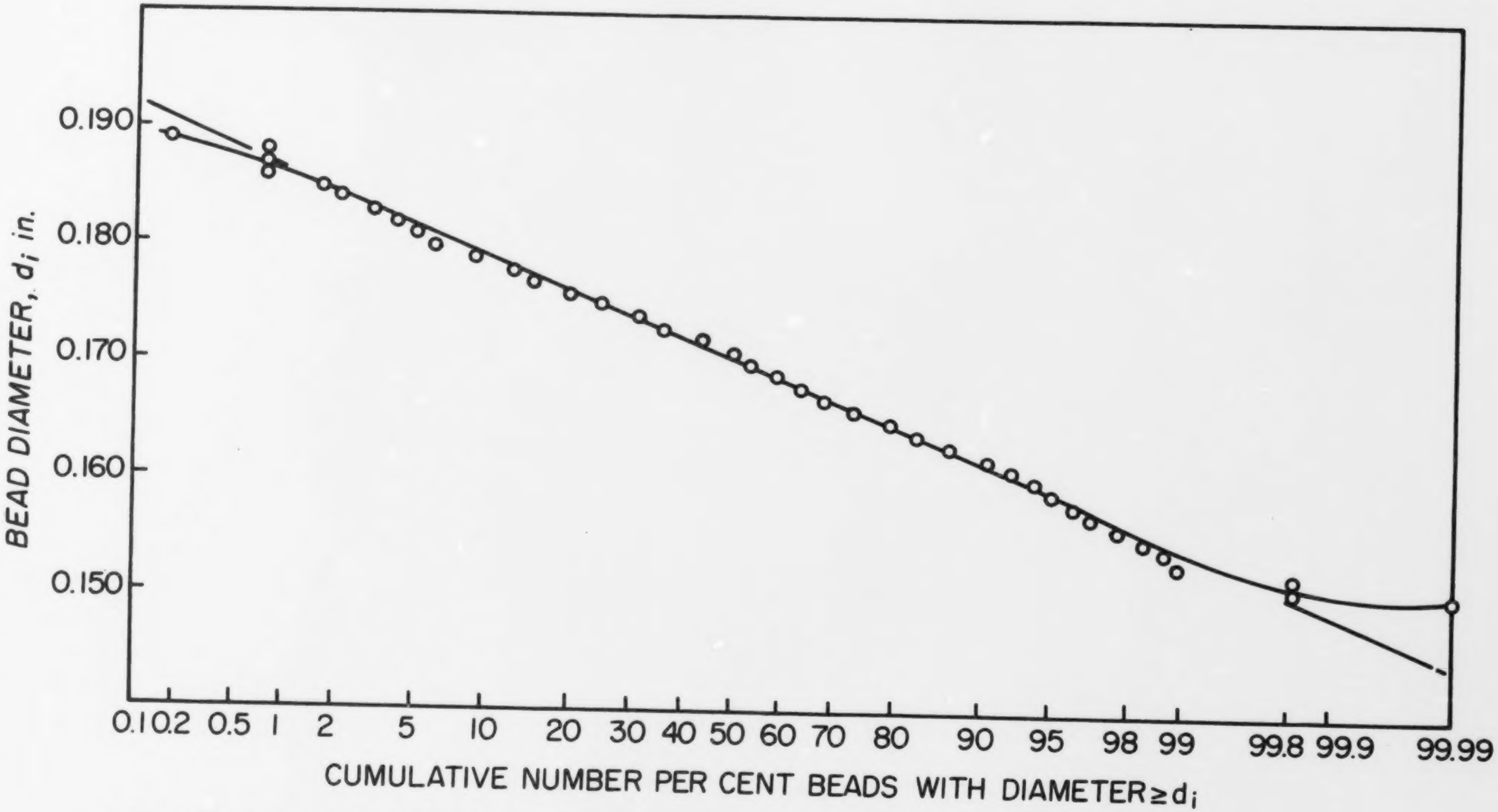

FIGURE 5. SIZE DISTRIBUTION FOR 4380μ SPHERES

4000μ - 4760μ, which is determined from screening measurements, and the range given in (i). The correspondence between the (4000μ-4760μ)-size range and the range given in (ii) is considerably closer and confirms our conclusions with respect to the presence of non-spherical particles. Under these circumstances, we chose to use as the mean particle size the average of the two limiting values obtained by screening, i.e. 4380μ. This value is quite close to the number average diameter given in (iii). The rest of the size data shown in Table 3.2 were determined in a similar fashion.

4.2 Operation of the Flow System and Experimental Procedure

4.2-1. Calibration of the Magnetic Flowmeter

The magnetic flowmeter was calibrated using the weigh tank and circulating water. The calibration was repeated using a slurry consisting of 214μ beads. It was found that on a volumetric basis the calibration of the flowmeter was not affected by the presence of solids. The magnetic flowmeter was used for measuring flowrates through the 2-inch pipeline only.

4.2-2. Charging and Recovery of Solids

For each bead size the flow experiments were carried out with the lowest solids concentration first. To increase the solids concentration additional amount of solids were added into the slurry reservoir. This was done while the slurry already present in the system was circulating. The charging of the initial slurry, i.e. the lowest concentration for each bead size, was done as follows. A measured quantity of water was poured into the reservoir tank. The liquid was circulated in the system by starting the pump, and the necessary quantity of solids was gradually poured into the reservoir while the mixer was running. The gradual addition of solids helps prevent any solid plugs from forming in the pump or other parts of the system, where they could obstruct the circulation. The system was operated in closed circuit in order to attain the highest possible flow rates without need of an excessively large quantity of slurry. Under these operating conditions attrition and grinding of the solids might become important if the circulation is maintained for long periods. In our case, however, these problems were not significant. No appreciable quantity of broken glass spheres was detected even though we often operated with the same slurry system intermittently over a period of several days using the same charge of beads.

It took several days to gather flow data for several concentrations for each size of beads. Clearly, it was quite convenient to be able to keep the same slurry in the system for several days, since to increase the concentration merely entailed adding the required quantity of solids. Before shutting off the system between experiments the slurry was diverted into the weigh tank with its bottom outlet valve shut. As the slurry filled the weigh tank, most of the solids settled at the bottom, and the liquid overflow returned to the reservoir through the two overflow outlets on the weigh tank and two additional removable siphon tubes. The circulation in this mode, i.e. with the weigh tank bottom outlet shut, was maintained until most of the solids were transferred into the weigh tank whereupon the system was shut off. To restart the system the mixing in the weigh tank and the circulation in the system were started, and the butterfly valve at the weigh tank bottom outlet was gradually opened, returning the bulk of the solids as a concentrated slurry back into circulation.

The procedure used for recovery of the beads after completion of the experiments entailed using graded filter bags of varying fineness depending on solid size. These filter bags made from Nylon by Afco Filter Products, were slipped on an adapter end of the 3-inch outlet pipe leading from the weigh tank into the reservoir. When the slurry was diverted into the weigh tank the solids were collected in the filter bag and the liquid filtered through back into the system. In this way it was possible to recover about 90% of the solids in the system.

4.2-3. Determination of Concentration

One disadvantage of operating a slurry flow system in closed circuit is that generally the concentration of solids coming out of the outlet pipe (discharge concentration), the concentration across any given cross-section of the pipe (spatial concentration), and the concentration originally charged to the system are all different. This is true even though the circulation has been maintained for a sufficiently long time for steady-state conditions, as indicated by the steadiness of the flow rate and pressure drops, to have been attained. Of course, the spatial and discharge concentrations are generally different even when the slurry flow system is operated on a once through feed basis. However, in this latter mode of operation it is possible to maintain the transport concentration fixed as the flow rate is varied, whereas in closed circuit operation one cannot do this. The observed difference between spatial and discharge concentrations is due to the fact that there is slip between solids and liquid, and that the concentration profile across any cross-section of the pipe is neither uniform nor symmetric (for a horizontal pipe) about the pipe axis. Furthermore, in closed circuit operation, accumulations of solids in insufficiently agitated regions of the flow system tend to aggravate this situation. Obviously, these effects are especially prominent for large density differences between solids and liquid, for larger particle sizes, and for lower flow rates.

4.2-3.a. Discharge Concentration

The discharge concentration was measured for each flow rate. For flow in the 2-inch pipeline, slurry samples were taken from the discharge end of the flow loop. The solids concentration was measured using calibrated graduated cylinders. For flow in the 1 and 1/2-inch pipelines, the discharge concentrations were measured by emptying the contents of the square plexiglas column, described in Section 3.1, through the column drain valve into a calibrated graduated cylinder allowing the water to flow over. Solids remaining in the column were rinsed down into the graduated cylinder by a spray of water.

4.2-3.b. Spatial Concentration

In the earlier series of experiments using the 2-inch pipeline only, measurements of the spatial concentration within the pipe were made. This was done by suddenly cutting off the flow in the removable section of the 2-inch flow loop, but the circulation was continued by simultaneously opening the bypass. The slurry in the removable section was flushed out into a graduated cylinder for measurement of solids volume. Since the volume of the material contained in the removable pipe section was known, the solids volume could be computed. The spatial concentration measurements were quite tedious, and they were not made in the second series of slurry experiments, in which all three test pipes, the 2, 1, and 1/2-inch lines, were used. The data for the 2-inch pipe are given in Appendix B-2.

4.3 Flow Experiments

4.3-1. Pressure Drop

Preceding each series of experiments with a given solid size, the pressure drop-flow rate data for water were taken. These data provided a periodic check on the procedure, and on whether the pipeline characteristics had been affected by the circulating slurries. The pressure drop-flow rate data for water in the 2, 1, and 1/2-inch pipelines are shown in Figures 6, 7, and 8, respectively. The temperature of the circulating water was recorded, and so was the ambient temperature.

The flow experiments with the slurries were carried out in the same way, and, in addition, the discharge concentration of solids was determined for each flow rate. To check on reproducibility the measurements at each flow rate were repeated, sometimes several times. These data are given in Appendix A

4.3-2. Critical Velocities

In the first series of experiments using the 2-inch pipeline only, we attempted to determine the critical velocity at which the solids in the pipe settle, forming a stationary bed with the flow taking place above the bed. This was done by slowing down the flow until bed formation occurred, and also by increasing the flow, starting from a low value, until the bed of solids was dispersed. The main difficulty associated with this measurement is undoubtedly the uncertainty in the interpretation of the observed flow regime in the pipe. Pressure drop and concentration determinations were made at the critical velocity. These measurements are tabulated in Appendix B-2.

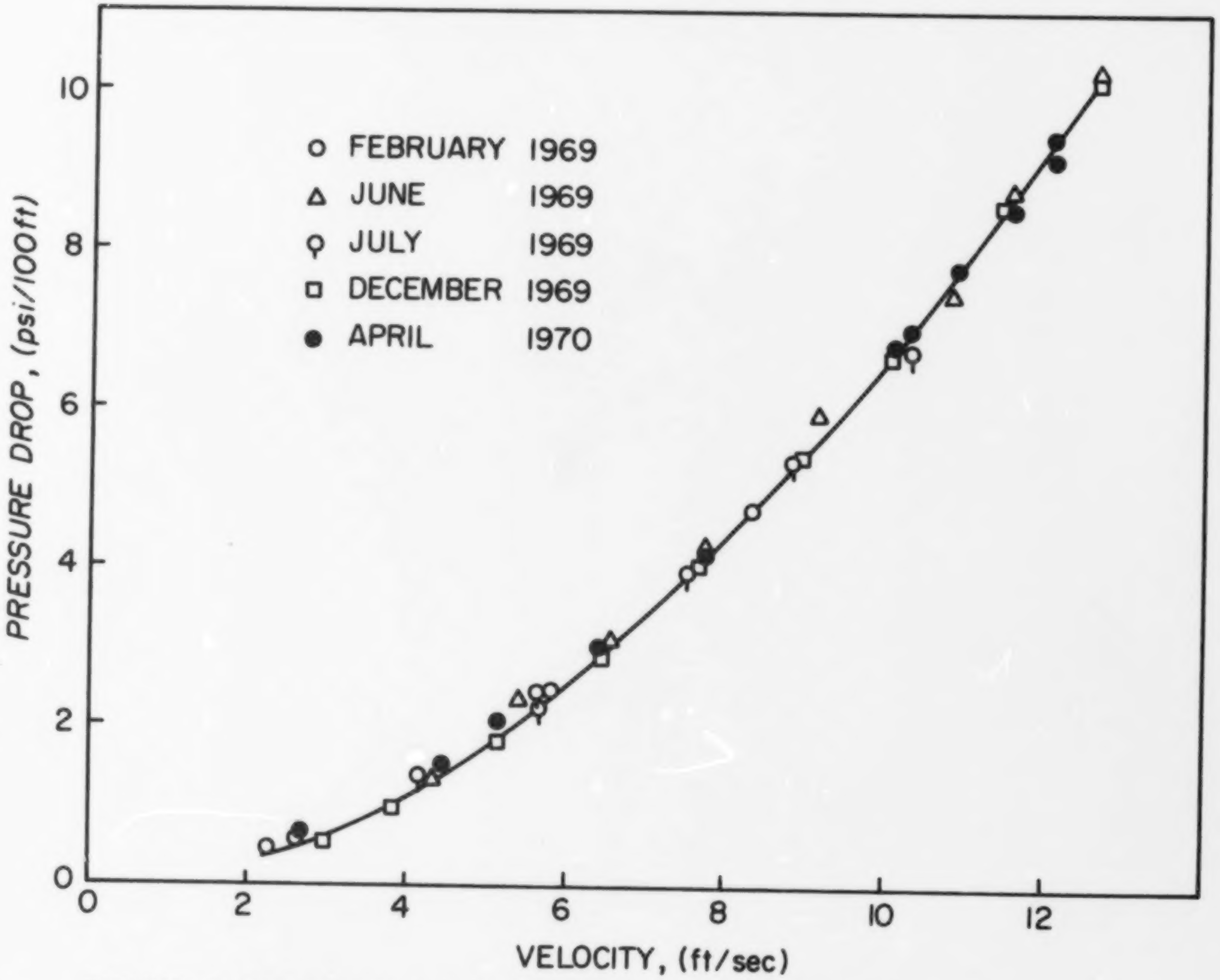

FIGURE 6. PRESSURE DROP - VELOCITY FOR WATER IN THE 2 INCH PIPE

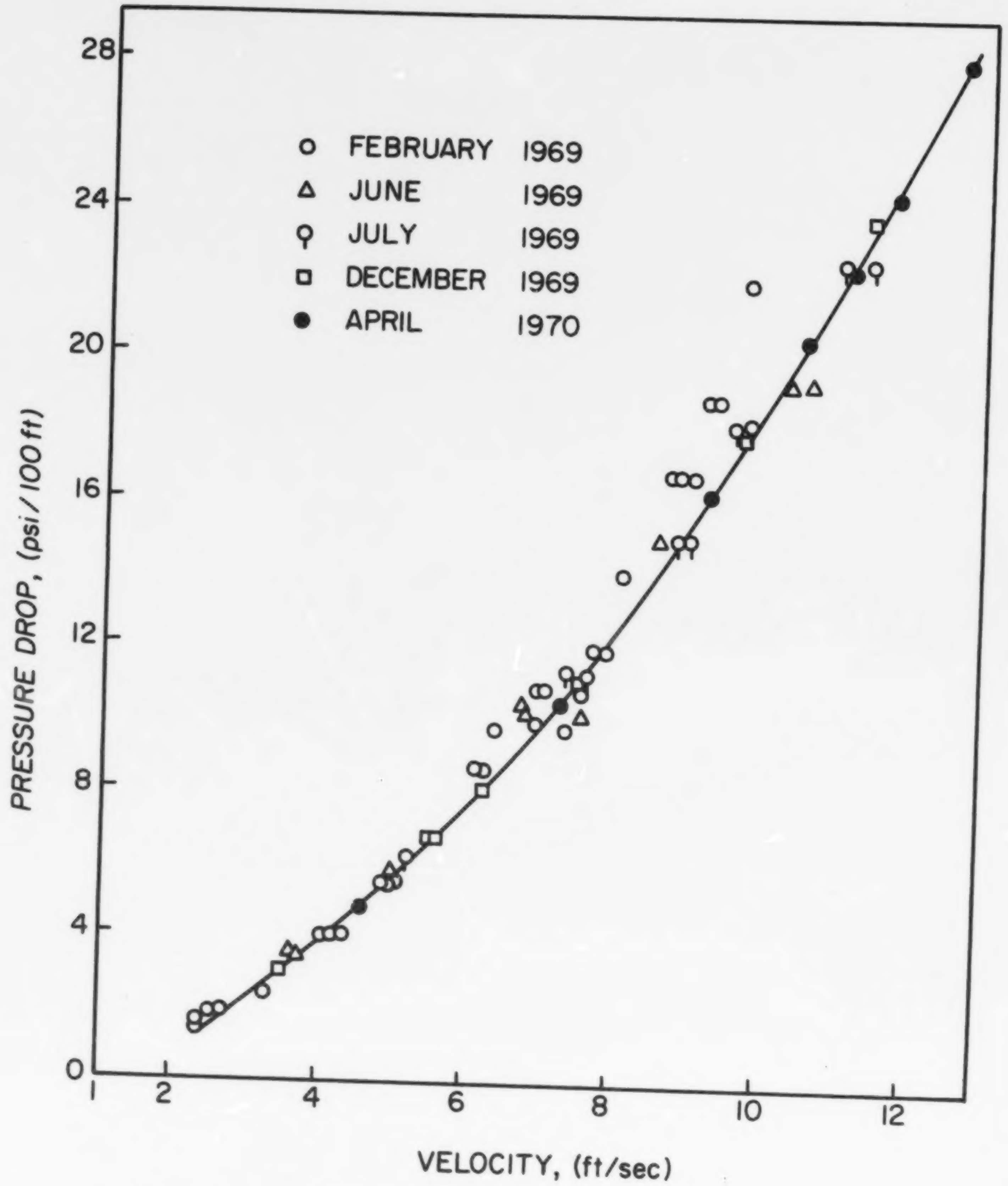

FIGURE 7. PRESSURE DROP - VELOCITY FOR WATER IN THE 1 INCH PIPE

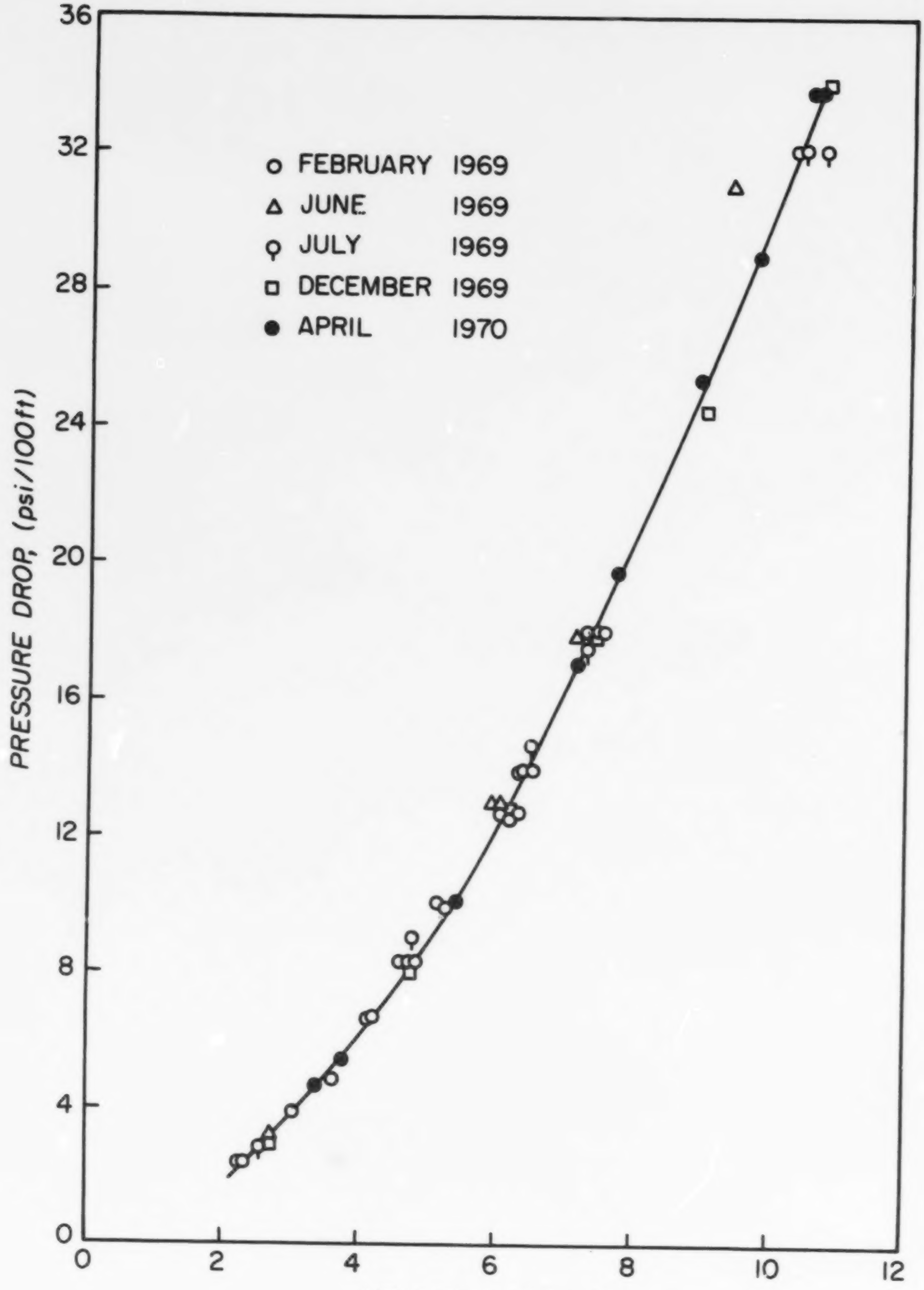

FIGURE 8. PRESSURE DROP - VELOCITY FOR WATER IN THE 1/2 INCH PIPE

CHAPTER V

EXPERIMENTAL RESULTS AND CORRELATIONS

5.1 Introduction

The results of the experiments described in the preceding chapter will be presented here. Two series of slurry flow data were taken in this research work; an early series of experiments in which the 2-inch pipeline only was used, followed by a more extensive series of experiments in which the 2, 1, and 1/2-inch pipelines were used. The data taken in the early series were of a more or less preliminary nature, but they included measurements of spatial concentration and critical velocity. These data are tabulated in Appendix B-2, and also in Mauri's thesis (36) where additional details may be found. The data from the second more extensive series of experiments are given in Appendix A, and were used in the slurry flow correlation presented here.

5.2 Critical Velocities

The critical velocity is defined here as the velocity at which a stationary deposit of solids forms in the pipe and the main flow takes place above this bed of solids. In our experiments the critical velocity was measured by decreasing the flow rate until a bed of solids was seen to form in the transparent section of the 2-inch line. In fact the value was estimated twice for each concentration of solids in the first series of experiments; the first value was obtained by approaching the critical condition from above (decreasing flow rate) and the second by approaching from below (increasing flow rate). These data are shown in Appendix B-2 together with the corresponding measurements for pressure drop. Table 5.1 lists the measured critical velocities together with estimates for V_c calculated using Equation (9) of Durand for concentrations equivalent to those used in our experiments.

TABLE 5.1 - Measured and Calculated Critical Slurry Velocities

Glass Beads μ	Charged Concentration wt.%	Critical Velocity (ft./sec.)		
		Experimental		Estimated Equation(9)
		(1)	(2)	
48.8	10	2.16	2.20	3
	15	2.96	2.16	
214	10	2.79	2.58	3.8
	20	3.99	3.64	
	25	2.90	2.03	
314	20	3.75	3.98	6
475	10	2.95	2.79	5
	20	2.93	2.93	
	30	2.69	2.33	

(1) Estimated by decreasing velocity to approach critical condition.
(2) Estimated by increasing velocity to approach critical condition.

The determination of the critical velocity is based upon observation of the flow under conditions in which, presumably, transitions in flow regime are taking place. The experimental data are difficult to get under these circumstances, and are subject to individual interpretation. In an attempt to preclude dependence of the critical velocity determinations on personal observation, an alternative procedure was used. At the critical condition the discharge concentration becomes vanishingly small. Accordingly, the ratio $[(i_m-i_w)/i_wC]$, defined in Chapter II, becomes very large under the same circumstances. Based on these considerations the inverse of this ratio was plotted against velocity, as shown in Figure 9, and the critical velocity was determined by extrapolating to the value $[i_wC/(i_m-i_w)] = 0$. For the slurries with sphere sizes of 214, 314, and 475μ the critical velocity obtained by this extrapolation procedure was between 2.2 and 2.4 ft./sec. The data for the 48.8μ spheres were not used, because due to scatter they could not be extrapolated with ease.

The foregoing comparisons demonstrate the elusive nature of the critical velocity, and the uncertainties surrounding its determination,

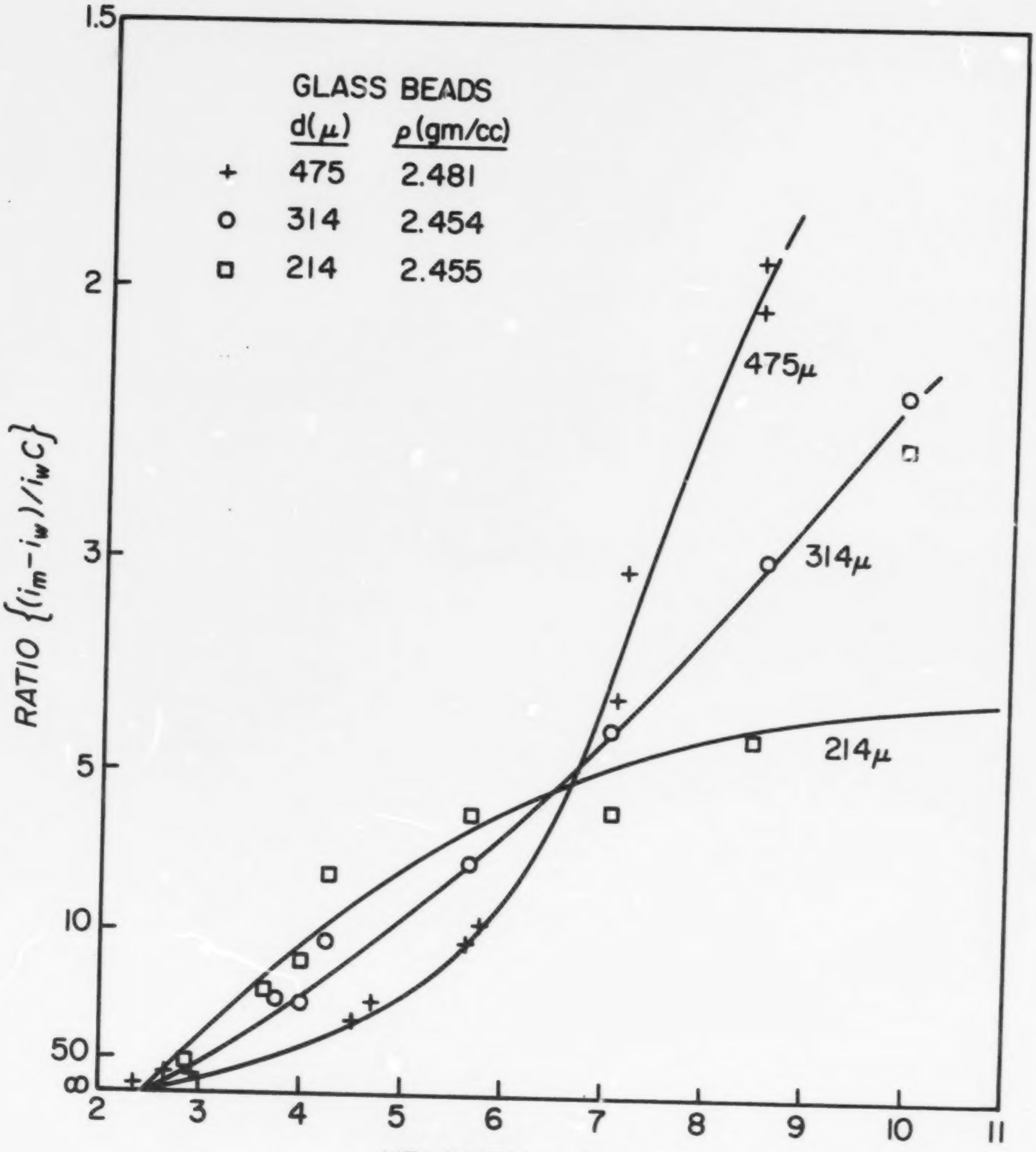

FIGURE 9. PLOT OF RECIPROCAL $\{(i_m - i_w)/i_w C\}$ AGAINST SLURRY VELOCITY

particularly through judgement based on observation of the flow patterns. These types of difficulties often arise with transitional phenomena of this sort. The extrapolation procedure represented by Figure 9 is not sufficiently satisfactory, or, more precisely perhaps, it is not yet demonstrably effective. However, the procedure demonstrates merely the type of approach that must be followed if an effective method to determine the critical velocity is to be developed, i.e. the determination should be based on a measure of the flow which is particularly sensitive to the type of flow regime prevailing. This may not be the ratio $[(i_m-i_w)/i_wC]$ that we have used. Besides there are no grounds for assuming that the flow regime, characterized by a stationary bed of solids in the pipe, is associated with a well-defined value of the flow velocity for any given system. Indeed transitions between flow regimes are, without any doubt, not so abrupt. The problem is, of course, intimately connected with the one of establishing overall criteria relating to the nature of the flow regime, and this, as has been pointed out with respect to even the very extensive work of Durand, remains unresolved.

5.3 Free Falling Velocity of Spheres

In order to use the slurry flow correlations developed in this work the free falling velocity of the solid spheres as well as the associated drag coefficient must be known. The flow past a sphere is a classical problem with an extensive literature. In a recently completed study in this laboratory relating to the settling of spheres in macromolecular solutions*, Carey (37) made extensive accurate measurements of the terminal velocities of spheres in Newtonian fluids. One of the aims of Carey's thesis research was to determine the extent of drag reduction for settling of spheres in very dilute solutions of viscoelastic materials, and, in particular, to predict the onset of the drag reduction. This latter aspect of the work, namely, the determination of the conditions under which the drag reduction phenomenon first appears, necessitates the use of very accurate Newtonian falling-sphere data for comparison. A comprehensive search of the literature revealed that, with few exceptions, the overwhelming body of available experimental work on settling of spheres in Newtonian fluids was unsuitable for this purpose. The two chronic main objections were that the data had been taken under conditions of poor temperature control, and that no provisions had been made for accounting for wall effects.

---

*The results of this work will be published by Carey and Turian. Only those aspects of the results pertaining to this report are summarized here.

Carey used two experimental setups; one for slow sphere velocities in which the fall times were determined visually, and the other for fast velocities in which the fall times were determined automatically using a photocell arrangement. The slow velocity apparatus consisted of five 15-inch thermostated cylindrical columns of various diameters, and the fast speed apparatus consisted of four 6-foot thermostated cylindrical plexiglas columns of various diameters. Using precision spheres ranging in size from 1/64 inch to 1-1/2 inches, made of materials as diversive as nylon, Teflon, glass, aluminum, ruby, steel, and tungsten carbide, together with distilled water and various concentrations of glycerine in water, the fall times were determined in two sections of the fall cylinder to insure attainment of terminal velocity. Each of these data were replicated five times. All the data were extrapolated to infinite cylinder diameter to obtain the free settling velocities in an unbounded medium.

These free settling velocity data are shown in Figure 10. The plot includes the data of Bacon (38) and McPherson (39), who also carried out experiments under carefully controlled conditions, but as shown in Figure 10,

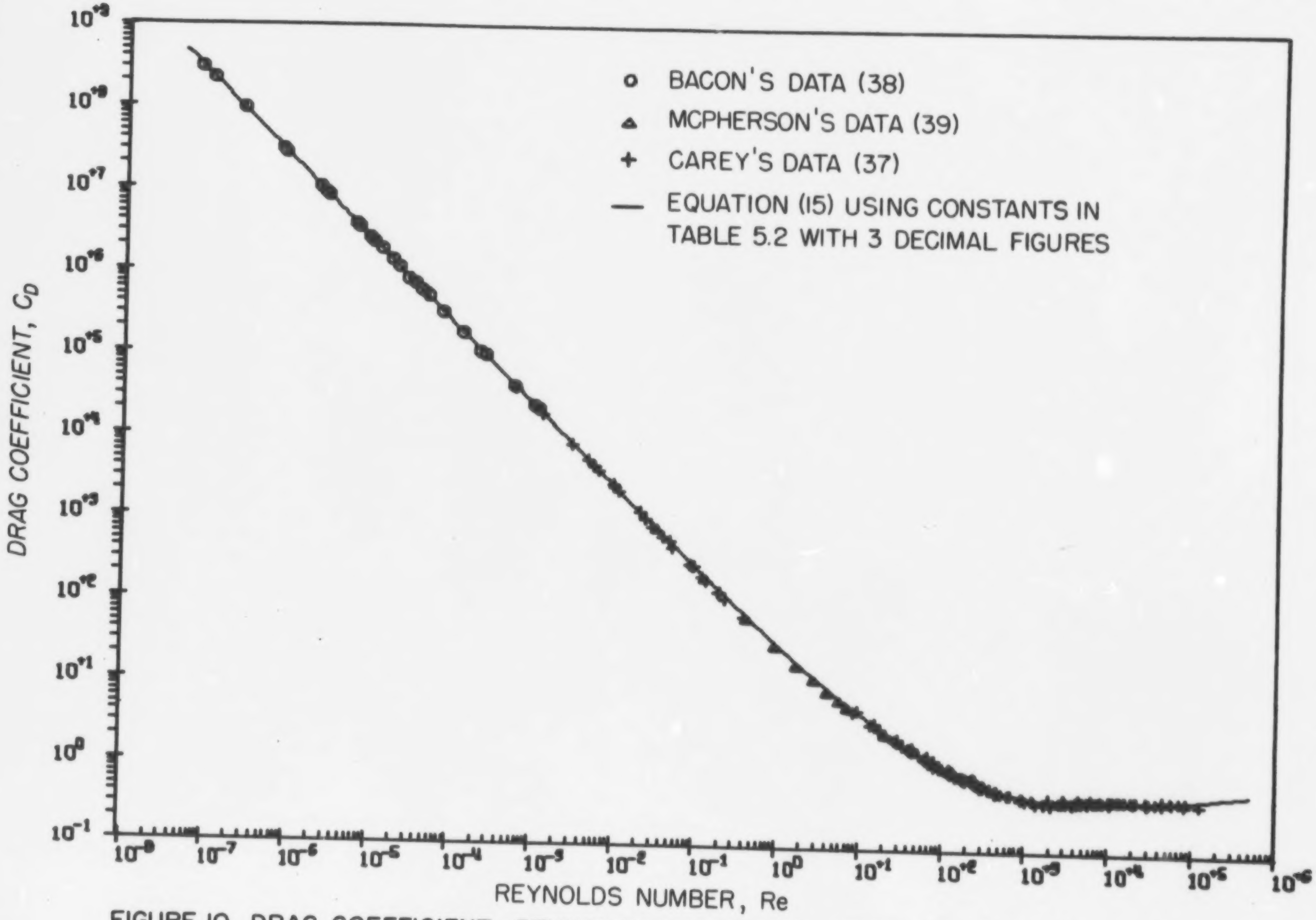

FIGURE 10. DRAG COEFFICIENT - REYNOLDS NUMBER RELATION FOR SOLID SPHERES SETTLING IN UNBOUNDED NEWTONIAN FLUIDS

over limited ranges of the Reynolds number*. The definitions of the drag coefficient, C_D, and the Reynolds number, Re, used in this plot are

$$C_D = \frac{4}{3} \frac{gd(\rho_s - \rho_\ell)}{\rho_\ell v_\infty^2} = \frac{4}{3} \frac{gd(s-1)}{v_\infty^2} \tag{12}$$

and

$$Re = \frac{d \rho_\ell v_\infty}{\mu} \tag{13}$$

in which

g = the gravitational constant,

d = the diameter of the sphere,

v_∞ = the terminal velocity of the sphere in an unbounded medium,

ρ_s = the density of the sphere,

ρ_ℓ = the density of the liquid,

μ = the viscosity of the liquid, and

s = ρ_s/ρ_ℓ, ratio of solid to liquid densities.

Because of the extensive Reynolds number range (almost 14 cycles), it would be convenient to express the information contained in Figure 10 in an analytical form. Carey developed the empirical relation

$$Re\, C_D^{1/2} = (24\, Re)^{1/2} + A_1 Re \left\{ Re^{A_2} + \frac{1}{A_3 + A_4 Re} \right\} \tag{14}$$

in which the constants A_i (i=1, 2, 3, 4) were evaluated by a nonlinear least squares scheme using the total number of 210 data points in Figure 10. These values are shown in Table 5.2, where the first and second sets of values apply when five decimal places and three decimal places are retained in the calculations, respectively. In the form depicted by Equation (14) the term ($Re\ C_D^{1/2}$) does not involve the sphere velocity explicitly. The relation between C_D and Re, which is the one shown in Figure 10, can be derived easily from Equation (14). It is given by

---

*Because of the large number of data (210 points) and the extensive Reynolds number range (14 cycles) the plot in Figure 10 was drawn using a Calcomp Plotter driven by an IBM 360/50 Computer. The solid line represents Equation (15), and its slightly jagged nature arises from the limitations of resolution attainable on this plotting system. The same system was used for plotting the data points in Figures 11, 12, and 13 which contain up to 1511 points.

$$C_D = \left\{ \left(\frac{24}{Re}\right)^{1/2} + A_1 \left(Re^{A_2} + \frac{1}{A_3 + A_4 Re}\right) \right\}^2 \qquad (15)$$

TABLE 5.2 - Constants for Equations (14) and (15)

i	A_i	
	5 Decimal Places	3 Decimal Places
1	0.34035	0.340
2	0.06071	0.060
3	1.72013	1.720
4	0.01800	0.018

It is important to point out how well the empirical expressions given by Equations (14) and (15) describe the data. The absolute average error in the value of ($Re\ C_D^{1/2}$), as calculated from Equation (14) using the constants A_i to five decimal places, is 1.87% for the 210 data points, while the maximum error is 9.54%, and is associated with the highest value of Re measured ($Re = 1.275 \times 10^5$). When the constants A_i to three decimal places are used with Equation (14) the absolute average error increases to 1.92%, while the maximum error decreases to 8.54% and is again associated with $Re = 1.275 \times 10^5$. The absolute average error in the value of C_D, as calculated from Equation (15) using the constants A_i to five decimal places, is 3.73% with a maximum error of 19.88% at $Re = 1.275 \times 10^5$. Furthermore, of the total number of 210 data points the error for only 11 points exceeds 10% with the remaining 199 data points having errors below 10%. When the constants to three decimal places are used in Equation (15) to calculate C_D, the absolute average error increases to 3.83%, the maximum error (at $Re = 1.275 \times 10^5$) decreases to 17.72%, and the number of data points with errors in excess of 10% increases to 12.

From the foregoing results we conclude that Equations (14) and (15) can be used to calculate results relating to the free settling of spheres in Newtonian fluids. In fact these equations describe the falling sphere data to a level of accuracy considerably surpassing that which may be required for use with slurry flow correlations, and the relatively simple forms of these equations are valid over an enormous (certainly unprecedented) range of the Reynolds number. However, they should not be used for calculations at Reynolds numbers exceeding 1.5×10^5 inasmuch as the so-called "drag crisis", relating to an abrupt drop in the drag coefficient, occurs in the neighborhood of $Re = 2.5 \times 10^5$. The forms of Equations (14) and (15) could be modified, of course, to extend the range beyond $Re = 1.5 \times 10^5$, but available data pertaining to these higher Reynolds numbers have usually been taken in wind tunnel experiments with varying levels of turbulent intensities. The turbulent intensity of the stream affects the drag force, and must, therefore, be considered in the interpretation of the data. None of the solids that might conceivably be transported hydraulically would have a free fall velocity exceeding the range represented by Equations (14) and (15), and this limitation is, therefore, of no consequence.

The value of the settling velocity of a single solid particle, v_∞, must be calculated for use with existing slurry correlations, and also with the correlations developed in this work. Of course Equation (14) can be used for this purpose because the term ($Re\ C_D^{1/2}$), as stated previously, does not contain v_∞, but the calculation must be carried out by trial and error, or by means of a Newton-Raphson iteration. In order to avoid the need for trial and error calculations, and, more importantly, to provide equations which can be used in straightforward and simple calculations, the drag coefficient relationship was expressed in the following different empirical form:

$$\log_{10}\mathrm{Re} = a_o + a_1\log_{10}\Lambda + a_2(\log_{10}\Lambda)^2$$

$$+ a_3(\log_{10}\Lambda)^3 + a_4(\log_{10}\Lambda)^4 + a_5(\log_{10}\Lambda)^5 \qquad (16)$$

In Equation (16) we have used

$$\Lambda = \mathrm{Re}\ C_D^{1/2} = \left\{\frac{4}{3}\ \frac{gd^3\rho_\ell(\rho_s-\rho_\ell)}{\mu^2}\right\}^{1/2} \qquad (17)$$

The constants a_i were evaluated by a nonlinear least squares scheme applied to Equation (16). These results are listed in Table 5.3. Two sets of constants are shown in this table; one set obtained by retaining seven significant figures, and the second by rounding off the values in the first set to three significant figures.

TABLE 5.3 - Constants for Equation (16)

i	a_i	
	7 Significant Figures	Rounded to 3 Significant Figures
0	-1.379270	-1.38
1	1.937020	1.94
2	-8.599308×10^{-2}	-8.60×10^{-2}
3	-2.516838×10^{-2}	-2.52×10^{-2}
4	9.185859×10^{-4}	9.19×10^{-4}
5	5.346710×10^{-4}	5.35×10^{-4}

If we define the percent error by

$$\%\ \mathrm{Error} = \frac{C_{D\mathrm{calc.}} - C_{D\mathrm{exp.}}}{C_{D\mathrm{calc.}}} \times 100 \qquad (18)$$

then the absolute average error using Equation (16) with the constants in Table 5.3 including all seven significant figures, is 2.68% for the 210 data points, and the maximum error is 11.83%. When the constants rounded to three significant figures are used the absolute average error becomes 3.12%, and the maximum error increases to 12.87%.

5.4 Pipe Flow of Homogeneous Liquids

Homogeneous liquid pipe flow correlations, analogous to those obtained in the preceding section for falling spheres, would permit straightforward calculations to be possible with the slurry flow correlations to be presented in the next section. For fully-developed laminar flow the Hagen-Poiseuille law applies. For the more prevalent case of turbulent flow the Blasius equation

$$f_w = 0.0791(Re_w)^{-1/4} \tag{19}$$

may be used. In Equation (19) the friction factor, f_w, and the Reynolds number, Re_w, relating to the homogeneous liquid (water) are defined by

$$f_w = \frac{\Delta p_w}{2\ \rho_\ell V^2}\ \frac{D}{L} \tag{20}$$

$$Re_w = \frac{D\ \rho_\ell V}{\mu} \tag{21}$$

where Δp_w is the pressure drop observed when the homogeneous suspending liquid is flowing in a circular pipe of diameter D, and length L at the velocity V. ρ_ℓ and μ are the density and viscosity of the liquid, respectively.

Blasius' Equation (19) is approximate, and in order to get a better description of the $f_w(Re_w)$ relation for the pipes used in the slurry flow studies we will be concerned with, we developed alternative expressions which gave closer fits to the data. Using the curves in Figures 6, 7, and 8 for water flowing in our 2, 1, and 1/2-inch pipelines, respectively, we obtain the following relations:

$$\text{2-inch pipe:}\quad \log_{10} f_w = -\ 1.306\ -\ 0.2044\ \log_{10} Re_w \tag{22}$$

$$\text{1-inch pipe:}\quad \log_{10} f_w = -\ 0.8395 - 0.2899\ \log_{10} Re_w \tag{23}$$

$$\text{1/2-inch pipe:}\quad \log_{10} f_w = -\ 0.9912 - 0.2640\ \log_{10} Re_w \tag{24}$$

Equations (22), (23) and (24) describe their respective curves in Figures 6, 7 and 8 with deviations not exceeding 1.5%. In addition to our own slurry flow data we have used the data reported by Murphy, Young, and Burian (40). They used only a 1/2-inch pipe and their water data can be represented by

$$\log_{10} f_w = -0.5201 - 0.5137 \log_{10} Re_w + 0.02942(\log_{10} Re_w)^2 \qquad (25)$$

Equation (25) describes the 1/2-inch water data of Murphy et al with an absolute average deviation of 0.82% and a maximum deviation of 3.51%.

There are other expressions for describing $f_w(Re_w)$, or the equivalent relation, for homogeneous pipe flow; the most famous being Prandtl's resistance law

$$\frac{1}{\sqrt{f_w}} = 4.0 \log_{10}(Re_w \sqrt{f_w}) - 0.40 \qquad (26)$$

The problem relating to pipe flow in the absence of suspended matter has been studied exhaustively, of course. We will not dwell further upon this subject here, since our aim in this section was to describe the particular empirical expressions for water flow that we will be using in subsequent analyses; the foregoing results fulfill this objective.

5.5 Slurry Flow Correlation

The complicated nature of the pipeline flow of suspended solids has already been discussed. It is instructive to enumerate the different variables which govern this type of flow, as shown in Table 5.4, which also includes their dimensions in terms of the fundamental units of mass (M), length (L) and time (T). Obviously, we are restricting the discussion to isothermal conditions, which have been implicitly assumed throughout.

TABLE 5.4 - Variables Relating to Pipeline Flow of Suspended Solids

No.	Variable	Description	Dimensions
1.	Δp	Pressure Drop	$ML^{-1}T^{-2}$
2.	L	Pipe Length	L
3.	D	Inside Diameter of Pipe	L
4.	V	Slurry Velocity	LT^{-1}
5.	ρ_ℓ	Liquid Density	ML^{-3}
6.	μ	Liquid Viscosity	$ML^{-1}T^{-1}$
7.	ρ_s	Suspended Particle Density	ML^{-3}
8.	d	Mean Particle Diameter	L
9.	ψ	Particle Size Distribution Function	--
10.	C	Concentration of Solids by Volume	--
11.	ε	Shape Factor for Particles	--
12.	g	Acceleration of Gravity	LT^{-2}

In the listing in Table 5.4, we have excluded pipeline roughness and solids density distribution for suspended solids of mixed densities.

The total number of 12 variables can be reduced to nine independent dimensionless groups which can be used to display their functional dependence. One way of expressing this, is through a relation of the type

$$f = \frac{\Delta p}{2\,\rho_\ell V^2}\,\frac{D}{L} = \phi\left[\frac{D\,\rho_\ell V}{\mu},\ \frac{d\,\rho_\ell V}{\mu},\ \frac{L}{D},\ \frac{\rho_s}{\rho_\ell},\ \frac{V^2}{gD},\ C,\ \psi,\ \varepsilon\right] \tag{27}$$

Under some conditions, certain simplifications can be made in Equation (27). For example, if the pipe length is large the dependence on the (L/D) ratio becomes insignificant, and this term can be dropped. The entrance length requirements, unlike the case for flow in the absence of solids, are not known for slurry flows, and their possible influence must be ascertained by measurement of axial variations in pressure drop. A few other simplifications in the dependence depicted by Equation (27) will accrue upon imposition of various restrictions, and these include the dropping of the dependence on ψ for iso-dimensional particles, and ε for spherical solids.

For fully developed pipe flow in the absence of suspended materials all but the first dimensionless groups on the right hand side of Equation (27) can be dropped. For fully developed pipe flow of a suspension composed of identical spherical solid particles, the dimensionless groups which can be dropped are (L/D), ψ and ε; the possible dependence on the so-called Froude number, (V^2/gD), must, unlike the case in the absence of solids, be retained. Accordingly, for this case Equation (27) takes the form

$$f = \frac{\Delta p}{2\,\rho_\ell V^2}\,\frac{D}{L} = \tilde{\phi}\left[\frac{D\,\rho_\ell V}{\mu}, \frac{d\,\rho_\ell V}{\mu}, \frac{\rho_s}{\rho_\ell}, \frac{V^2}{gD}, C\right] \tag{28}$$

Despite the substantial reduction in the number of variables in going from Equation (27) to Equation (28), the functional dependence is still unknown. A purely experimental approach designed to establish the relationship stated in Equation (28), even for modest ranges of the dimensionless groups appearing, would entail so massive an effort as to be impracticable. In addition, the dimensionless groups appearing on the right hand side of Equation (28), although they are quite legitimate choices for defining the problem in a general sense, do not, on the whole, bear an obvious relationship to the friction loss. An entirely different approach is utilized in this work, and it will be described following a brief discussion of the relationship between the flow of suspended solids and the free settling velocity of a single particle.

As might already have been suspected, information relating to the free settling of single solid particles will be incorporated in the slurry flow correlation developed in this work. The free settling velocity, v_∞, of a solid sphere of diameter d and density ρ_s in a fluid of viscosity μ and density ρ_ℓ does not appear in any of the groups in Equation (27) or (28). It will be shown that the dimensionless groups in these equations are sufficient to define fully the quantity Λ given by Equation (17), and, therefore, using the results in Section 5.3, the drag coefficient, C_D, and the corresponding Reynolds, Re, for this flow are also fully defined*. It will be convenient to use the definitions

$$X_1 = \frac{D\,\rho_\ell V}{\mu} \; ; \; X_2 = \frac{d\,\rho_\ell V}{\mu} \; ; \; X_3 = \frac{\rho_s}{\rho_\ell} \; ; \; X_4 = \frac{V^2}{gD} \qquad (29)$$

Using these definitions and Equation (17), Λ is given by

$$\Lambda = \text{Re}\; C_D^{1/2} = \left\{ \frac{4}{3} \; \frac{X_2^3}{X_1 X_4} \,(X_3 - 1) \right\}^{1/2} \qquad (30)$$

Equation (30) provides the connection between the general friction loss relationship depicted in Equation (28), and the drag coefficient-Reynolds number dependence for the single particle.

We now proceed to a discussion of the slurry flow correlation. The idea behind our approach is quite simple. The starting point is to consider the various forces involved in the pipeline flow of a slurry, and to represent these, or more correctly, quantities related to their orders of magnitude in the flow by suitable mathematical expressions. Next, we form dimensionless ratios among these various terms, and assume that the friction loss factor, f, for the slurry is a function of these ratios, and also of additional variables which are known, or presumed, to be pertinent. The final steps involve establishing a correlation, by curve-fitting, which is consistent with the experimental data.

In accordance with the foregoing idea, we consider the inertial and viscous forces relating to the flow, and the gravitational force on the suspended solids. We assume that the order of magnitude of the inertial force, F_I, and viscous force, F_V, are depicted by the relations

---

*The settling velocity, v_∞, per se cannot be defined without additional specific information inasmuch as it is dimensional.

$$F_I \sim \rho_\ell V^2/D \tag{31}$$

$$F_V \sim \mu\ V/D^2 \tag{32}$$

where the symbol $\sim$ is used to designate an ordering statement; no equality being implied, or for that matter necessary. Furthermore, these relations are expressed in terms of the density, ρ_ℓ, and the viscosity, μ, of the suspending liquid. It is very important to recognize that the statements depicted in Equations (31) and (32) relate to forces per unit volume, while the net force of gravity and buoyancy on the solid, F_D, represented by

$$F_D \sim \frac{\pi}{6} d^3 g\ (\rho_s - \rho_\ell) \tag{33}$$

is based on the particle volume. The force ratios are:

$$F_I/F_V = \frac{D\ \rho_\ell V}{\mu} = Re_w \tag{34}$$

$$F_D/(\frac{\pi}{6} d^3 F_I) = \frac{g(\rho_s - \rho_\ell)}{\rho_\ell V^2} = \frac{g(s-1)D}{V^2} \tag{35}$$

The first ratio is the Reynolds number for the pure liquid with density ρ_ℓ and viscosity μ flowing at the suspension velocity V. In the second ratio we have taken into account the fact that F_I and F_D are defined relative to different bases, as previously mentioned.

We postulate that the friction factor, f, for the slurry depends on the dimensionless ratios (34) and (35), on the drag coefficient C_D defined in Equation (12), and the discharge concentration, C, of suspended solids. The inclusion of the drag coefficient, C_D, for single free falling spheres reflects our desire to account, in some way, for slurry settling effects. The fate of a single particle in the pipe, where it is surrounded by other particles in a shear field, is, of course, vastly different from that of a single sphere settling in a quiescent unbounded fluid. However, in the absence of knowledge pertaining to the true situation, this choice is inevitable, and, moreover, it has a rather appealing feature; it is a well defined quantity and can be determined readily. It should be emphasized that C_D is independent of the quantity defined in Equation (35). Thus, the slurry friction factor, f, is taken to have the functional representation given by

$$f = \frac{\Delta p}{2\,\rho_\ell V^2}\,\frac{D}{L} = \bar{F}\left[\mathrm{Re}_w\,,\ C_D\,,\ \frac{g(s-1)D}{V^2}\,,\ C\right]$$

$$= F\left[f_w(\mathrm{Re}_w)\,,\ C_D\,,\ \frac{g(s-1)D}{V^2}\,,\ C\right] \qquad (36)$$

In the second functional form of Equation (36), we have replaced the Reynolds number for the liquid in the absence of solids, Re_w, by its corresponding friction factor, f_w; a permissible step because Re_w defines f_w completely (we exclude possible ambiguities associated with the laminar-turbulent transition here), and an appropriate one because the overall relationship itself pertains to the friction factor.

We must now assume a specific functional form for Equation (36) which, in the absence of solids (C=0), reduces to the value f_w. The form we chose is given by

$$f - f_w = K\,C^{\alpha}\,f_w^{\beta}\,C_D^{\gamma}\left\{\frac{g(s-1)D}{V^2}\right\}^{\delta} \qquad (37)$$

The constants K, α, β, γ and δ were determined by means of nonlinear least squares using Equation (37) together with 1511 data points. The concentration C used in this equation is the discharge concentration, and C_D was calculated using Equation (16), and the definition $C_D = \Lambda^2/\mathrm{Re}^2$. The least squares adjusted values of the correlation constants are listed in Table 5.5, in which the second set represents values rounded to four significant figures.

TABLE 5.5 - Constants for Equation (37)

	7 Significant Figures	Rounded to 4 Significant Figures
K	0.3202320	0.3202
α	0.4925438	0.4925
β	0.5586016	0.5586
γ	-0.1094677	-0.1095
δ	0.9002440	0.9002

The total collection of 1511 data points consisted of 917 data taken in this work, and 594 from Murphy, Young, and Burian's (40) report. Our own data were taken using water suspensions of the solids listed in Table 3.2 in 2, 1, and 1/2-inch pipelines. The complete set of data pertaining to the solids listed in Table 3.2 is presented in Appendix A. For our own data, the values of f_w for use in Equation (37) were calculated from Equations (22), (23) and (24) which represent the flow data for water in the 2-inch, 1-inch and 1/2-inch pipes. Murphy et al used only a 1/2-inch pipe, but made tests on a large number of slurries as shown in Table 5.6. The value of f_w for use with their data was calculated from Equation (25), which represents the curve fit for their water data. We should point out that the apparent discrepancy between the total number of 631 data points, shown in Table 5.6, and the 594 data points we used, can be explained by the fact that for 37 data points in Murphy and his co-worker's report the value of $(f-f_w)$ was negative. These data are probably in error, and are, at any rate, inconsistent with the overwhelming body of their data. Moreover, as will be explained later, in obtaining the initial guesses for computation of the constants in Equation (37) the least squares adjusted values based on the linearized form of this equation were first calculated. The linearization entailed taking the logarithm of both sides of the equation which precluded negative arguments entirely.

In the nonlinear least squares scheme for determining the constants

TABLE 5.6 - Solid Particles Used in Suspension Flow Experiments in 1/2-inch Pipeline by Murphy, Young, and Burian (40)

Material	Diameter (μ)	Density gm/cc	Max.Discharge Conc.wt.%	No. of Data
Glass	31.0	2.344	10.0	6
	50.8	2.344	27.5	14
	66.0	2.790	34.8	81
	289.6	2.851	48.5	155
	797.6	2.504	59.6	86
Steel	378.5	7.503	47.8	71
	1834	7.503	30.5	46
Lead	1283	11.30	63.8	172

Total No. of Data = 631

in Equation (37) initial estimates for the constants are needed. We derived these initial guesses by applying the least squares computation to the following linearized form of the equation:

$$\log(f-f_w) = \log K^o + \alpha^o \log C + \beta^o \log f_w$$

$$+ \gamma^o \log C_D + \delta^o \log \left\{ \frac{g(s-1)D}{V^2} \right\} \qquad (38)$$

where the o superscript designates that the constants, computed using the linearized form, are to be considered as initial estimates. The values of the least squares adjusted constants for the linearized form are shown in Table 5.7.

TABLE 5.7 - Values of Constants Obtained by Least Squares Scheme Using the Linearized Equation (38)

	7 Significant Figures	4 Significant Figures
K^o	0.4549952×10^{-1}	0.4549×10^{-1}
α^o	0.8265064	0.8265
β^o	0.4737177	0.4737
γ^o	0.1025866	0.1025
δ^o	1.116589	1.116

The comparison between the data and Equation (38) using the constants in Table 5.7, pertaining to the linearized form, is shown in Figure 11. Defining the percent deviation by

$$\%\ \text{Deviation} = \frac{f_{exp.} - f_{calc.}}{f_{calc.}} \times 100 \qquad (39)$$

the absolute average deviation for all the data points is 13.97%, but 191 data points have a deviation exceeding 30%, and of these 122 have a deviation exceeding 50%. Precisely the same results, relating to percentage deviations, are obtained when the constants shown in Table 5.7 are truncated to four significant figures. These comparisons demonstrate that the constants computed by the least squares adjustment performed on the linearized form given by Equation (38) do not provide a sufficiently satisfactory agreement with the data.

In the nonlinear least squares analysis applied to the form given by Equation (37) using the entire set of 1511 data points, we used the constants listed in Table 5.7 as initial estimates in the computations. The values of the nonlinear least squares adjusted constants are shown in Table 5.5. Equation (37) with the constants given in Table 5.5 is represented by the straight line segment labelled $(f-f_w) = K\xi$ in Figure 12, where

$$\xi = C^{\alpha} f_w^{\beta} C_D^{\gamma} \left\{ \frac{g(s-1)D}{V^2} \right\}^{\delta} \tag{40}$$

The comparison of the line $(f-f_w) = K\xi$ with the actual data, depicted in Figure 12, shows that in the nonlinear least squares computations the data pertaining to the range $\xi > 1$ are weighted somewhat more heavily than those falling in the range $\xi < 1$. In order to circumvent this, we devised the following alternative correlation:

$$f-f_w = K\xi \qquad \text{for } \xi \geq 1 \tag{41}$$

and

$$f-f_w = K\xi^{1.358} \qquad \text{for } \xi < 1 \tag{42}$$

where ξ is defined by Equation (40) with K, α, β, γ, and δ given in Table 5.5. In obtaining Equation (42), pertaining to the range $\xi < 1$, we simply drew a straight line through the center of the black mass of data for this range in Figure 12, and determined its slope. Therefore, in using the set of equations for either range of ξ the same set of constants, namely, those listed in Table 5.5, is used.

Using the percentage deviation definition in Equation (39), the correlation represented by Equations (41) and (42) gives an absolute average deviation of 9.54% for all 1511 data points, with 74 data points having a deviation exceeding 30%, and only 9 points having deviations exceeding 50%. Moreover, the same results relating to percentage deviation are obtained regardless of whether the correlation constants K, α, β, γ, and δ are taken to seven or four significant figures. We present in Figure 13 a comparison between the correlation and our own data only. The comparison does not show any significant difference between our data, and the entire set shown in Figure 12.

5.6 Summary

A brief summary of the principal results obtained in this work, and discussed in detail in the preceding sections, is presented here.

The friction loss factor correlation for the flow of slurries in pipelines developed in this work is represented by

$$f = f_w + K\xi \qquad \text{for } \xi \geq 1 \qquad (41)$$

$$f = f_w + K\xi^{1.358} \qquad \text{for } \xi < 1$$

with

$$\xi = C^{\alpha} f_w^{\beta} C_D^{\gamma} \left\{ \frac{g(s-1)D}{V^2} \right\}^{\delta} \qquad (40)$$

The constants in these equations were determined using a total number of 1,511 slurry flow data relating to water suspensions of 12 different sizes of solid particles ranging from 31μ up to 4380μ, covering, in round figures, densities of 2.3, 3.0, 4.4, 7.5 and 11.3 gm/cc, and pipe diameters of 2, 1, and 1/2-inch. The nonlinear least squares adjusted values of the constants are (see Table 5.5):

$$K = 0.3202,\ \alpha = 0.4925,\ \beta = 0.5586,$$

$$\gamma = -\,0.1095,\ \delta = 0.9002$$

FIGURE 11

PLOT OF $(f-f_w)$ AGAINST $\xi^\circ = C^{\alpha^\circ} f_w^{\beta^\circ} C_D^{\gamma^\circ} \left\{\frac{g(s-1)D}{V^2}\right\}^{\delta^\circ}$ FOR SUSPENSION FLOW THROUGH 2, 1, AND 1/2 INCH PIPES

VALUES OF PARAMETERS

Obtained by least squares adjustment of linearized form given by equation (38), and listed in Table 5.7.

$K^\circ = 0.4549 \times 10^{-1}$
$\alpha^\circ = 0.8265$
$\beta^\circ = 0.4737$
$\gamma^\circ = 0.1025$
$\delta^\circ = 1.116$

SYMBOLS

Experimental data for glass sphere slurries from this work

Symbol	Diameter (μ)	Density (gm/cc)
▣	40	4.434
×	5C5	4.430
◈	1015	4.400
+	475	2.486
⊙	1340	2.977
△	4380	2.964

Experimental data of Murphy, Young, and Burian (40) in 1/2 inch pipe

✤ Suspensions of glass beads (see Table 5.6)
⌧ Suspension of steel and lead particles (see Table 5.6)

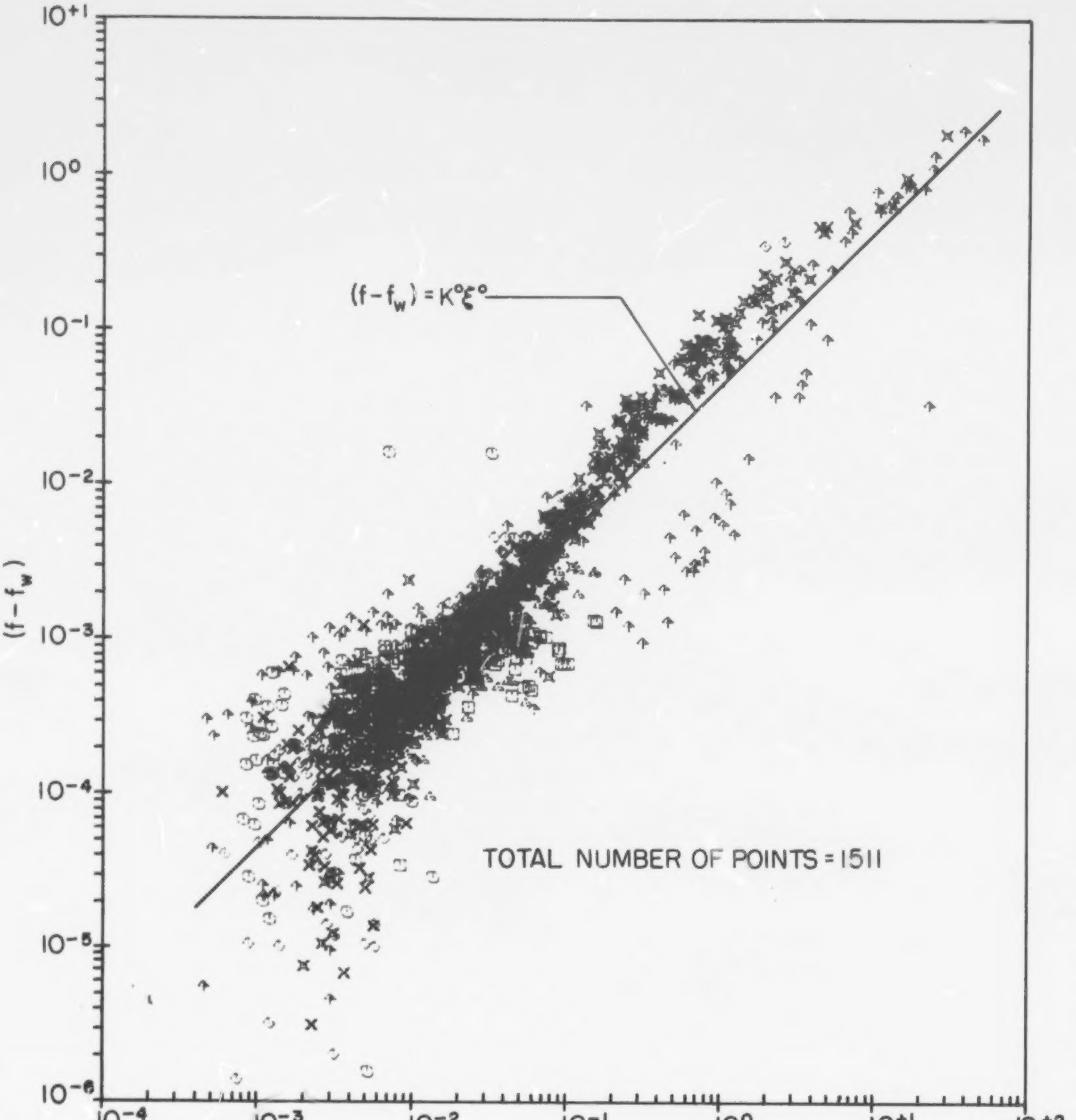

$$\xi^\circ = C^{\alpha^\circ} f_w{}^{\beta^\circ} C_D{}^{\gamma^\circ} \left\{\frac{g(s-1)D}{V^2}\right\}^{\delta^\circ}$$

FIGURE 11

FIGURE 12

PLOT OF $(f-f_w)$ AGAINST $\xi = C^{a} f_w^{\beta} C_D^{\gamma} \left\{\frac{g(s-1)D}{V^2}\right\}^{\delta}$ FOR SUSPENSION FLOW THROUGH 2, 1, AND 1/2 INCH PIPES

VALUES OF PARAMETERS

Obtained by nonlinear least squares adjustment of form given by equation (37), and listed in Table 5.5.

$K = 0.3202$
$a = 0.4925$
$\beta = 0.5586$
$\gamma = -0.1095$
$\delta = 0.9002$

SYMBOLS

Experimental data for glass sphere slurries from this work

Symbol	Diameter (μ)	Density (gm/cc)
⊡	40	4.434
×	505	4.430
⟐	1015	4.400
+	475	2.486
⊙	1340	2.977
◬	4380	2.964

Experimental data of Murphy, Young, and Burian (40) in 1/2 inch pipe

⍋ Suspensions of glass beads (see Table 5.6)
⌧ Suspension of steel and lead particles (see Table 5.6)

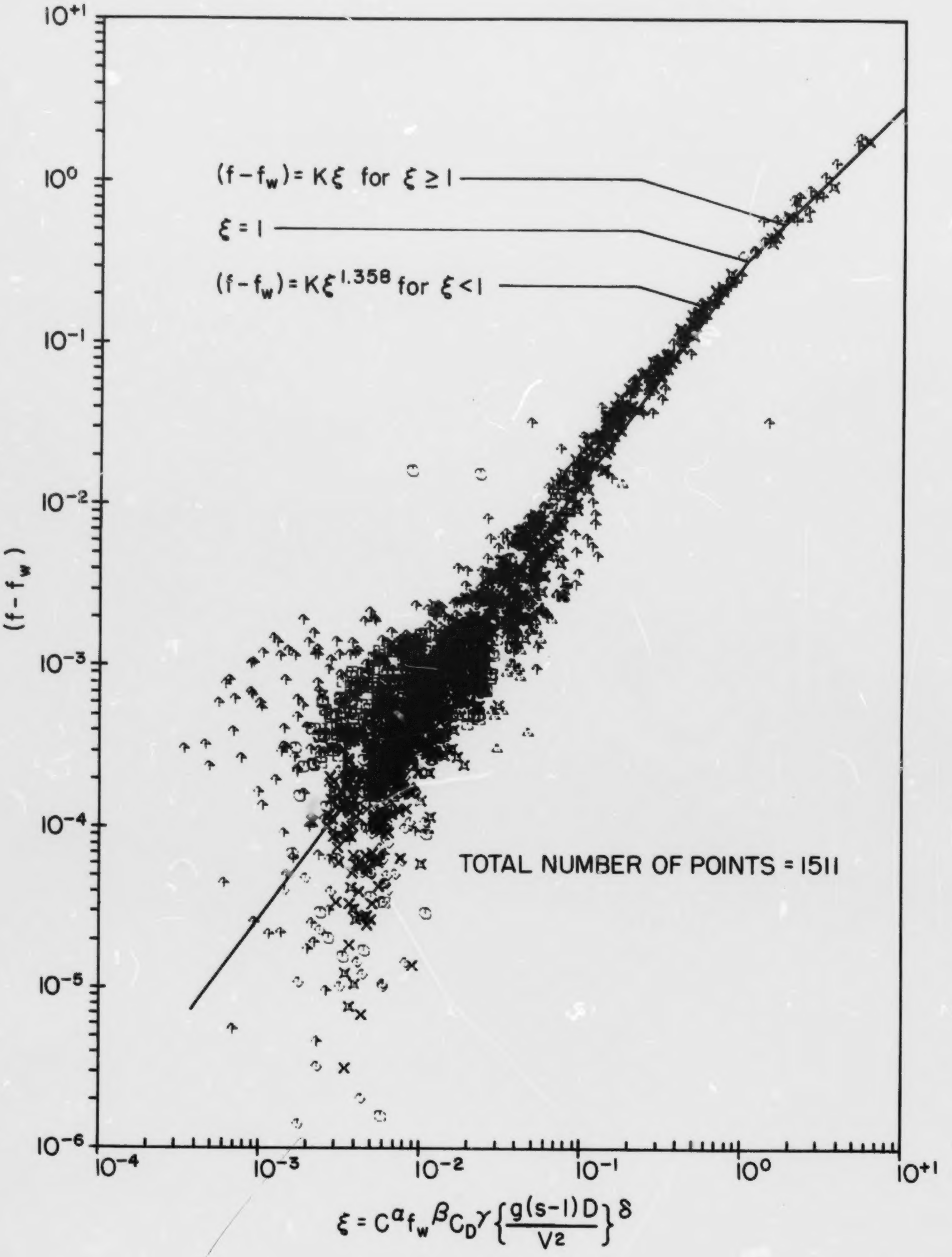
10^{+1}
10^{0}
10^{-1}
10^{-2}
10^{-3}
10^{-4}
10^{-5}
10^{-6}
$(f-f_w)$
$(f-f_w)=K\xi$ for $\xi \geq 1$
$\xi = 1$
$(f-f_w)=K\xi^{1.358}$ for $\xi<1$
TOTAL NUMBER OF POINTS = 1511
10^{-4}
10^{-3}
10^{-2}
10^{-1}
10^{0}
10^{+1}
$\xi = C^{\alpha} f_w{}^{\beta} C_D{}^{\gamma} \left\{\frac{g(s-1)D}{V^2}\right\}^{\delta}$

FIGURE 12

FIGURE 13

PLOT OF $(f-f_w)$ AGAINST $\xi = C^{\alpha} f_w^{\beta} C_D^{\gamma} \left\{\frac{g(s-1)D}{V^2}\right\}^{\delta}$ FOR SUSPENSION FLOW THROUGH 2, 1, AND 1/2 INCH PIPES

DATA TAKEN IN THIS WORK SHOWN ONLY

VALUES OF PARAMETERS

Obtained by nonlinear least squares adjustment of form given by equation (37), and listed in Table 5.5.

$K = 0.3202$
$\alpha = 0.4925$
$\beta = 0.5586$
$\gamma = -0.1095$
$\delta = 0.9002$

SYMBOLS

Experimental data for glass sphere slurries from this work

Symbol	Diameter (μ)	Density (gm/cc)
⊡	40	4.434
×	505	4.430
◈	1015	4.400
+	475	2.486
⊙	1340	2.977
△	4380	2.964

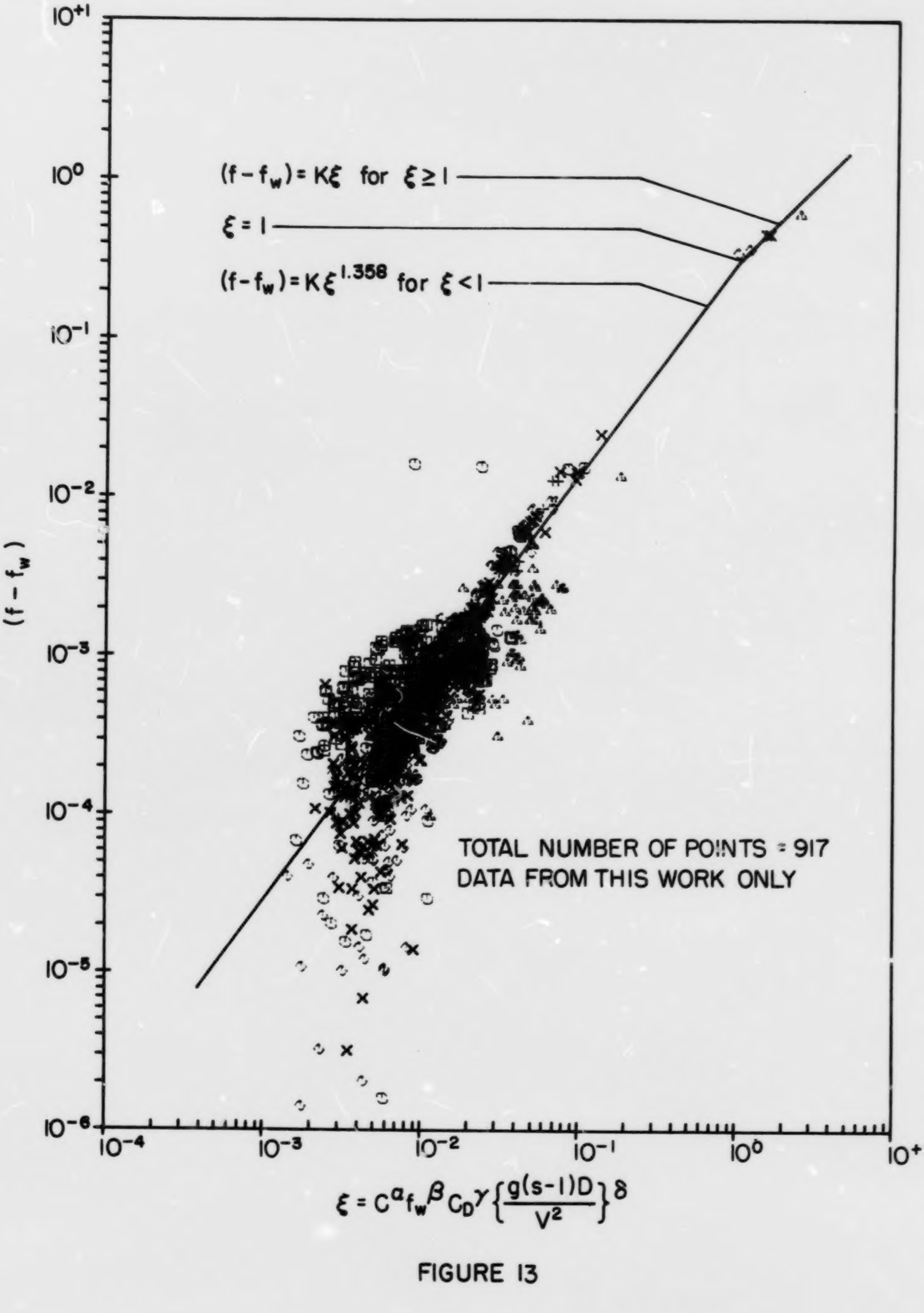
10^{+1}
10^{0}
10^{-1}
10^{-2}
10^{-3}
10^{-4}
10^{-5}
10^{-6}
$(f - f_w)$
$(f-f_w) = K\xi$ for $\xi \geq 1$
$\xi = 1$
$(f-f_w) = K\xi^{1.358}$ for $\xi < 1$
TOTAL NUMBER OF POINTS = 917
DATA FROM THIS WORK ONLY
10^{-4}
10^{-3}
10^{-2}
10^{-1}
10^{0}
10^{+1}
$\xi = C^{\alpha} f_w{}^{\beta} C_D{}^{\gamma} \left\{\frac{g(s-1)D}{V^2}\right\}^{\delta}$

FIGURE 13

The drag coefficient, C_D, for a free falling sphere appearing in the slurry flow correlation is calculated using the relation

$$\log_{10}\mathrm{Re} = a_o + a_1\log_{10}\Lambda + a_2(\log_{10}\Lambda)^2 + a_3(\log_{10}\Lambda)^3 + a_4(\log_{10}\Lambda)^4 + a_5(\log_{10}\Lambda)^5 \tag{16}$$

and the definition

$$\Lambda = \mathrm{Re}\ C_D^{1/2} = \left\{\frac{4}{3}\ \frac{g d^3 \rho_\ell(\rho_s-\rho_\ell)}{\mu^2}\right\}^{1/2} \tag{17}$$

The constants a_i based on a large collection of falling sphere data, which were stringently scrutinized with respect to accuracy, have the following values (see Table 5.3):

$a_o = -1.38$ $a_1 = 1.94$ $a_2 = -8.60 \times 10^{-2}$

$a_3 = -2.52 \times 10^{-2}$ $a_4 = 9.19 \times 10^{-4}$ $a_5 = 5.35 \times 10^{-4}$

Equation (16) is valid over the wide range $10^{-7} \leq \mathrm{Re} \leq 10^5$, and describes the data with an average deviation of 3.12%, with no deviations exceeding 12.87% within this entire range.

The friction factor, f_w, pertaining to pipe flow in the absence of solids can be approximated through use of Blasius' formula

$$f_w = 0.0791\ (\mathrm{Re}_w)^{-1/4} \tag{19}$$

or other available expressions for turbulent pipe flow, such as, for example, the logarithmic resistance law of Prandtl given by Equation (26). Alternatively, suitable curve fits of actual data to forms of the type given by

$$f_w = a\ \mathrm{Re}_w^b \tag{43}$$

can be used, as was done in this work (see Section 5.4).

The results established provide the necessary basis for slurry pipeline design, and they entail entirely straightforward calculations. Comparison of the slurry flow correlation with the data shows that the average deviation for the total number of 1,511 points is 9.54%, with 74 points having deviations exceeding 30% and only 9 points with deviations exceeding 50%.

CHAPTER VI

CONCLUSION

The slurry flow correlation developed in this work provides a description of the suspension flow data which is satisfactory for design purposes, particularly in view of the fact that even for flow in the absence of solids (a much simpler and a considerably more intensively researched problem) available design methods cannot, as they should not, claim predictive tolerances to within less than 5 to 10%. Indeed, had it been warranted, the correlation could have been extended to provide a comparatively closer agreement with all the data tested, but a rather convincing case could be made for deferring such an investment of effort pending the accumulation of more data. A strong preoccupation with merely the problem of splitting the percent deviation by successive extensions of the empirical correlation would, aside from allocating to this aspect of the problem a great deal more importance than it deserves, soon lead to diminishing returns.

In considering suspended solid flows, particularly those in which settling effects are quite pronounced, an important characteristic which emerges is that the system is unstable, in the sense described at the outset in this report, and, therefore, there are inherent limitations on the accuracy of the data which may be obtained. Fortunately, some properties of the flow, among them the observed pressure drop, are not as terribly sensitive to effects arising from this nature of the system as, say, the discharge or spatial concentrations seem to be. The use of a broader base of data will not alter this aspect of the problem, namely, the part associated with uncertainties in the observed data arising from effects which are neither easy to detect nor to evaluate, but, at the very least, it will submerge it by the sheer force of factual evidence.

Oddly enough many authors of published research on hydraulic transport of solids are mute with respect to quantitative statements on the predictive effectivenesses of their correlations. They deprive the rest of us, no doubt unwittingly, from sharing this important facet of their experiences; a sharing which might facilitate the evolution of criteria on what one could realistically expect from slurry flow design calculations.

Unlike the correlations relating to flow in the absence of solids, which relate friction loss to flow rate, the slurry flow correlation provides a relation between solids concentration and friction loss for a given flow rate. Therefore, for a given flow rate, the friction loss is indeterminate unless the concentration is specified, and vice versa. This type of relationship can, in principle, be used as the basis of optimization calculations relating to hydraulic transport of solids. Optimization calculations within the context of the present status of knowledge in this area, characterized by (besides the limitations residing in uncertainties with respect to predictive effectiveness, as discussed above) the absence of information on the important role of particle size distribution, among others, would amount to, what they usually do in other problems burdened by similar circumstances: sterile mathematical exercises.

The collection of data that we have used as the basis for our correlation represents a reasonably wide range of particle sizes and densities, and a rather modest range of pipe diameters, although the largest pipeline we used may be considered to be on a pilot scale. Viewed within the overall context of hydraulic transport of solids the range of variables represented by our collection of data is far from extravagant, of course. Nevertheless, if unlimited data were available studies of this sort would, of course, be superfluous; the aim here is to establish, on the basis of laboratory data, the means to predict the behavior on the practical scale.

The total number of 1,511 data points, most of which we took ourselves, is not small by most standards of measurement. Our use of this particular set of data, covering the range of variables that it does, and the number and type of data that we took ourselves, reflect, in part, an attempt to measure ends to means.

NOMENCLATURE

A, A' = constants

A_i = constants ($i=1,2,3,4$) Eqs. (14) and (15)

a_i = constants ($i=0,1,2,3,4$) Eq. (16)

C = discharge concentration of solids, volume %

C_D = $\frac{4}{3} \frac{gd(\rho_s-\rho_\ell)}{\rho_\ell v_\infty^2}$, drag coefficient for free falling sphere

D = inside diameter of pipe

d = mean particle diameter of suspended solids

d_e = $\Sigma w_i/\Sigma(w_i/d_i)$, equivalent particle diameter, Eq. (10)

d_i = particle diameter of ith solid species in mixture

$\bar{d}_n$ = $\Sigma(n_i d_i)/\Sigma n_i$

f = $(\Delta pD)/(2\rho_\ell V^2 L)$, friction factor for pipe flow of slurry

f_w = $(\Delta p_w D)/(2\rho_\ell V^2 L)$, friction factor for pipe flow in absence of solids

F_D = gravitational force (see Eq. 33)

F_I = inertial force (see Eq. 31)

F_L = dimensionless function in critical velocity correlation, Eq. (9)

F_V = viscous force (see Eq. 32)

g = gravitational constant

h_m = head loss for pipe flow of slurry, in feet of water per foot of pipe

h_w = head loss for pipe flow in absence of solids, in feet of water per foot of pipe

i_m = pressure drop or friction factor for pipe flow of slurry

i_w = pressure drop or friction factor for pipe flow in absence of solids

K = constant

NOMENCLATURE (Cont'd.)

$\bar{K}$ = constant

L = pipe length

n_i = number of particles of diameter d_i

Δp = pressure drop in length L of pipe for slurry

Δp_w = pressure drop in length L of pipe in absence of solids

Re = $d\rho_\ell v_\infty/\mu$, Reynolds number for free settling sphere

Re_w = $D\rho_\ell V/\mu$, Reynolds for pipe flow in absence of solids

s = ρ_s/ρ_ℓ, ratio of solid to liquid densities

V = mean velocity of mixture for slurry flow in pipeline

V_c = critical velocity of slurry (see Eq. 9)

v_∞ = terminal velocity of sphere settling in an unbounded fluid

w_i = weight fraction of particles of diameter d_i

$K,\alpha,\beta,\gamma,\delta$ = slurry flow correlation constants obtained by nonlinear least squares adjustment (Eq. 37)

$K^o,\alpha^o,\beta^o,\gamma^o,\delta^o$ = correlation constants in linearized form of slurry flow equation (Eq. 38)

ϵ = shape factor for suspended particles

Λ = $Re\ C_D^{1/2}$

μ = liquid viscosity

ξ = $C^\alpha f_w^\beta C_D^\gamma\ [g(s-1)D/V^2]^\delta$

ξ^o = $C^{\alpha^o} f_w^{\beta^o} C_D^{\gamma^o}\ [g(s-1)D/V^2]^{\delta^o}$

ρ_ℓ = liquid density

ρ_s = solid particle density

X_1 = $D\rho_\ell V/\mu$, dimensionless group (see Eq. 30)

X_2 = $d\rho_\ell V/\mu$, dimensionless group (see Eq. 30)

X_3 = ρ_s/ρ_ℓ, dimensionless group (see Eq. 30)

NOMENCLATURE (Cont'd.)

χ_4 = V^2/gD, dimensionless group (see Eq. 30)

ψ = particle size distribution function

LITERATURE CITED

1. Goldsmith, H.L., and Mason, S.G., *J. Colloid Sci.* *17*, 448, 1962; *18*, 237, 1963.

2. Goldsmith, H.L., and Mason, S.G., *Proc. Roy. Soc. London*, *A282*, 569, 1964.

3. Happel, J., and Byrne, B.J., *Ind. Eng. Chem.*, *46*, 1181, 1954.

4. Happel, J., and Brenner, H., *A.I.Ch.E. J.*, *3*, 506, 1957

5. Bagnold, R.A., *Proc. Inst. Civil Engrs.*, *4*, III, 174, 1955.

6. Bagnold, R.A., *Proc. Roy. Soc. London*, *A225*, 49, 1954.

7. Bagnold, R.A., *Phil. Trans.*, *A249*, 235, 1954.

8. Daniel, S.M., *Ph.D. Thesis*, *University of Saskatchewan*, Saskatoon, Saskatchewan, September 1965.

9. Rutgers, I.R., *Rheologica Acta*, *2*, 202, 1962.

10. Kynch, G.J., *Proc. Roy. Soc. London*, *A237*, 90, 1956.

11. Ting, A.P., and Luebbers, R.H., *A.I.Ch.E. J.*, *3*, 111, 1957.

12. Einstein, A., *Ann. Physik*, *19*, 289, 1906; *34*, 591, 1911.

13. Thomas, D.G., *Ind. Eng. Chem.*, *55* (11), 18, 1963; *55* (12), 27, 1963.

14. Metzner, A.B., "Non-Newtonian Technology: Fluid Mechanics, Mixing, and Heat Transfer", pp. 77-153 in "Advances in Chemical Engineering", Vol. 1, T.B. Drew, and J.W. Hoopes (eds.), Academic Press, N.Y., 1956.

15. Meter, D.M., *A.I.Ch.E. J.*, *10*, 881, 1964.

16. Caldwell, D.H., and Babbitt, M.E., *Indust. Eng. Chem.*, *33* (2), 249, 1941.

17. Wilhelm, R.H., Wroughton, D.M., and Loeffel, W.F., *Indust. Eng. Chem.*, *31* (5), 622, 1939.

18. Hazen and Hardy, *Trans. A.S.C.E.*,*57*, 1036, 1906.

19. Howard, G.W., *Proc. A.S.C.E.*, *64*, 1337, 1938; *Trans. A.S.C.E.*, *104*, 1334, 1938.

20. Wilson, W.E., *A.I.M.E.*, *169*, 675, 1946.

21. Newitt, D.M., Richardson, J.F., Abbott, M., and Turtle, R.B., *Trans. Instn. Chem. Engrs.*, *33*, 93, 1955.

LITERATURE CITED (Cont'd.)

22. Durand, R., *La Houille Blanche*, *6*, 384 (May-June) 1951.

23. Durand, R., *La Houille Blanche*, *6*, 609 (Special No. B) 1951.

24. Durand, R., and Condolios, E., *Proc. Minn. Int. Hydr. Conf.*, *I.A.H.R.*, Sept. 1953; also *Compte Rendu des Deuxiémes Journées de l'Hydraulique*, p. 29, June 1952 (Société Hydrotechnique de France, Paris).

25. Danel, P., Durand, R., and Condolios, E., *Memoires et Travaux de la Société Hydrotech. de France*, *8* (2), 217, 1953; also *La Houille Blanche*, *8*, 815, 1953.

26. Ellis, H.S. and Round, G.F., paper presented at the A.G.M. of *Can. Inst. Min.*, quoted in *Indust. Eng. Chem.* *55*, 18, 1963.

27. Worster, R.D., and Denny, D.F., *Proc. Inst. Mech. Eng.*, *169*, 32, 1955.

28. Smith, R.A., Trans. *Instn. Chem. Engrs.*, *33*, 85, 1955.

29. Cloete, F.L.D., Miller, A.I., and Streat, M., *Trans. Instn. Chem. Engrs.* *45*, T392, 1967.

30. Miller, A.I., *Ph.D. Thesis*, University of London, 1966.

31. Buchanan, R.H., Davies, D., and Oedjoe, D., *Austr. Chem. Proc.*, *15*, 3, 1962.

32. Oedjoe, D., Davies, D., and Buchanan, R.H., *Austr. Chem. Engng.*, *4*, 9, 1963.

33. Oedjoe, D., *Ph.D. Thesis*, The University of New South Wales, 1964.

34. Oedjoe, D., and Buchanan, R.H., *Trans. Instn. Chem. Engrs.*, *44*, T364, 1966.

35. Gay, E.C., *Sc. D. Thesis*, Washington University, St. Louis, 1967.

36. Mauri, G., *M.S. Thesis*, Syracuse University, November 1968.

37. Carey, W.W., *Ph.D. Thesis*, Syracuse University, July 1970.

38. Bacon, L.R., *J. Franklin Inst.*, *221*, 251, 1936.

39. McPherson, M.B., *M.S. Thesis*, University of Iowa, August 1947.

40. Murphy, G., Young, D.F., and Burian, R.J., *U.S. Atomic Energy Commission*, Report ISC-474, April 1, 1954.

APPENDIX A

GLASS SPHERE SLURRY FLOW IN 2, 1, AND 1/2-INCH PIPELINES

NOT REPRODUCIBLE

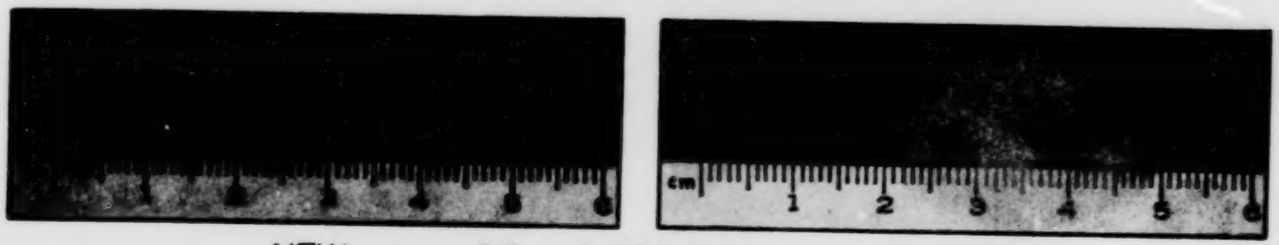
NEW 90μ, 4.434 gm/cc USED

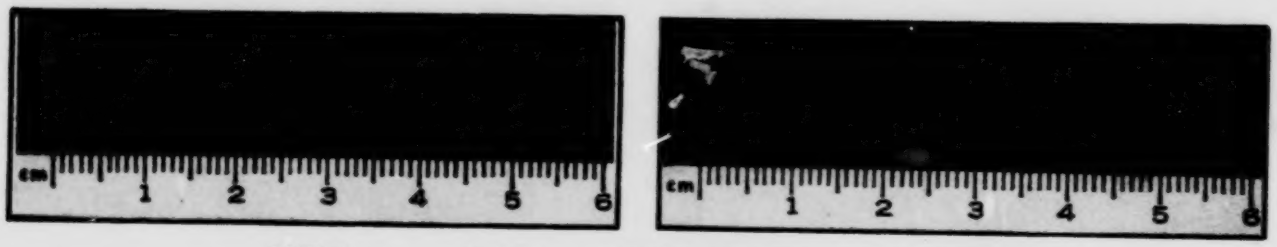
NEW 505μ, 4.430 gm/cc USED

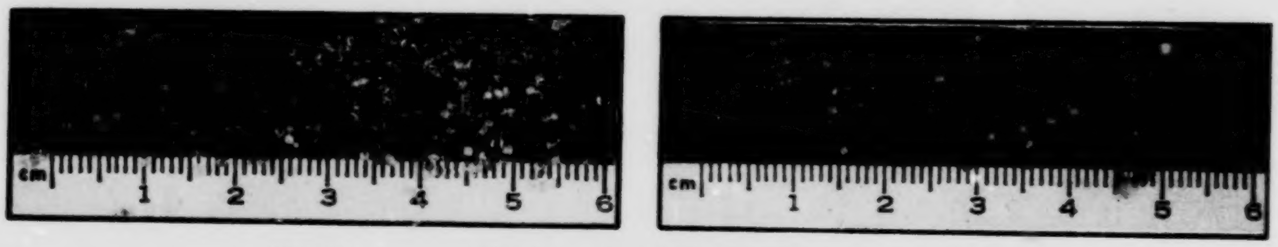
NEW 1015μ, 4.400 gm/cc USED

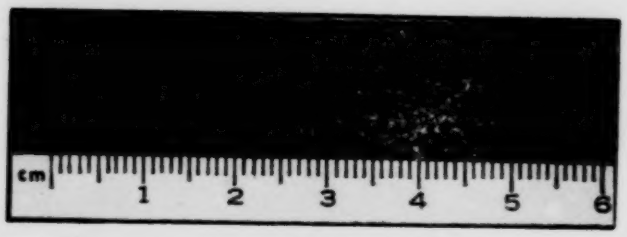
USED 475μ, 2.486 gm/cc

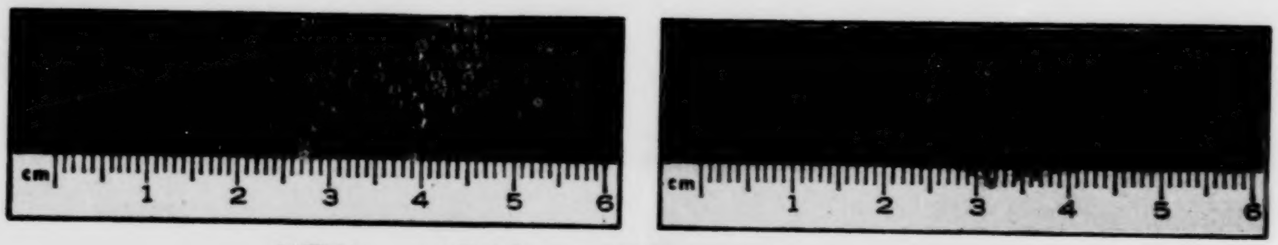
NEW 1340μ, 2.977 gm/cc USED

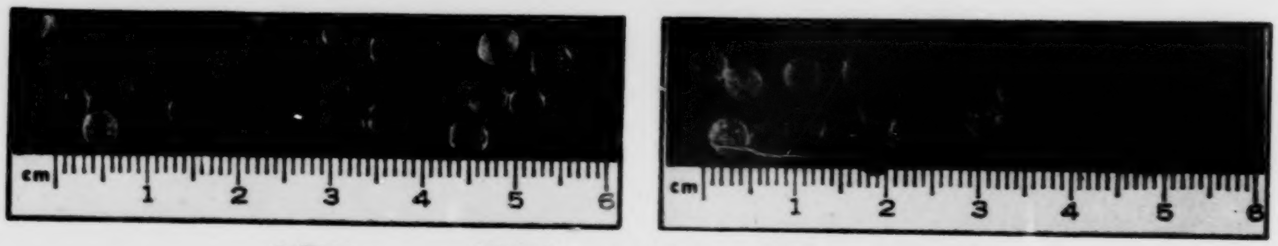
NEW 4380μ, 2.964 gm/cc USED

TABLE 1

Glass Beads : Average Diameter = 90.0 Microns
Density = 4.434 g/cc
Charged Conc. = 5.05 % by wt.

PVC Pipe : Inside Diameter = 2.067 in.

Reference No.	Temperature (Deg.C)	Pressure Drop (Psi/ft) x 100	Flow Rate (GPM)	Concentration (% by volume)
1	23.0	4.12	76.8	0.202
2	23.0	4.14	77.1	0.199
3	23.0	4.16	77.1	0.240
4	23.0	4.16	77.1	0.215
5	23.0	4.16	77.4	0.245
6	23.0	4.18	77.4	0.240
7	23.0	6.25	96.6	0.319
8	23.0	6.25	96.6	0.292
9	23.3	6.28	96.9	0.309
10	24.4	9.14	120.	0.432
11	24.4	9.20	120.	0.444
12	24.4	9.25	120.	0.458
13	24.4	9.25	120.	0.464
14	23.3	2.18	53.3	0.125
15	23.3	2.17	54.6	0.133
16	23.3	2.18	54.6	0.121
17	24.0	10.8	132.	0.403
18	24.5	10.9	132.	0.499
19	24.5	10.9	132.	0.453

TABLE 2

Glass Beads : Average Diameter = 90.0 Microns
Density = 4.434 g/cc
Charged Conc. = 5.05 % by wt.

PVC Pipe : Inside Diameter = 0.957 in.

Reference No.	Temperature (Deg.C)	Pressure Drop (Psi/ft) x 100	Flow Rate (GPM)	Concentration (% by volume)
1	23.5	7.34	13.0	0.227
2	23.0	7.37	12.6	0.233
3	23.0	7.39	13.0	0.221
4	23.0	11.3	15.9	0.302
5	23.0	11.3	17.5	0.316
6	23.0	11.4	16.0	0.325
7	24.0	18.8	21.0	0.434
8	24.0	18.8	21.3	0.434
9	24.0	19.0	21.4	0.456
10	24.0	21.7	23.4	0.508
11	24.0	22.0	23.8	0.531
12	24.2	22.1	23.7	0.505
13	24.5	25.2	26.3	0.576
14	24.5	25.5	25.7	0.605
15	24.5	25.5	26.1	0.617

TABLE 3

Glass Beads: Average Diameter = 90.0 Microns
Density = 4.434 g/cc
Charged Conc. = 5.05 % by wt.
PVC Pipe : Inside Diameter = 0.622 in.

Reference No.	Temperature (Deg.C)	Pressure Drop (Psi/ft) x 100	Flow Rate (GPM)	Concentration (% by volume)
1	23.5	12.1	5.40	0.266
2	23.5	12.1	5.38	0.275
3	23.5	12.1	5.41	0.275
4	23.5	17.0	6.53	0.403
5	23.5	17.0	6.54	0.377
6	23.5	17.0	6.42	0.375
7	23.5	4.46	3.00	0.386
8	23.5	4.46	3.00	0.403
9	23.5	4.46	2.98	0.398
10	23.5	23.8	8.04	0.478
11	23.5	23.8	7.91	0.472
12	24.0	23.8	8.03	0.451
13	24.0	30.9	9.27	0.565
14	24.0	30.9	9.11	0.566
15	24.0	30.9	9.30	0.578
16	24.0	21.7	7.66	0.459
17	23.7	21.8	7.51	0.494
18	23.6	21.9	7.50	0.490

TABLE 4

Glass Beads: Average Diameter = 90.0 Microns
Density = 4.434 g/cc
Charged Conc. = 9.98 % by wt.
PVC Pipe : Inside Diameter = 2.067 in.

Reference No.	Temperature (Deg.C)	Pressure Drop (Psi/ft) x 100	Flow Rate (GPM)	Concentration (% by volume)
1	22.5	1.92	50.0	0.586
2	22.5	1.96	50.3	0.567
3	22.5	1.95	50.3	0.516
4	22.5	1.96	50.7	0.425
5	23.0	4.66	80.7	0.762
6	22.5	4.74	81.0	0.803
7	22.5	4.77	81.4	0.853
8	23.0	7.54	105.	0.909
9	23.0	7.57	105.	1.05
10	23.0	7.57	105.	0.973
11	23.0	7.57	105.	0.996
12	23.0	9.50	119.	1.18
13	23.4	9.53	119.	1.11
14	23.5	9.53	119.	1.13
15	23.5	10.7	127.	1.17
16	23.5	10.7	127.	1.30
17	23.6	10.7	127.	1.40

TABLE 5

Glass Beads: Average Diameter = 90.0 microns
Density = 4.434 g/c.c.
Charged Conc. = 9.98 % by Wt.

PVC Pipe: Inside Diameter = 0.957 in.

Reference No.	Temperature (Deg.C)	Pressure Drop (psi/ft)x100	Flow Rate (GPM)	Concentration (% by Volume)
1	24.0	9.73	13.9	0.909
2	24.0	9.73	15.1	0.889
3	24.0	9.73	14.2	0.875
4	23.3	4.63	9.68	0.332
5	23.3	4.63	9.54	0.331
6	23.3	4.63	9.56	0.357
7	23.5	19.0	21.1	1.08
8	23.8	19.3	20.7	1.03
9	24.0	19.1	21.3	1.12
10	24.2	19.3	21.0	1.10
11	24.5	24.7	25.5	1.03
12	24.8	25.0	25.9	1.10
13	25.0	25.1	24.7	1.09
14	25.0	24.9	25.4	1.20
15	24.7	23.6	24.1	0.984
16	24.7	23.8	23.8	0.971
17	24.7	23.9	24.6	1.01

TABLE 6

Glass Beads: Average Diameter = 90.0 microns
Density = 4.434 G/C.C.
Charged Conc. = 9.98 % by Wt.

PVC Pipe: Inside Diameter = 0.622 in.

Reference No.	Temperature (Deg.C)	Pressure Drop (psi/ft)x100	Flow Rate (GPM)	Concentration (% by Volume)
1	23.7	7.38	3.96	0.406
2	23.6	7.45	4.06	0.320
3	23.6	7.53	4.05	0.367
4	23.6	7.62	4.11	0.420
5	23.8	14.6	5.96	0.698
6	24.0	14.6	5.93	1.06
7	24.0	14.7	5.74	1.05
8	24.0	14.8	5.85	1.11
9	24.0	22.3	7.52	1.30
10	24.2	22.3	7.54	1.40
11	24.1	22.4	7.53	1.38
12	24.1	18.6	6.70	1.29
13	24.0	18.6	6.78	1.29
14	24.0	18.6	6.77	1.32
15	24.0	29.5	8.64	1.64
16	24.0	29.8	8.77	1.58

TABLE 7

Glass Beads: Average Diameter = 90.0 Microns
Density = 4.434 g/cc
Charged Conc. = 14.7 % by wt.
PVC Pipe : Inside Diameter = 2.067 in.

Reference No.	Temperature (Deg.C)	Pressure Drop (Psi/ft) x 100	Flow Rate (GPM)	Concentration (% by volume)
1	23.0	4.76	80.0	2.01
2	22.5	4.88	80.3	1.88
3	22.7	4.89	80.0	1.83
4	22.7	4.89	80.4	1.97
5	22.6	2.77	58.9	1.51
6	22.6	2.78	58.8	1.54
7	22.5	2.78	58.8	1.48
8	23.2	7.36	101.	1.80
9	23.2	7.39	102.	1.89
10	23.2	7.41	102.	2.08
11	24.3	10.5	123.	2.24
12	24.3	10.6	124.	2.41
13	24.4	10.6	124.	1.99
14	24.4	10.6	124.	2.13
15	24.2	8.64	111.	1.69
16	24.2	8.71	111.	2.02
17	24.2	8.72	111.	2.03

TABLE 8

Glass Beads: Average Diameter = 90.0 Microns
Density = 4.434 g/cc
Charged Conc. = 14.7 % by wt.
PVC Pipe : Inside Diameter = 0.957 in.

Reference No.	Temperature (Deg.C)	Pressure Drop (Psi/ft) x 100	Flow Rate (GPM)	Concentration (% by volume)
1	24.0	6.77	11.3	1.29
2	23.8	6.80	11.3	1.37
3	23.8	6.80	11.6	1.41
4	23.7	10.6	14.7	1.80
5	23.8	10.6	14.8	1.82
6	23.8	10.7	14.4	1.92
7	24.4	17.4	19.2	2.18
8	24.7	17.6	19.2	2.15
9	24.7	17.6	19.7	2.12
10	25.0	21.7	22.8	2.07
11	25.3	21.9	23.0	2.10
12	25.4	21.9	23.4	2.11
13	24.2	5.39	10.6	0.256
14	24.2	5.44	10.4	0.252
15	24.2	5.44	10.2	0.245
16	25.1	26.4	26.7	1.39
17	25.2	26.4	25.8	1.41
18	25.2	26.5	25.8	1.57

TABLE 9

Glass Beads: Average Diameter = 90.0 microns
Density = 4.434 g/c.c.
Charged Conc. = 14.7 % by Wt.

PVC Pipe: Inside Diameter = 0.622 in.

Reference No.	Temperature (Deg.C)	Pressure Drop (psi/ft)x100	Flow Rate (GPM)	Concentration (% by Volume)
1	23.3	12.3	5.14	1.69
2	23.2	12.5	5.21	1.74
3	23.2	12.6	5.28	1.87
4	23.4	7.59	3.95	1.11
5	23.4	7.62	3.95	1.06
6	23.4	7.70	4.00	1.16
7	23.4	7.75	3.98	1.16
8	23.8	20.7	6.92	2.44
9	24.0	20.9	7.09	2.43
10	24.0	20.9	6.90	2.46
11	24.0	27.2	8.03	2.79
12	24.2	27.4	8.30	2.60
13	24.3	27.4	8.03	2.72
14	24.3	27.4	8.08	2.63
15	24.5	34.9	9.30	3.18
16	25.0	35.6	9.38	3.22
17	25.0	35.6	9.47	3.13

TABLE 10

Glass Beads: Average Diameter = 90.0 microns
Density = 4.434 g/c.c.
Charged Conc. = 20.8 % by Wt.

PVC Pipe: Inside Diameter = 2.067 in.

Reference No.	Temperature (Deg.C)	Pressure Drop (psi/ft)x100	Flow Rate (GPM)	Concentration (% by Volume)
1	23.7	4.54	78.5	4.06
2	23.7	4.54	78.5	3.74
3	23.7	4.54	78.5	3.59
4	23.7	8.54	107.	3.31
5	24.0	8.50	107.	3.69
6	24.0	8.54	107.	3.75
7	23.0	3.39	62.9	3.45
8	23.0	3.41	63.2	3.66
9	23.0	3.42	63.3	3.69
10	22.5	6.09	88.8	3.83
11	22.5	6.15	89.0	3.49
12	22.5	6.18	89.4	3.51
13	23.7	11.1	124.	3.98
14	23.9	11.2	124.	4.04
15	24.8	11.2	124.	4.03

TABLE 11

Glass Beads: Average Diameter = 90.0 microns
Density = 4.434 g/c.c.
Charged Conc. = 20.8 % by Wt.

PVC Pipe: Inside Diameter = 0.957 in.

Reference No.	Temperature (Deg.C)	Pressure Drop (psi/ft)x100	Flow Rate (GPM)	Concentration (% by Volume)
1	23.5	10.7	14.6	1.84
2	23.5	10.7	14.7	1.82
3	23.0	10.7	14.5	1.81
4	22.5	4.50	9.02	0.695
5	22.5	4.50	9.29	0.669
6	22.5	4.50	9.21	0.666
7	23.3	18.8	19.6	3.61
8	23.3	18.9	19.7	3.34
9	23.3	18.9	19.7	3.28
10	23.5	25.2	24.8	3.87
11	24.0	25.4	23.7	3.75
12	24.4	23.8	23.3	4.28
13	24.6	24.3	23.8	4.19
14	24.7	24.3	23.2	4.47

TABLE 12

Glass Beads: Average Diameter = 90.0 microns
Density = 4.434 g/c.c.
Charged Conc. = 20.8 % by Wt.

PVC Pipe: Inside Diameter = 0.622 in.

Reference No.	Temperature (Deg.C)	Pressure Drop (psi/ft)x100	Flow Rate (GPM)	Concentration (% by Volume)
1	24.1	14.7	5.59	2.58
2	24.1	14.9	5.81	2.45
3	24.1	14.9	5.70	2.80
4	24.0	8.04	4.12	1.14
5	24.0	8.02	4.15	1.13
6	24.0	8.01	4.09	1.04
7	23.2	21.6	7.05	3.01
8	23.2	21.6	7.07	2.93
9	23.2	21.6	6.92	3.08
10	22.7	5.05	3.13	0.850
11	22.7	5.10	3.17	0.866
12	22.7	5.09	3.20	0.819
13	23.3	28.4	8.20	4.17
14	23.5	28.4	8.09	3.80
15	23.5	28.4	8.12	3.92
16	23.5	28.4	8.13	3.84

TABLE 13

Glass Beads: Average Diameter = 1340. microns
Density = 2.977 g/c.c.
Charged Conc. = 5.05 % by Wt.

PVC Pipe: Inside Diameter = 2.067 in.

Reference No.	Temperature (Deg.C)	Pressure Drop (psi/ft)x100	Flow Rate (GPM)	Concentration (% by Volume)
1	22.0	2.24	51.7	0.635
2	22.0	2.24	51.7	0.644
3	22.5	2.31	51.0	0.698
4	22.5	3.88	73.4	0.838
5	22.5	3.95	73.4	0.743
6	22.5	3.95	74.1	0.741
7	23.5	6.57	102.	0.764
8	23.5	6.58	102.	0.570
9	22.0	6.63	101.	0.619
10	22.0	10.2	130.	0.704
11	22.5	10.3	131.	1.22
12	23.0	7.96	114.	1.54
13	23.0	7.96	114.	0.585
14	23.0	8.03	114.	0.731

TABLE 14

Glass Beads: Average Diameter = 1340. microns
Density = 2.977 g/c.c.
Charged Conc. = 5.05 % by Wt.

PVC Pipe: Inside Diameter = 0.957 in.

Reference No.	Temperature (Deg.C)	Pressure Drop (psi/ft)x100	Flow Rate (GPM)	Concentration (% by Volume)
1	21.5	10.5	14.9	0.388
2	21.5	10.5	15.7	0.379
3	22.5	10.5	15.6	0.449
4	23.0	10.6	15.7	0.441
5	22.5	10.5	15.8	0.201
6	22.5	10.5	15.4	0.150
7	22.5	10.5	15.5	0.148
8	23.0	18.8	21.3	0.306
9	23.0	18.8	22.9	0.275
10	23.0	18.8	21.7	0.240
11	22.5	5.44	11.0	0.037
12	22.5	5.44	10.8	0.035
13	22.0	5.53	10.9	0.033
14	22.0	10.5	16.6	0.136
15	22.5	10.6	15.8	0.193
16	22.5	10.7	16.0	0.162
17	22.5	10.7	16.5	0.260
18	23.5	5.55	11.1	0.076
19	22.5	5.65	11.3	0.070
20	22.5	5.64	11.2	0.083
21	22.5	18.7	21.9	0.272
22	23.5	18.8	21.8	0.303
23	23.5	18.8	22.0	0.339
24	23.5	18.8	22.1	0.287
25	23.5	28.6	29.1	0.322
26	23.5	28.8	13.8	0.725
27	23.0	23.3	25.2	0.314
28	22.5	23.3	24.9	0.345

TABLE 15

Glass Beads: Average Diameter = 1340. microns
Density = 2.977 g/c.c.
Charged Conc. = 5.05 % by Wt.
PVC Pipe: Inside Diameter = 0.622 in.

Reference No.	Temperature (Deg.C)	Pressure Drop (psi/ft)x100	Flow Rate (GPM)	Concentration (% by Volume)
1	22.5	7.07	4.05	0.055
2	22.5	7.09	4.05	0.041
3	22.5	7.09	4.09	0.054
4	22.5	16.6	6.72	0.251
5	22.5	16.6	6.62	0.214
6	22.5	16.6	6.77	0.229
7	22.5	11.4	5.40	0.105
8	22.5	11.4	5.38	0.104
9	22.5	11.4	5.38	0.081
10	22.5	23.7	8.37	0.352
11	22.5	23.8	8.31	0.316
12	22.5	23.8	8.32	0.303
13	22.5	36.0	10.4	0.474
14	22.5	36.1	10.2	0.475

TABLE 16

Glass Beads: Average Diameter = 1340. microns
Density = 2.977 g/c.c.
Charged Conc. = 10.0 % by Wt.
PVC Pipe: Inside Diameter = 2.067 in.

Reference No.	Temperature (Deg.C)	Pressure Drop (psi/ft)x100	Flow Rate (GPM)	Concentration (% by Volume)
1	22.5	6.44	93.3	3.88
2	22.5	6.44	93.3	2.46
3	22.5	6.44	93.9	1.99
4	22.5	6.59	93.3	2.03
5	22.5	10.4	129.	1.86
6	22.5	10.3	129.	1.52
7	22.5	10.3	130.	0.959
8	22.5	10.2	129.	1.99
9	23.5	10.2	130.	1.33
10	22.0	5.00	74.5	2.45
11	22.5	4.89	74.8	2.12
12	22.5	5.06	75.4	2.88
13	22.5	4.06	55.0	2.39
14	22.0	4.12	55.6	1.92
15	22.0	4.14	55.6	2.41
16	23.0	8.01	108.	2.49
17	23.0	8.11	108.	2.12
18	23.0	8.07	109.	2.17

TABLE 17

Glass Beads: Average Diameter = 1340. microns
Density = 2.977 g/c.c.
Charged Conc. = 10.0 % by Wt.

PVC Pipe: Inside Diameter = 0.957 in.

Reference No.	Temperature (Deg.C)	Pressure Drop (psi/ft)x100	Flow Rate (GPM)	Concentration (% by Volume)
1	22.5	9.52	14.7	1.09
2	22.5	9.65	14.8	1.10
3	22.5	9.72	14.8	1.04
4	22.5	18.7	21.3	2.27
5	22.5	18.8	21.3	2.33
6	22.5	26.2	27.2	3.33
7	23.0	26.4	26.8	3.58
8	22.5	26.4	26.9	3.06
9	22.5	20.8	23.4	3.29
10	22.5	20.8	23.2	2.75
11	22.5	20.8	23.2	3.57
12	22.5	5.27	9.90	1.31
13	22.5	5.27	9.80	1.47
14	22.5	5.27	9.70	1.45

TABLE 18

Glass Beads: Average Diameter = 1340. microns
Density = 2.977 g/c.c.
Charged Conc. = 10.0 % by Wt.

PVC Pipe: Inside Diameter = 0.622 in.

Reference No.	Temperature (Deg.C)	Pressure Drop (psi/ft)x100	Flow Rate (GPM)	Concentration (% by Volume)
1	22.0	9.63	4.85	1.15
2	22.0	9.64	4.77	1.28
3	22.0	9.69	4.71	1.25
4	22.5	20.2	7.37	1.91
5	22.5	20.2	7.50	1.82
6	23.0	20.2	7.37	2.41
7	22.5	20.4	7.42	1.67
8	22.5	20.6	7.50	2.01
9	22.5	20.6	7.50	1.65
10	24.0	5.35	3.17	1.65
11	23.0	5.35	3.21	1.55
12	22.0	5.35	3.21	1.60
13	22.0	24.1	8.26	1.91
14	22.5	24.4	8.39	1.66
15	22.5	24.4	8.35	1.68

TABLE 19

Glass Beads: Average Diameter = 1340. microns
Density = 2.977 g/c.c.
Charged Conc. = 15.0 % by Wt.

PVC Pipe: Inside Diameter = 2.067 in.

Reference No.	Temperature (Deg.C)	Pressure Drop (psi/ft)x100	Flow Rate (GPM)	Concentration (% by Volume)
1	22.5	6.27	64.9	5.81
2	22.5	6.36	64.9	5.94
3	22.5	6.49	64.9	5.64
4	23.0	9.29	114.	3.34
5	23.0	9.32	114.	3.78
6	23.0	9.31	115.	3.41
7	23.5	7.00	90.6	3.04
8	23.5	7.02	91.3	3.55
9	23.5	6.98	90.6	3.01
10	23.5	7.00	91.3	3.45
11	22.5	3.82	36.1	2.51
12	23.0	3.97	36.5	4.23
13	24.0	10.5	127.	2.41
14	24.5	10.5	128.	2.61
15	24.5	10.5	128.	2.32

TABLE 20

Glass Beads: Average Diameter = 1340. microns
Density = 2.977 g/c.c.
Charged Conc. = 15.0 % by Wt.

PVC Pipe: Inside Diameter = 0.957 in.

Reference No.	Temperature (Deg.C)	Pressure Drop (psi/ft)x100	Flow Rate (GPM)	Concentration (% by Volume)
1	22.5	11.4	15.1	3.22
2	22.5	11.4	15.4	2.97
3	22.5	11.5	15.3	3.45
4	22.5	18.4	20.4	3.74
5	22.5	18.4	20.6	3.99
6	22.5	18.4	20.6	4.08
7	22.5	24.8	25.3	4.98
8	23.0	24.8	29.6	4.57
9	24.0	24.8	25.8	5.12
10	24.0	25.0	25.8	5.07
11	23.0	21.2	23.2	4.42
12	23.5	21.2	23.6	4.85
13	24.0	21.2	23.6	4.65
14	23.5	7.12	11.7	1.99
15	22.5	7.12	11.7	2.09
16	22.5	7.12	11.6	2.26

TABLE 21

Glass Beads: Average Diameter = 1340. Microns
Density = 2.977 g/cc
Charged Conc. = 15.0 % by wt.
PVC Pipe : Inside Diameter = 0.622 in.

Reference No.	Temperature (Deg.C)	Pressure Drop (Psi/ft) x 100	Flow Rate (GPM)	Concentration (% by volume)
1	23.0	16.4	6.65	4.09
2	23.0	16.4	6.51	4.25
3	23.0	16.5	6.78	3.82
4	23.0	33.7	9.88	4.74
5	23.5	34.2	9.93	3.89
6	22.5	33.7	9.56	4.14
7	22.5	28.1	8.93	3.34
8	23.0	28.1	8.88	4.57
9	23.0	28.1	8.92	3.96
10	22.5	23.2	7.87	3.64
11	23.0	23.2	7.97	3.75
12	23.0	23.4	7.99	3.22
13	23.0	23.8	8.01	3.85
14	22.8	25.8	4.42	3.62
15	23.0	9.71	4.41	3.30
16	23.0	9.93	4.41	2.88

TABLE 22

Glass Beads: Average Diameter = 4380. Microns
Density = 2.964 g/cc
Charged Conc. = 5.05 % by wt.
PVC Pipe : Inside Diameter = 2.067 in.

Reference No.	Temperature (Deg.C)	Pressure Drop (Psi/ft) x 100	Flow Rate (GPM)	Concentration (% by volume)
1	22.5	4.32	74.5	1.78
2	22.5	4.32	76.1	2.54
3	22.5	2.53	55.0	2.51
4	22.5	2.53	55.0	2.32
5	22.5	3.50	69.1	3.34
6	22.5	3.50	69.1	1.14
7	22.5	3.50	69.1	1.64
8	22.5	3.50	69.1	1.99
9	23.0	6.18	96.6	1.96
10	23.0	6.18	96.6	0.788
11	24.0	6.10	96.6	1.56

TABLE 23

Glass Beads: Average Diameter = 4380. Microns
Density = 2.964 g/cc
Charged Conc. = 5.05 % by wt.
PVC Pipe : Inside Diameter = 2.067 in.

Reference No.	Temperature (Deg.C)	Pressure Drop (Psi/ft) x 100	Flow Rate (GPM)	Concentration (% by volume)
1	19.0	1.71	41.8	1.41
2	19.0	1.71	41.8	0.923
3	19.0	1.71	41.8	1.63
4	20.5	4.91	81.4	3.04
5	21.0	4.91	81.4	2.64
6	21.5	4.91	81.4	2.43
7	22.0	4.91	81.4	2.38
8	24.0	7.37	109.	1.70
9	24.0	7.37	109.	2.02
10	24.0	7.37	109.	1.22
11	24.0	7.37	109.	1.36
12	24.0	8.93	120.	1.10
13	24.0	8.93	120.	1.97
14	24.0	8.93	120.	1.05
15	24.0	8.93	120.	1.69
16	24.0	8.93	120.	1.43
17	25.0	10.3	130.	1.84
18	25.0	10.3	130.	1.42
19	25.0	10.3	130.	1.42
20	25.0	10.3	130.	1.04

TABLE 24

Glass Beads: Average Diameter = 4380. Microns
Density = 2.964 g/cc
Charged Conc. = 5.05 % by wt.
PVC Pipe : Inside Diameter = 0.957 in.

Reference No.	Temperature (Deg.C)	Pressure Drop (Psi/ft) x 100	Flow Rate (GPM)	Concentration (% by volume)
1	23.0	4.47	8.36	3.92
2	23.0	4.47	8.64	3.29
3	23.0	4.47	8.30	4.09
4	23.0	4.47	8.75	4.76
5	23.0	4.47	8.49	5.77
6	23.0	4.47	8.14	6.75
7	23.0	4.47	8.35	4.12
8	23.0	4.47	8.13	6.87
9	23.0	4.47	8.45	3.30
10	22.0	6.96	10.9	6.98
11	18.0	2.54	6.48	0.771
12	19.0	2.54	6.71	1.13
13	19.0	2.54	4.07	2.24
14	19.0	2.54	6.47	0.706
15	20.0	9.47	13.8	5.03
16	20.5	9.54	13.8	4.40
17	21.5	9.83	14.3	5.17
18	22.0	10.0	14.4	3.73
19	22.0	10.0	14.8	4.41

TABLE 25

Glass Beads: Average Diameter = 4380. Microns
Density = 2.964 g/cc
Charged Conc. = 5.05 % by wt.
PVC Pipe : Inside Diameter = 0.957 in.

Reference No.	Temperature (Deg.C)	Pressure Drop (Psi/ft) x 100	Flow Rate (GPM)	Concentration (% by volume)
1	19.5	11.5	15.8	4.55
2	19.5	11.5	15.0	4.91
3	19.5	11.5	15.7	5.39
4	20.0	11.5	15.5	4.65
5	20.0	11.5	15.7	3.64
6	20.5	7.70	12.4	3.58
7	21.0	7.70	12.6	3.19
8	21.0	7.70	12.7	3.47
9	21.0	7.70	12.7	3.17
10	21.5	7.70	12.4	3.67
11	21.5	5.24	9.99	1.50
12	21.5	5.24	9.91	2.92
13	22.0	5.24	10.2	2.34
14	22.0	5.24	10.2	2.93

TABLE 26

Glass Beads: Average Diameter = 380. Microns
Density = 2.964 g/cc
Charged Conc. = 5.05 % by wt.
PVC Pipe : Inside Diameter = 0.622 in.

Reference No.	Temperature (Deg.C)	Pressure Drop (Psi/ft) x 100	Flow Rate (GPM)	Concentration (% by volume)
1	21.5	17.2	6.53	3.42
2	21.5	17.2	6.68	3.16
3	21.5	17.2	6.75	4.34
4	21.5	17.2	7.09	4.51
5	21.5	17.2	0.687	26.1
6	21.5	17.2	6.81	3.27
7	20.0	2.24	2.05	0.276
8	21.0	23.8	8.24	0.270
9	22.5	34.9	10.5	3.85
10	22.5	34.9	9.95	3.95
11	22.5	34.9	9.74	4.12
12	22.0	11.7	5.32	2.31
13	22.0	11.7	5.29	2.49
14	22.0	11.7	5.24	3.13
15	21.5	24.1	8.18	3.01
16	21.5	24.1	8.09	3.48
17	21.5	24.1	8.16	3.31

TABLE 27

Glass Beads: Average Diameter = 4380. Microns
Density = 2.964 g/cc
Charged Conc. = 10.1 % by wt.
PVC Pipe : Inside Diameter = 2.067 in.

Reference No.	Temperature (Deg.C)	Pressure Drop (Psi/ft) x 100	Flow Rate (GPM)	Concentration (% by volume)
1	21.0	8.38	134.	3.61
2	21.0	8.38	134.	3.57
3	21.0	8.38	134.	2.61
4	22.5	1.80	39.8	0.437
5	22.5	1.80	39.8	2.54
6	22.5	1.80	39.8	1.31
7	22.5	5.99	88.6	2.49
8	22.5	5.99	88.6	2.22
9	22.5	5.99	88.6	3.00
10	21.0	4.18	62.2	4.38
11	21.0	4.18	62.2	3.85
12	21.0	3.86	62.2	2.86
13	21.0	4.18	62.2	4.13
14	23.0	8.26	111.	2.96
15	23.5	8.26	111.	3.16
16	23.5	8.26	111.	2.56

TABLE 28

Glass Beads: Average Diameter = 4380. Microns
Density = 2.964 g/cc
Charged Conc. = 10.1 % by wt.
PVC Pipe : Inside Diameter = 0.957 in.

Reference No.	Temperature (Deg.C)	Pressure Drop (Psi/ft) x 100	Flow Rate (GPM)	Concentration (% by volume)
1	22.5	21.9	24.0	7.40
2	22.5	21.9	24.2	7.17
3	22.5	21.9	23.1	8.18
4	20.5	8.73	11.9	7.33
5	21.0	8.73	12.0	8.32
6	21.0	8.84	12.4	6.62
7	21.5	8.95	12.2	7.68
8	22.0	2.65	6.23	1.52
9	22.0	2.65	6.55	0.849
10	22.0	2.65	6.30	1.09
11	22.0	2.65	6.67	0.855
12	22.0	18.9	18.1	8.68
13	22.0	18.9	20.0	7.74
14	21.5	18.9	21.2	7.51
15	21.0	12.6	16.0	6.84
16	21.0	12.6	16.3	6.73
17	21.0	12.6	15.4	7.57

TABLE 29

Glass Beads: Average Diameter = 4380. Microns
Density = 2.964 g/cc
Charged Conc. = 10.1 % by wt.
PVC Pipe : Inside Diameter = 0.622 in.

Reference No.	Temperature (Deg.C)	Pressure Drop (Psi/ft) x 100	Flow Rate (GPM)	Concentration (% by volume)
1	21.5	9.29	3.82	9.07

TABLE 30

Glass Beads: Average Diameter = 4380. Microns
Density = 2.964 g/cc
Charged Conc. = 11.5 % by wt.
PVC Pipe : Inside Diameter = 2.067 in.

Reference No.	Temperature (Deg.C)	Pressure Drop (Psi/ft) x 100	Flow Rate (GPM)	Concentration (% by volume)
1	21.5	6.19	82.7	4.59
2	21.5	5.64	82.7	5.04
3	21.5	5.64	82.7	4.69
4	22.5	8.88	108.	6.00
5	22.5	8.42	108.	3.90
6	22.5	8.30	108.	3.12
7	22.0	4.46	55.0	3.76
8	21.5	4.31	55.0	4.26
9	21.5	4.25	55.0	4.37
10	22.5	10.9	131.	3.48
11	23.5	10.9	131.	4.01
12	24.0	10.9	131.	3.42
13	22.5	6.49	93.3	3.74
14	22.0	6.32	93.3	3.04

TABLE 31

Glass Beads: Average Diameter = 4380. Microns
Density = 2.964 g/cc
Charged Conc. = 11.5 % by wt.
PVC Pipe : Inside Diameter = 0.957 in.

Reference No.	Temperature (Deg.C)	Pressure Drop (Psi/ft) x 100	Flow Rate (GPM)	Concentration (% by volume)
1	22.5	5.78	9.58	5.40
2	22.5	5.78	9.53	4.20
3	22.5	5.78	9.36	5.40
4	22.0	23.2	23.1	10.2
5	22.5	23.2	24.2	10.3
6	22.5	23.2	29.3	11.3
7	22.5	12.8	15.2	9.58
8	22.5	12.8	16.5	7.99
9	22.0	12.8	15.8	8.57
10	22.0	18.7	20.3	10.4
11	22.5	18.7	19.6	9.25
12	22.5	18.7	20.9	8.89
13	22.5	3.51	7.38	1.15
14	22.5	3.51	7.67	1.45
15	21.5	3.51	9.35	1.11

TABLE 32

Glass Beads: Average Diameter = 505. Microns
Density = 4.430 g/cc
Charged Conc. = 5.05 % by wt.
PVC Pipe : Inside Diameter = 2.067 in.

Reference No.	Temperature (Deg.C)	Pressure Drop (Psi/ft) x 100	Flow Rate (GPM)	Concentration (% by volume)
1	23.0	4.66	83.3	0.139
2	19.5	4.71	83.3	0.303
3	20.5	4.71	83.3	0.311
4	21.5	7.52	107.	0.514
5	22.5	7.58	108.	0.235
6	22.0	7.58	108.	0.356
7	23.0	1.82	47.7	0.082
8	21.5	1.83	47.7	0.115
9	20.5	1.83	47.7	0.189
10	22.5	10.2	130.	0.659
11	22.5	10.2	130.	0.816
12	22.5	10.3	130.	0.903
13	22.0	6.06	95.9	0.445
14	22.0	6.08	95.9	0.422
15	22.0	6.28	95.9	0.477

TABLE 33

Glass Beads: Average Diameter = 505. Microns
Density = 4.430 g/cc
Charged Conc. = 5.05 % by wt.
PVC : Inside Diameter = 0.957 in.

Reference No.	Temperature (Deg.C)	Pressure Drop (Psi/ft) x 100	Flow Rate (GPM)	Concentration (% by volume)
1	20.5	4.95	10.3	0.008
2	20.5	4.95	10.3	0.009
3	21.5	11.4	16.3	0.100
4	22.0	11.4	16.6	0.083
5	22.5	11.4	16.7	0.090
6	22.0	18.0	21.7	0.206
7	21.0	18.0	21.4	0.196
8	21.5	18.1	21.5	0.177
9	22.0	20.6	23.6	0.466
10	21.5	20.6	24.0	0.283
11	21.0	20.6	23.6	0.281
12	22.0	24.5	26.3	0.511
13	23.0	24.5	26.3	0.475
14	23.0	24.5	26.2	0.503

TABLE 34

Glass Beads: Average Diameter = 505. Microns
Density = 4.430 g/cc
Charged Conc. = 5.05 % by wt.
PVC Pipe : Inside Diameter = 0.622 in.

Reference No.	Temperature (Deg.C)	Pressure Drop (Psi/ft) x 100	Flow Rate (GPM)	Concentration (% by volume)
1	22.0	11.2	5.18	0.0410
2	22.0	11.2	5.34	0.0300
3	22.0	11.2	5.35	0.0360
4	21.5	17.1	6.62	0.401
5	21.5	17.2	6.60	0.294
6	22.0	17.2	6.52	0.320
7	22.5	21.6	7.77	0.348
8	22.5	21.6	7.78	0.315
9	23.0	21.6	7.81	0.465
10	21.5	25.5	8.47	0.447
11	22.0	25.5	8.47	0.595
12	21.0	25.5	8.48	0.557
13	21.0	32.6	9.70	0.854
14	21.0	32.6	9.83	0.930
15	22.5	32.6	9.94	0.799

TABLE 35

Glass Beads: Average Diameter = 505. Microns
Density = 4.430 g/cc
Charged Conc. = 9.99 % by wt.
PVC Pipe : Inside Diameter = 2.067 in.

Reference No.	Temperature (Deg.C)	Pressure Drop (Psi/ft) x 100	Flow Rate (GPM)	Concentration (% by volume)
1	23.0	10.1	126.	1.17
2	24.5	9.94	127.	0.851
3	21.0	10.2	128.	0.834
4	23.5	10.2	128.	1.56
5	22.0	8.25	113.	0.947
6	21.5	8.42	114.	0.874
7	22.5	8.36	114.	1.04
8	22.5	8.36	114.	0.909
9	21.0	6.21	94.6	0.938
10	22.0	6.22	94.6	0.852
11	22.5	6.22	95.2	0.734
13	22.0	4.54	72.8	0.887
14	22.0	4.56	72.8	0.841
15	22.0	2.99	6.65	0.572
16	20.0	2.99	6.65	0.501

TABLE 36

Glass Beads: Average Diameter = 505. Microns
Density = 4.430 g/cc
Charged Conc. = 9.99 % by wt.
PVC Pipe : Inside Diameter = 0.957 in.

Reference No.	Temperature (Deg. C)	Pressure Drop (Psi/ft) x 100	Flow Rate (GPM)	Concentration (% by volume)
1	20.0	9.83	15.2	0.127
2	20.0	9.83	14.9	0.179
3	20.5	9.82	15.1	0.149
4	22.0	5.34	10.7	0.060
5	21.5	5.36	10.7	0.079
6	21.0	5.36	10.6	0.080
7	21.5	18.4	20.9	0.941
8	22.0	18.4	21.2	0.708
9	22.5	18.5	21.6	0.680
10	23.0	25.5	26.2	1.71
11	22.5	25.5	25.5	1.67
12	20.0	25.7	27.0	1.47
13	21.0	20.0	23.5	0.969
14	21.5	19.8	22.8	0.927

TABLE 37

Glass Beads: Average Diameter = 505. Microns
Density = 4.430 g/cc
Charged Conc. = 9.99 % by wt.
PVC Pipe : Inside Diameter = 0.957 in.

Reference No.	Temperature (Deg.C)	Pressure Drop (Psi/ft) x 100	Flow Rate (GPM)	Concentration (% by volume)
1	22.5	2.12	6.63	----
2	22.5	2.06	6.31	----
3	22.5	2.08	6.31	----
4	23.0	3.81	9.02	0.008
5	23.0	3.81	8.94	0.008
6	23.0	3.81	9.02	0.008
7	23.5	5.91	11.4	0.026
8	23.5	5.91	11.6	0.027
9	22.5	10.6	16.0	0.129
11	24.0	5.38	11.0	0.029
12	22.0	5.38	10.9	0.022
13	21.5	5.49	10.8	0.022
14	22.0	10.4	14.3	0.217
15	22.0	10.4	15.8	0.203
16	22.5	10.4	15.6	0.172
18	24.5	16.0	19.6	0.539
19	21.5	16.0	19.5	0.471
20	20.5	16.0	19.9	0.489
21	20.0	20.1	23.1	1.85
22	21.0	20.1	22.7	1.23
23	22.0	20.1	22.8	0.871
24	21.5	20.1	23.1	0.839
25	22.0	20.1	23.0	1.01
26	22.5	20.1	23.4	1.05
27	22.5	20.1	23.4	0.851
28	23.0	20.1	23.0	0.833
29	23.5	24.5	26.7	1.40
30	23.0	24.5	26.0	1.10
31	22.5	24.5	26.1	1.21
32	22.5	24.5	26.4	1.33
33	22.0	30.2	29.0	1.02
34	23.0	30.5	29.2	1.03
35	22.0	30.7	29.7	0.816

TABLE 38

Glass Beads: Average Diameter = 505. Microns
Density = 4.430 g/cc
Charged Conc. = 9.99 % by wt.
PVC Pipe : Inside Diameter = 0.622 in.

Reference No.	Temperature (Deg.C)	Pressure Drop (Psi/ft) x 100	Flow Rate (GPM)	Concentration (% by volume)
1	21.0	14.0	5.97	0.245
2	21.5	14.0	6.01	0.243
3	21.5	14.0	6.03	0.238
4	20.5	4.16	2.97	0.004
5	22.0	22.8	8.07	0.196
6	22.0	22.8	7.90	0.221
7	22.0	22.8	7.89	0.689
8	22.0	22.8	7.98	0.474
9	21.5	23.0	7.91	0.338
10	21.5	23.0	7.89	0.478
11	21.5	23.0	8.01	0.421
12	22.0	23.4	7.95	0.369
13	20.5	23.9	8.10	0.422
14	22.5	34.9	9.97	0.788
15	22.0	34.9	9.77	1.52
16	21.5	35.1	9.93	2.08
17	22.0	30.2	9.13	0.733
18	22.5	30.2	9.15	0.664
19	22.0	30.2	9.15	1.30

TABLE 39

Glass Beads: Average Diameter = 505. Microns
Density = 4.430 g/cc
Charged Conc. = 14.9 % by wt.
PVC Pipe : Inside Diameter = 2.067 in.

Reference No.	Temperature (Deg.C)	Pressure Drop (Psi/ft) x 100	Flow Rate (GPM)	Concentration (% by volume)
1	21.0	6.92	89.0	2.38
2	22.0	6.92	90.0	1.96
3	23.0	6.66	91.3	1.33
4	22.0	6.92	89.3	2.08
5	22.0	6.92	89.6	1.77
6	22.0	5.77	75.3	1.72
7	22.5	5.77	75.4	1.86
8	23.0	5.84	75.4	1.94
9	22.0	8.00	105.	1.53
10	24.0	8.23	104.	1.87
11	23.5	8.23	105.	1.74
12	21.0	8.33	105.	1.76
13	22.5	4.69	62.2	1.40
14	22.0	4.69	61.8	1.43
15	22.0	4.69	61.6	1.69
16	22.5	3.76	49.0	1.01
17	22.5	3.76	49.0	1.12
18	22.5	3.76	49.0	1.81
19	22.0	9.82	120.	1.78
20	22.5	9.82	120.	1.99
21	22.5	9.82	120.	2.22
22	22.5	10.5	126.	1.78
23	22.5	10.6	126.	1.99
24	22.5	10.6	126.	2.14

TABLE 40

Glass Beads: Average Diameter = 505. Microns
Density = 4.430 g/cc
Charged Conc. = 10.1 % by wt.

PVC Pipe : Inside Diameter = 0.957 in.

Reference No.	Temperature (Deg.C)	Pressure Drop (Psi/ft) x 100	Flow Rate (GPM)	Concentration (% by volume)
1	23.0	6.78	12.2	0.347
2	22.5	6.78	12.0	0.395
3	22.5	6.79	12.1	0.278
4	22.5	6.75	12.0	0.234
5	23.0	6.79	12.2	0.241
6	23.0.	4.81	10.1	0.079
7	22.5	4.81	10.1	0.099
8	22.0	4.81	10.0	0.088
9	21.5	9.80	14.7	0.658
10	21.5	9.80	14.6	0.548
11	23.0	16.6	20.1	1.26
12	23.0	16.7	20.1	1.19
13	23.0	16.7	19.8	1.26
14	23.0	21.9	25.1	1.59
15	23.0	21.7	24.2	1.69
16	23.0	21.7	24.1	1.52
17	23.5	25.0	26.1	1.69
18	23.5	25.0	26.6	1.55
19	23.5	25.2	26.0	1.55
20	22.5	29.5	29.6	1.93
21	22.0	29.5	29.2	1.80

TABLE 41

Glass Beads: Average Diameter = 505. Microns
Density = 4.430 g/cc
Charged Conc. = 14.9 % by wt.

PVC Pipe : Inside Diameter = 0.622 in.

Reference No.	Temperature (Deg.C)	Pressure Drop (Psi/ft) x 100	Flow Rate (GPM)	Concentration (% by volume)
1	24.0	5.13	3.28	0.499
2	23.0	5.15	3.21	0.476
3	22.5	5.15	3.23	0.425
4	23.0	11.2	5.08	0.996
5	23.0	11.4	5.19	0.954
6	23.0	11.4	5.17	0.895
7	23.0	17.1	6.61	1.27
8	23.0	17.1	6.54	1.38
9	23.0	17.1	6.57	1.28
10	23.0	25.1	8.60	0.885
11	23.0	25.5	8.59	0.753
12	23.0	25.5	8.72	0.722
13	22.5	3.33	2.60	----
14	21.0	20.1	7.33	1.00
15	22.0	20.1	7.33	1.18
16	23.0	20.1	7.37	0.940
17	24.0	30.9	9.46	1.32
18	22.5	30.9	9.71	1.01
19	22.0	30.9	9.21	2.38
20	22.5	4.87	3.17	0.182
21	23.0	4.87	3.13	0.138
22	23.0	4.87	3.11	0.178
23	23.5	37.3	10.8	0.290
24	21.5	37.3	10.5	0.395
25	22.0	37.3	10.0	0.415

TABLE 42

Glass Beads: Average Diameter = 505. Microns
Density = 4.430 g/cc
Charged Conc. = 20.8 % by wt.

PVC Pipe : Inside Diameter = 2.067 in.

Reference No.	Temperature (Deg.C)	Pressure Drop (Psi/ft) x 100	Flow Rate (GPM)	Concentration (% by volume)
1	23.5	9.12	93.9	4.45
2	21.5	9.12	94.6	4.11
3	23.0	9.12	95.2	3.95
4	23.5	10.3	112.	4.22
5	23.0	10.3	114.	3.21
6	22.5	10.2	115.	3.20
7	23.0	7.00	64.2	3.74
8	23.5	6.92	64.2	3.44
9	22.0	7.29	64.2	4.07
10	23.0	11.1	122.	2.86
11	24.0	10.7	122.	2.69
12	24.5	10.8	122.	3.13
13	23.5	8.52	84.0	5.03
14	22.5	8.56	84.0	4.31
15	21.2	8.56	84.0	4.16
16	23.0	7.55	70.1	3.67
17	23.5	7.70	70.1	4.19
18	23.5	7.70	70.1	4.01
19	23.0	5.10	42.8	2.80
20	23.0	5.10	42.4	1.65
21	23.0	5.10	42.4	2.84

TABLE 45

Glass Beads: Average Diameter = 1015. Microns
Density = 4.400 g/cc
Charged Conc. = 5.08 % by wt.

PVC Pipe : Inside Diameter = 2.067 in.

Reference No.	Temperature (Deg.C)	Pressure Drop (Psi/ft) x 100	Flow Rate (GPM)	Concentration (% by volume)
1	22.8	4.69	84.7	0.095
2	23.5	4.69	84.7	0.134
3	23.0	4.70	84.7	0.121
4	23.0	6.33	101.	0.117
5	23.5	6.33	101.	0.070
6	23.5	7.82	113.	0.129
7	23.3	7.85	113.	0.086
8	23.0	7.85	113.	0.336
9	23.0	9.73	127.	0.127
10	23.0	9.76	127.	0.309
11	23.0	9.76	127.	0.238
12	23.0	9.76	127.	0.138
13	22.5	3.66	71.9	0.180
14	22.5	3.67	71.9	0.208
15	22.5	3.67	71.9	0.241
16	22.5	2.75	58.9	0.361
17	23.0	6.35	101.	0.079
18	23.0	6.36	101.	0.104
19	23.0	2.46	57.6	0.067
20	23.0	2.57	57.6	0.232
21	23.0	2.75	7.09	0.355
22	23.0	2.62	7.14	0.256

TABLE 43

Glass Beads: Average Diameter = 505. Microns
Density = 4.430 g/cc
Charged Conc. = 20.8 % by wt.

PVC Pipe : Inside Diameter = 0.957 in.

Reference No.	Temperature (Deg.C)	Pressure Drop (Psi/ft) x 100	Flow Rate (GPM)	Concentration (% by volume)
1	22.0	8.20	12.5	1.34
2	22.0	8.21	12.3	1.28
3	22.0	7.86	12.3	1.42
4	22.5	15.6	17.4	3.18
5	22.5	15.6	17.6	3.08
6	23.0	15.6	17.8	3.04
7	22.5	4.85	9.49	0.438
8	22.5	4.85	9.53	0.487
9	22.5	4.85	9.37	0.528
10	23.5	20.7	22.6	3.47
11	23.5	20.7	22.4	3.00
12	23.0	20.7	22.4	3.06
13	23.0	24.8	24.9	3.18
14	23.0	24.8	25.1	3.64
15	21.5	35.0	31.8	1.56
16	23.0	35.0	31.1	1.67
17	23.5	35.0	30.1	1.69

TABLE 44

Glass Beads: Average Diameter = 505. Microns
Density = 4.430 g/cc
Charged Conc. = 20.8 % by wt.

PVC Pipe : Inside Diameter = 0.622 in.

Reference No.	Temperature (Deg.C)	Pressure Drop (Psi/ft) x 100	Flow Rate (GPM)	Concentration (% by volume)
1	23.0	15.5	5.52	3.16
2	23.5	15.6	5.61	3.31
3	23.0	15.6	5.55	3.32
4	22.5	26.2	8.30	3.86
5	22.5	26.5	8.34	3.16
6	23.5	26.2	7.87	5.13
7	23.0	26.2	7.75	5.71
8	23.5	23.0	7.44	3.93
9	23.0	23.0	7.37	4.13
10	23.0	23.0	7.39	4.34
11	22.5	32.8	8.96	5.78
13	23.0	32.8	9.08	6.01
14	22.5	10.8	4.55	2.23
15	22.0	10.8	4.43	2.27
16	22.3	10.8	4.49	2.18
17	20.0	6.09	2.20	1.63
18	20.5	6.56	1.82	1.68

TABLE 46

Glass Beads: Average Diameter = 1015. Microns
Density = 4.400 g/cc
Charged Conc. = 5.08 % by wt.

PVC Pipe : Inside Diameter = 0.957 in.

Reference No.	Temperature (Deg.C)	Pressure Drop (Psi/ft) x 100	Flow Rate (GPM)	Concentration (% by volume)
1	23.0	14.4	19.8	0.252
2	23.0	14.5	19.9	0.225
3	23.0	14.6	19.9	0.263
4	23.0	21.8	25.0	0.307
5	23.0	21.8	24.8	0.319
6	23.0	21.8	25.5	0.294
7	23.0	21.9	25.1	0.269
8	23.0	21.9	25.1	0.239
9	23.0	22.0	24.8	0.254
10	23.0	22.1	25.1	0.228
11	23.0	22.1	25.2	0.203
12	23.0	7.62	13.8	0.055
13	23.0	7.62	13.8	0.073
14	23.0	7.62	13.7	0.078
15	23.0	7.62	13.8	0.089
16	23.0	7.62	13.8	0.080
17	23.0	28.1	28.6	0.333
18	23.0	28.1	28.4	0.487
19	23.0	28.1	29.0	0.402
20	23.0	28.1	29.0	0.378
21	23.0	28.1	28.5	0.360
22	23.0	34.9	32.4	0.323
23	23.0	34.9	32.5	0.350
24	23.0	34.9	32.3	0.386
25	23.0	35.1	32.8	0.206
26	23.0	35.1	32.4	0.211

TABLE 47

Glass Beads: Average Diameter = 1015. Microns
Density = 4.400 g/cc
Charged Conc. = 5.08 % by wt.

PVC Pipe : Inside Diameter = 0.622 in.

Reference No.	Temperature (Deg.C)	Pressure Drop (Psi/ft) x 100	Flow Rate (GPM)	Concentration (% by volume)
1	23.0	16.0	6.59	0.122
2	23.0	16.2	6.60	0.121
3	23.5	16.2	6.70	0.106
4	23.0	16.2	6.68	0.111
5	23.0	16.2	6.64	0.098
6	23.0	23.9	8.32	0.160
7	23.0	23.9	8.31	0.126
8	23.0	23.9	8.40	0.120
9	23.0	23.9	8.43	0.125
10	23.0	24.0	8.40	0.124
11	23.0	32.8	9.92	0.183
12	23.0	32.7	9.96	0.157
13	23.0	32.7	10.0	0.183
14	23.0	32.7	10.0	0.201
15	23.0	32.7	9.92	0.193
16	23.0	6.19	3.81	0.043
17	23.0	6.19	3.81	0.055
18	23.0	42.6	11.6	0.205
19	23.0	42.6	11.6	0.207
20	23.0	42.6	11.7	0.181

TABLE 48

Glass Beads: Average Diameter = 1015. Microns
Density = 4.400 g/cc
Charged Conc. = 10.0 % by wt.

PVC Pipe : Inside Diameter = 2.067 in.

Reference No.	Temperature (Deg.C)	Pressure Drop (Psi/ft) x 100	Flow Rate (GPM)	Concentration (% by volume)
1	23.0	8.13	112.	0.673
2	23.0	8.13	112.	0.949
3	23.5	8.13	112.	0.743
4	22.6	8.13	112.	0.708
5	22.6	8.13	112.	0.692
6	22.6	5.51	88.6	0.781
7	23.0	5.52	88.2	0.744
8	23.0	5.63	88.2	0.835
9	23.0	5.63	88.2	0.691
10	23.0	5.63	88.2	0.830
11	23.0	4.06	66.2	0.693
12	23.0	4.06	66.2	0.911
13	23.0	4.06	66.2	0.826
14	23.0	4.06	66.2	0.806
15	23.0	4.06	66.2	0.878
16	23.5	10.2	126.	1.83
17	23.5	10.3	127.	1.66
18	23.5	10.3	126.	1.34
19	23.5	10.3	127.	1.44
20	23.5	10.3	127.	1.13
21	23.0	3.50	53.6	0.653
22	23.0	3.50	54.3	1.02

TABLE 49

Glass Beads: Average Diameter = 1015. Microns
Density = 4.400 g/cc
Charged Conc. = 10.0 % by wt.

PVC Pipe : Inside Diameter = 0.957 in.

Reference No.	Temperature (Deg.C)	Pressure Drop (Psi/ft) x 100	Flow Rate (GPM)	Concentration (% by volume)
1	23.5	20.0	23.3	1.45
2	23.5	20.1	23.7	1.27
3	23.5	20.1	23.4	1.15
4	23.5	20.2	23.5	1.08
5	23.5	20.2	23.6	1.06
6	23.0	20.2	23.7	0.614
7	23.5	27.1	27.7	1.77
8	23.0	27.1	27.8	1.42
9	23.5	27.1	27.7	1.64
10	23.5	27.1	27.8	1.46
11	23.5	27.2	27.6	1.47
12	23.0	14.5	19.5	0.771
13	23.0	14.6	19.5	0.878
14	23.0	14.6	19.7	0.731
15	23.0	14.6	19.6	0.845
16	23.0	14.6	19.2	0.921
17	23.0	7.10	13.0	0.279
18	23.0	7.10	12.9	0.272
19	23.0	7.10	13.0	0.287
20	23.0	7.10	12.9	0.310
21	23.0	7.10	12.8	0.322
22	23.5	35.8	32.6	0.848
23	23.5	35.8	32.4	0.906
24	23.5	36.0	34.2	0.822
25	23.5	35.9	33.1	0.919
26	23.5	35.9	32.2	1.02

TABLE 50

Glass Beads: Average Diameter = 1015. Microns
Density = 4.400 g/cc
Charged Conc. = 10.0 % by wt.

PVC Pipe : Inside Diameter = 0.622 in.

Reference No.	Temperature (Deg.C)	Pressure Drop (Psi/ft) x 100	Flow Rate (GPM)	Concentration (% by volume)
1	23.5	33.5	10.0	1.21
2	23.5	33.3	10.0	1.04
3	23.5	33.4	10.0	1.02
4	23.5	33.5	9.93	1.31
5	23.5	33.5	9.90	1.22
6	23.5	18.9	7.16	0.652
7	23.5	18.9	7.18	0.702
8	23.5	18.9	7.20	0.607
9	23.5	18.9	7.21	0.645
10	23.5	18.9	7.16	0.623
11	23.3	26.9	8.87	0.755
12	23.5	27.1	8.86	0.691
13	23.5	27.1	8.90	0.668
14	23.5	27.1	8.91	0.769
15	23.5	27.1	8.87	0.780
16	23.0	12.0	5.57	0.419
17	23.0	12.1	5.55	0.408
18	23.0	12.1	5.56	0.382
19	23.0	12.1	5.53	0.457
20	22.5	6.79	3.99	0.058
21	22.5	6.79	3.99	0.067
22	22.5	6.79	4.01	0.063

TABLE 51

Glass Beads: Average Diameter = 1015. Microns
Density = 4.400 g/cc
Charged Conc. = 14.8 % by wt.

PVC Pipe : Inside Diameter = 2.067 in.

Reference No.	Temperature (Deg.C)	Pressure Drop (Psi/ft) x 100	Flow Rate (GPM)	Concentration (% by volume)
1	23.5	10.5	126.	1.78
2	23.5	10.5	126.	1.68
3	23.5	10.5	125.	2.06
4	23.5	10.5	125.	1.56
5	23.5	10.5	127.	1.12
6	23.5	8.24	102.	1.68
7	23.5	8.24	102.	1.87
8	23.5	8.24	103.	1.86
9	23.5	8.09	103.	1.66
10	23.5	8.02	103.	1.79
11	23.5	6.09	82.7	1.25
12	23.5	6.48	80.7	1.50
13	23.5	6.48	81.4	1.50
14	23.5	6.52	80.7	1.96
15	23.5	6.48	81.4	1.51
16	23.0	4.67	62.6	1.05
17	23.0	4.67	62.6	1.07
18	23.0	4.67	62.2	0.995
19	23.5	3.94	54.3	0.730
20	23.5	3.94	54.3	0.603
21	23.5	3.94	54.3	1.58

TABLE 52

Glass Beads: Average Diameter = 1015. microns
Density = 4.400 g/c.c.
Charged Conc. = 14.8 % by Wt.

PVC Pipe Inside Diameter = 0.957 in.

Reference No.	Temperature (Deg.C)	Pressure Drop (psi/ft)x100	Flow Rate (GPM)	Concentration (% by Volume)
1	23.5	27.1	27.8	1.87
2	24.0	27.2	28.1	2.11
3	23.5	27.1	27.4	2.12
4	23.5	27.1	27.6	2.07
5	23.5	20.0	23.1	1.90
6	23.5	20.0	23.0	1.76
7	23.5	19.8	22.6	1.77
8	23.5	19.8	22.9	2.40
9	23.5	13.3	17.8	1.39
10	23.5	13.3	18.1	1.48
11	23.5	13.3	18.0	1.44
12	23.5	13.3	18.0	1.50
13	23.0	7.29	13.3	0.309
14	23.0	7.29	13.3	0.287
15	23.5	7.29	12.9	0.320
16	23.5	7.29	13.4	0.303
17	23.5	34.8	32.0	1.28
18	23.5	35.2	32.0	1.36
19	23.5	35.3	32.9	1.17
20	23.5	35.5	33.4	1.32

TABLE 53

Glass Beads: Average Diameter = 1015. microns
Density = 4.400 g/c.c.
Charged Conc. = 14.8 % by Wt.

PVC Pipe: Inside Diameter = 0.622 in.

Reference No.	Temperature (Deg.C)	Pressure Drop (psi/ft)x100	Flow Rate (GPM)	Concentration (% by Volume)
1	23.5	36.6	10.4	2.85
2	23.5	36.6	10.3	2.72
3	23.5	36.6	10.4	2.66
4	23.5	36.6	10.4	2.54
5	23.5	14.3	5.95	1.18
6	23.5	14.3	5.91	1.35
7	23.5	14.3	5.94	1.19
8	23.5	14.3	5.96	1.14
9	23.5	28.6	8.93	2.52
10	23.5	28.6	8.99	2.75
11	23.5	28.6	8.96	2.50
12	23.5	29.1	9.03	2.65
13	23.5	21.1	7.42	2.15
14	23.5	21.1	7.36	1.90
15	23.5	21.1	7.43	2.26
16	23.5	21.1	7.35	2.59
17	23.5	7.73	4.21	0.363
18	23.5	7.73	4.23	0.365
19	23.5	7.73	4.23	0.363

TABLE 54

Glass Beads: Average Diameter = 1015. microns
Density = 4.400 g/c.c.
Charged Conc. = 20.7 % by Wt.

PVC Pipe: Inside Diameter = 2.067 in.

Reference No.	Temperature (Deg.C)	Pressure Drop (psi/ft)x100	Flow Rate (GPM)	Concentration (% by Volume)
1	23.5	11.5	118.	4.11
2	23.5	11.5	118.	3.58
3	23.5	11.5	118.	3.43
4	23.5	11.5	118.	2.36
5	23.5	10.1	93.9	4.19
6	23.5	10.1	93.9	4.10
7	23.5	10.1	93.9	4.08
8	23.5	8.90	75.0	4.41
9	23.5	8.90	74.4	4.37
10	23.2	7.67	63.5	3.16
11	23.5	7.52	63.5	2.99
12	23.5	7.44	64.9	3.74
13	23.1	5.02	51.0	2.31
14	23.1	5.40	51.0	2.20
15	23.3	5.40	51.0	2.55

TABLE 55

Glass Beads: Average Diameter = 1015. microns
Density = 4.400 g/c.c.
Charged Conc. = 20.7 % by Wt.

PVC Pipe: Inside Diameter = 0.957 in.

Reference No.	Temperature (Deg.C)	Pressure Drop (psi/ft)x100	Flow Rate (GPM)	Concentration (% by Volume)
1	23.0	13.6	19.1	0.802
2	23.5	14.1	19.3	0.512
3	23.5	14.1	19.1	0.519
4	23.5	14.1	19.3	0.843
5	23.5	7.38	13.5	0.051
6	23.8	19.5	22.2	3.32
7	23.6	19.8	22.2	3.22
8	23.5	20.0	22.3	3.35
9	23.5	25.7	25.9	4.06
10	23.5	25.7	25.8	4.92
11	23.5	26.0	25.9	4.81
12	23.5	26.0	25.9	5.77
13	23.5	31.0	29.7	2.62
14	23.5	31.0	29.5	3.18
15	23.5	31.0	29.9	3.48
16	23.5	31.0	29.4	2.85

TABLE 56

Glass Beads: Average Diameter = 1015. microns
Density = 4.400 g/c.c.
Charged Conc. = 20.7 % by Wt.

PVC Pipe: Inside Diameter = 0.622 in.

Reference No.	Temperature (Deg.C)	Pressure Drop (psi/ft)x100	Flow Rate (GPM)	Concentration (% by Volume)
1	23.5	31.2	9.03	5.29
2	23.5	31.2	9.06	5.03
3	23.5	31.2	9.17	4.84
4	23.2	24.1	7.79	3.62
5	23.5	24.1	7.75	3.96
6	23.5	23.9	7.71	4.14
7	23.5	23.9	7.68	3.82
8	23.5	17.6	6.35	2.86
9	23.5	17.6	6.51	2.81
10	23.5	17.6	6.49	2.90
11	23.5	9.51	4.70	0.670
12	23.5	9.61	4.74	0.772
13	23.5	9.61	4.75	0.722
14	23.0	9.61	4.53	1.11
15	23.5	36.6	10.2	3.33
16	23.5	36.8	10.3	3.19
17	23.5	36.8	10.3	3.42

TABLE 57

Glass Beads: Average Diameter = 475. microns
Density = 2.486 g/c.c.
Charged Conc. = 5.00 % by Wt.

PVC Pipe: Inside Diameter = 2.067 in.

Reference No.	Temperature (Deg.C)	Pressure Drop (psi/ft)x100	Flow Rate (GPM)	Concentration (% by Volume)
1	25.0	2.35	60.9	0.358
2	24.5	10.2	131.	1.60
3	23.5	3.83	74.1	0.606
4	23.0	1.82	47.7	0.403
5	23.0	5.10	88.0	0.875
6	23.5	1.38	41.1	0.178
7	24.0	8.26	116.	1.22
8	24.0	6.66	102.	1.20

TABLE 58

Glass Beads: Average Diameter = 475. Microns
Density = 2.486 g/cc
Charged Conc. = 10.0 % by wt.

PVC Pipe : Inside Diameter = 2.067 in.

Reference No.	Temperature (Deg.C)	Pressure Drop (Psi/ft) x 100	Flow Rate (GPM)	Concentration (% by volume)
1	23.5	3.54	54.3	3.36
2	24.0	5.06	80.7	4.33
3	24.0	7.67	107.	3.64
4	23.5	4.24	67.5	3.94
5	24.5	9.40	120.	4.11
6	25.0	2.44	43.7	2.72
7	25.0	2.42	44.8	2.38
8	25.5	6.44	93.9	4.41
9	26.0	6.51	93.3	3.34
10	26.5	6.18	93.9	3.26
11	23.0	2.38	42.4	1.92
12	23.0	2.23	42.4	1.45
13	23.0	2.20	42.4	2.33
14	23.5	4.21	67.5	2.98
15	24.0	4.21	66.9	3.99
16	23.5	5.25	80.7	3.32
17	24.5	7.85	107.	4.56
18	25.0	3.42	54.3	3.50
19	26.5	9.57	122.	3.99
20	28.5	6.37	93.9	2.22

TABLE 59

Glass Beads: Average Diameter = 475. Microns
Density = 2.486 g/cc
Charged Conc. = 15.0 % by wt.

PVC Pipe : Inside Diameter = 2.067 in.

Reference No.	Temperature (Deg.C)	Pressure Drop (Psi/ft) x 100	Flow Rate (GPM)	Concentration (% by volume)
1	24.0	8.11	102.	7.94
2	24.0	8.11	102.	7.94
3	25.0	8.11	102.	8.28
4	26.5	8.86	103.	6.98
5	26.5	8.86	103.	6.98
6	24.0	4.54	54.3	7.29
7	24.5	4.54	54.3	7.29
8	23.5	4.47	54.3	7.22
9	23.5	4.47	54.3	7.22
10	24.0	4.47	54.3	7.79
11	23.0	5.25	67.5	9.25
12	24.0	9.90	122.	7.88
13	24.5	5.88	79.4	7.20
14	24.5	6.10	80.7	7.32
15	24.7	6.10	80.7	7.32
16	24.0	3.31	41.1	4.32
17	24.3	8.38	107.	6.74
18	24.3	8.38	107.	6.74
19	23.5	2.53	31.2	2.00
20	23.5	2.53	31.2	2.30

APPENDIX B-1

SIZE MEASUREMENTS OF GLASS SPHERES

TABLE 1 - Diameter Measurements for 48.8μ Glass Beads

Sample	Group	Bead No.	Diameter Reading(μ)
FIRST	FIRST	1	58.2
		2	52.8
		3	38.2
		4	45.5
		5	40.0
	SECOND	6	43.7
		7	49.1
		8	45.5
		9	45.5
		10	43.7
SECOND	FIRST	11	51.0
		12	47.3
		13	51.0
		14	45.5
		15	43.7
	SECOND	16	54.6
		17	58.2
		18	52.8
		19	58.2
		20	52.8

Mean Diameter = 48.8   Standard Deviation = 5.78μ

TABLE 2 - Diameter Measurements for 214μ Glass Beads

Sample	Group	Bead No.	Diameter Reading(μ)	
			1	2
FIRST	FIRST	1	246	247
		2	208	212
		3	201	204
		4	206	212
		5	221	222
	SECOND	6	209	214
		7	209	210
		8	213	213
		9	208	212
		10	226	227
SECOND	FIRST	11	235	239
		12	195	198
		13	214	213
		14	199	194
		15	195	194
	SECOND	16	209	206
		17	186	192
		18	225	227
		19	221	219
		20	253	251

Mean Diameter = 214μ   Standard Deviation = 16.2μ

TABLE 3 - Diameter Measurements for 314μ Glass Beads

Sample	Group	Bead No.	Diameter Reading(μ)	
			1	2
FIRST	FIRST	1	301	301
		2	315	319
		3	339	344
		4	360	350
		5	274	274
	SECOND	6	281	287
		7	338	331
		8	321	316
		9	277	270
		10	275	280
SECOND	FIRST	11	325	317
		12	331	340
		13	315	316
		14	259	276
		15	328	349
	SECOND	16	285	288
		17	352	358
		18	270	271
		19	284	288
		20	332	324

Mean Diameter = 314μ Standard Deviation = 29.8μ

TABLE 4 - Diameter Measurements for 475μ Glass Beads

Sample	Group	Bead No.	Diameter Reading(μ)	
			1	2
FIRST	FIRST	1	400	401
		2	516	539
		3	482	490
		4	495	495
		5	497	510
	SECOND	6	572	456
		7	464	478
		8	468	461
		9	486	484
		10	438	458
SECOND	FIRST	11	477	479
		12	529	522
		13	463	474
		14	456	438
		15	488	491
	SECOND	16	489	508
		17	484	488
		18	477	475
		19	462	445
		20	433	441

Mean Diameter = 475μ Standard Deviation = 28.9μ

APPENDIX B-2

GLASS SPHERE SLURRY FLOW IN 2-INCH PIPELINE

TABLE 1

Glass Beads: Average Diameter = 48.8 microns
Density = 2.451 gm/cc
Charged Conc. = 10.0% wt.

PVC Pipe: Inside Diameter = 2.067 in.

No.	Temp. (°C)	Velocity (ft./sec.)	Pressure Drop (psi/100 ft.)	Concentration(Vol.%) Discharge	Spatial
1	18	2.16(1)	0.37	3.80	--
2	19	2.20(2)	0.43	3.80	2.99
3	21	3.98	1.42	2.54	2.18
4	19	5.20	2.29	2.70	--
5	19	7.11	4.15	3.53	--
6	20	9.04	6.10	3.22	2.88
7	19	10.96	8.21	3.88	--
8	20	12.57	10.80	3.97	--
9	22	13.23	11.83	4.35	3.59

(1) Critical velocity approached from above.
(2) Critical velocity approached from below.

TABLE 2

Glass Beads: Average Diameter = 48.8 microns
Density = 2.451 gm/cc
Charged Conc. = 15.0% wt.

PVC Pipe: Inside Diameter = 2.067 in.

No.	Temp. (°C)	Velocity (ft./sec.)	Pressure Drop (psi/100 ft.)	Concentration(Vol.%) Discharge	Spatial
1	21	2.96(1)	0.83	3.18	--
2	20	2.16(2)	0.46	3.19	2.69
3	20	3.82	1.51	4.14	3.56
4	21	4.73	2.30	5.63	--
5	21	7.15	4.07	6.58	--
6	20	8.60	6.43	6.17	5.06
7	21	10.16	8.56	6.78	--
8	21	11.70	10.66	6.65	--
9	20	12.59	11.56	6.69	5.27

(1) Critical velocity approached from above.
(2) Critical velocity approached from below.

TABLE 3

Glass Beads: Average Diameter = 214 microns
Density = 2.455 gm/cc
Charged Conc. = 10% wt.

PVC Pipe: Inside Diameter = 2.067 in.

No.	Temp. (°C)	Velocity (ft./sec.)	Pressure Drop (psi/100 ft.)	Concentration(Vol.%)	
				Discharge	Spatial
1	20	2.79(1)	0.82	0.92	--
2	20	2.58(2)	0.76	0.92	1.83
3	19	2.83	0.86	0.68	--
4	19	4.24	1.51	0.32	--
5	19	5.66	2.68	1.24	--
6	19	7.07	3.89	0.81	0.53
7	19	8.48	5.30	0.93	--
8	20	9.97	6.96	1.84	--
9	20	12.02	9.92	1.77	1.58

(1) Critical velocity approached from above.
(2) Critical velocity approached from below.

TABLE 4

Glass Beads: Average Diameter = 214 microns
Density = 2.455 gm/cc
Charged Conc. = 20% wt.

PVC Pipe: Inside Diameter = 2.067 in.

No.	Temp. (°C)	Velocity (ft./sec.)	Pressure Drop (psi/100 ft.)	Concentration(Vol.%)	
				Discharge	Spatial
1	19	3.99(1)	1.68	2.76	--
2	19	3.64(2)	1.50	2.29	3.05
3	21	2.83	0.96	0.78	2.19
4	21	4.24	1.67	2.56	--
5	20	5.66	2.88	3.51	5.78
6	21	7.07	4.22	3.20	--
7	20	8.48	5.93	4.55	6.91
8	21	9.90	7.54	7.16	--
9	21	12.02	10.96	5.92	7.16

(1) Critical velocity approached from above.
(2) Critical velocity approached from below.

TABLE 5

Glass Beads: Average Diameter = 214 microns
Density = 2.455 gm/cc
Charged Conc. = 25% wt.

PVC Pipe: Inside Diameter = 2.067 in.

No.	Temp. (°C)	Velocity (ft./sec.)	Pressure Drop (psi/100 ft.)	Concentration(Vol.%)	
				Discharge	Spatial
1	24	2.90(1)	0.84	0.15	--
2	23	2.03(2)	0.42	0.07	--
3	22.5	2.83	0.92	0.55	2.51
4	22.5	4.24	1.85	3.44	--
5	23.5	5.67	2.57	3.34	--
6	23	7.45	4.21	2.15	1.88
7	22	8.48	5.22	1.62	--
8	23	9.90	6.77	6.57	--
9	21	11.31	8.68	5.18	--

(1) Critical velocity approached from above.
(2) Critical velocity approached from below.

TABLE 6

Glass Beads: Average Diameter = 314 microns
Density = 2.454 gm/cc
Charged Conc. = 20% wt.

PVC Pipe: Inside Diameter = 2.067 in.

No.	Temp. (°C)	Velocity (ft./sec.)	Pressure Drop (psi/100 ft.)	Concentration(Vol.%)	
				Discharge	Spatial
1	20	3.75(1)	3.14	10.8	--
2	20.5	3.98(2)	2.78	7.35	--
3	21.3	4.24	3.89	16.9	--
4	21.3	5.66	3.87	9.72	12.3
5	20	7.07	5.25	11.8	--
6	21.5	8.55	7.16	15.8	--
7	21.3	9.90	8.14	12.5	13.3
8	22.5	11.31	8.71	10.1	13.6

(1) Critical velocity approached from above.
(2) Critical velocity approached from below.

TABLE 7

Glass Beads: Average Diameter = 475 microns
Density = 2.481 gm/cc
Charged Conc. = 10% wt.

PVC Pipe: Inside Diameter = 2.067 in.

No.	Temp. (°C)	Velocity (ft./sec.)	Pressure Drop (psi/100 ft.)	Concentration(Vol.%)	
				Discharge	Spatial
1	19.5	2.95(1)	0.93	0.30	--
2	19.5	2.79(2)	0.76	0.17	0.44
3	20.5	2.86	0.91	0.50	1.83
4	21	4.95	2.04	1.56	--
5	19	5.66	2.52	0.71	0.86
6	19	7.07	4.05	2.54	--
7	21	8.41	5.15	2.76	2.73
8	19.5	9.97	7.41	3.94	--
9	20.5	11.81	9.14	4.29	5.23

(1) Critical velocity approached from above.
(2) Critical velocity approached from below.

TABLE 8

Glass Beads: Average Diameter = 475 microns
Density = 2.481 gm/cc
Charged Conc. = 20% wt.

PVC Pipe: Inside Diameter = 2.067 in.

No.	Temp. (°C)	Velocity (ft./sec.)	Pressure Drop (psi/100 ft.)	Concentration(Vol.%)	
				Discharge	Spatial
1	19.5	2.93(1)	1.67	1.18	6.23
2	21	2.93(2)	1.47	1.17	4.75
3	19	4.53	2.12	1.53	--
4	20	5.66	3.06	2.63	4.79
5	19	7.10	4.62	7.07	5.61
6	19.5	8.48	5.88	9.56	3.36
7	19.5	9.97	7.38	10.1	3.75
8	21	11.28	8.80	6.83	3.81

(1) Critical velocity approached from above.
(2) Critical velocity approached from below.

TABLE 9

Glass Beads: Average Diameter = 475 microns
Density = 2.481 gm/cc
Charged Conc. = 30% wt.

PVC Pipe: Inside Diameter = 2.067 in.

No.	Temp. (°C)	Velocity (ft./sec.)	Pressure Drop (psi/100 ft.)	Concentration(Vol.%) Discharge	Spatial
1	20	2.69[1]	2.70	5.01	9.39
2	21	2.33[2]	1.81	1.74	6.12
3	23	4.70	3.27	5.48	--
4	19	5.78	3.80	5.71	6.20
5	20	7.16	4.83	9.05	--
6	21.5	8.48	6.15	13.0	6.90
7	20	9.97	7.53	12.1	--
8	20	11.38	9.42	11.1	7.69

(1) Critical velocity approached from above.
(2) Critical velocity approached from below.